INL/RPT-24-78112
Revision 0

AGC-4 Specimen Post-Irradiation Examination Data Interim Report

May 2024

Austin C. Matthews, David T. Rohrbaugh, William E. Windes, and David L. Cottle
Idaho National Laboratory

INL is a U.S. Department of Energy National Laboratory operated by Battelle Energy Alliance, LLC

INL/RPT-24-78112
Revision 0

AGC-4 Specimen Post-Irradiation Examination Data Interim Report

Austin C. Matthews, David T. Rohrbaugh, William E. Windes, and David L. Cottle
Idaho National Laboratory

May 2024

Idaho National Laboratory
Advanced Reactor Technologies
Idaho Falls, Idaho 83415

http://www.art.inl.gov

Prepared for the
U.S. Department of Energy
Office of Nuclear Energy
Under DOE Idaho Operations Office
Contract DE-AC07-05ID14517

Page intentionally left blank

INL ART Program

AGC-4 Specimen Post-Irradiation Examination Data Interim Report

INL/RPT-24-78112
Revision 0

May 2024

Technical Reviewer: (Confirmation of mathematical accuracy, and correctness of data and appropriateness of assumptions.)

Michael E. Davenport INL ART Project Manager	Date

Approved by:

Travis Mitchell INL ART Program Manager	Date
Michelle T. Sharp INL Quality Assurance	Date

Page intentionally left blank

SUMMARY

This interim report documents preliminary results of the post-irradiation examination material-property testing from the fourth Advanced Graphite Creep (AGC) experiment campaign, AGC-4, capsule specimens. This is the fourth of a series of six irradiation test trains planned as part of the AGC experiment to fully characterize the neutron-irradiation effects and radiation-creep behavior of current nuclear graphite grades to moderate dose levels (≤15 dpa). The AGC-4 capsule was irradiated in Idaho National Laboratory's Advanced Test Reactor at a nominal temperature of 800°C and to a peak dose of 8 dpa. Half of the AGC-4 specimens were subjected to compressive stresses to induce irradiation creep. Post-irradiation testing and measurement results are reported here, with the exception of thermal testing, which is still in progress, and irradiation mechanical-strength testing. Additionally, some specimens initially deemed too hot to be examined in the Advanced Reactor Technologies (ART) Graphite Laboratory may still be measured. The data reported include dimensions for both stressed and unstressed specimens to establish irradiation-creep rates, mass, and dimensional data necessary to derive density, elastic constants (Young's modulus, shear modulus, and Poisson's ratio) from ultrasonic time-of-flight velocity measurements, Young's modulus from the fundamental frequency of vibration, and electrical resistivity. Not included in this report are additional specimens initially deemed too radiologically active to be examined in the ART Carbon Laboratory in 2023. However, new administrative controls specifically developed for these specimens may now allow them to be shipped and tested within the Carbon Laboratory. The actual number of these specimens remains to be determined based upon their measured activity levels.

A more complete evaluation of trends in the material property changes, the thermal property changes, as well as irradiation-induced creep analysis due to the irradiation environment and applied load on the specimens, will be reported at a later date in a full AGC-4 post-irradiation examination analysis report.

Page intentionally left blank

CONTENTS

FIGURES

TABLES

ACRONYMS

AG	Against-grain
AGC	Advanced graphite creep
ART	Advanced Reactor Technologies
ASTM	American Society for Testing and Materials
ATR	Advanced Test Reactor
COV	Coefficient of variance
DOE	Department of Energy
HDG	high-dose graphite
HFEF	Hot Fuels Examination Facility
HOPG	Highly ordered pyrolitic graphite
HTR	High-temperature reactor
INL	Idaho National Laboratory
IQR	Interquartile range
PIE	Post-irradiation examination
WG	With-grain

Page intentionally left blank

AGC-4 Specimen Post-Irradiation Examination Data Interim Report

1. INTRODUCTION

The Advanced Reactor Technologies Graphite Research and Development Program is conducting an extensive graphite-irradiation program to provide data to assist in licensing of a high-temperature reactor (HTR) design. In past applications, graphite has been used effectively as a structural and moderator material in both research and commercial high-temperature gas-cooled reactor designs (Burchell T. 2007) (Bratton 2005). Nuclear graphite H-451, used previously in the United States for nuclear-reactor graphite components, is no longer available. New nuclear-graphite grades have been developed and are considered suitable candidates for new HTR designs. To support the design and licensing of HTR core components within a commercial reactor, a complete properties database must be developed for these current grades of graphite. Quantitative data on in-service material performance is required for the physical, mechanical, and thermal properties of each graphite grade, with a specific emphasis on data accounting for the life-limiting effects of irradiation creep. Further details on the research and development activities and associated rationale required to qualify nuclear-grade graphite for use within the HTR are documented in the PLN-2497, "Graphite Technology Development Plan" (Windes 2010).

Based on experience with previous graphite core components, the phenomenon of irradiation-induced creep within the graphite has been shown to be a critical parameter in determining the total useful lifetime of graphite components. Irradiation-induced creep occurs under the simultaneous application of high temperatures, neutron irradiation, and applied stresses within the graphite components. A second, much more-significant internal stress is experienced within the graphite components due to irradiation-induced dimensional changes. These induced stresses result from neutron irradiation inducing physical changes in the graphite structure — first shrinking or densifying the microstructure and, with increasing neutron dose, inducing volumetric expansion. This disparity in material-volume change can induce significant internal stresses within graphite components. Irradiation-induced creep relaxes these large internal stresses, thus reducing the risk of crack formation and component failure. Obviously, higher irradiation-creep levels tend to relieve more internal stress, thus allowing the components longer useful lifetimes within the core. Determining the irradiation-creep rates of nuclear-graphite grades is critical for determining the useful lifetime of graphite components and is a major component of the Advanced Graphite Creep (AGC) experiment.

The overall AGC experiment determines the in-service behavior of new graphite grades for use in HTRs. This test series examines the properties and behaviors of nuclear-grade graphite over a large range of irradiation temperatures, moderate fluence levels, and applied stresses that are expected to induce physical property changes and irradiation-creep strains within HTR graphite components. Six irradiation capsules will be irradiated in a large flux trap of the Advanced Test Reactor (ATR) at Idaho National Laboratory (INL). AGC irradiation conditions are similar to the anticipated environment within a high-temperature core design. Each irradiation capsule contains over 400 graphite specimens that are characterized before and after irradiation to determine the irradiation-induced material-property changes and life-limiting irradiation creep rate for each graphite grade.

The data and information produced in this report and the referenced documents within were generated under the approved INL Quality Assurance Programs, in compliance with the applicable Nuclear Quality Assurance (NQA)-1 requirements (ASME 2009). It is anticipated that all data will be robust enough to stand up to a review by the American Society of Mechanical Engineers and Nuclear Regulatory Commission as support for an eventual graphite-reactor design selection.

2. ADVANCED GRAPHITE CREEP EXPERIMENT

The AGC test series is designed to provide data necessary to assist in determining the safe operating envelope of graphite core components for an HTR by measuring the irradiated-material property changes

and the behavior of several new nuclear-graphite grades over a large range of temperatures, moderate neutron fluence, and mechanical compressive loads. The experiment consists of five interrelated stages: pre-irradiation characterization of the graphite specimens, as-run irradiation reports for each test series (designated as six separate irradiation test-train capsules), capsule disassembly, post-irradiation examination (PIE), and analysis of the graphite specimens. Separate reports for each distinct stage are prepared after each individual activity is completed.

The pre-irradiation examination report details the total number of graphite grades and individual specimens, specimen-loading configuration designed to expose all specimens to the entire range of irradiation conditions, and pre-irradiation material-property testing data and results. The as-run irradiation report will detail the irradiation history of each capsule while in the reactor, noting any changes from the technical and functional specifications for each specific test-series capsule and identifying the possible improvements to the next test-series capsule design. The disassembly report details specimen recovery from the irradiation capsule, noting any damage to the specimens and providing an inventory of recovered specimens for PIE testing. This PIE data report details the changes in specimen dimensional measurements as well as irradiated material properties upon exposure to neutron irradiation. Finally, the PIE analysis report will analyze the irradiation results reported in the data-package reports, using the irradiation conditions recorded in the as-run irradiation report. The PIE analysis determines the irradiation-induced creep rates for the major grades of graphite and assesses any changes to the material properties in all graphite grades. The PIE analysis also interprets the irradiation behavior of graphite to assist in determining a credible, safe operating envelope for graphite core components in an HTR design and licensing application. This report is on AGC PIE data and provides the results and data from PIE for AGC-4 specimens. An abridged statistical analysis is performed here along with a limited comparison to pre- and post-irradiation data. In this way, the consistency and soundness of the data are initially tested. A more complete evaluation of trends in the material property changes, the thermal property changes, as well as irradiation-induced creep analysis due to the irradiation environment and applied load on the specimens, will be reported later in a full AGC-4 post-irradiation examination analysis report.

2.1 Design Parameters of AGC Experiment

The AGC test series is designed to measure changes in key thermal, physical, and mechanical material properties over the anticipated range of HTR operating conditions. By comparing the material properties of each specimen before and after irradiation, the experiment generates quantitative material-property-change data and irradiation-creep data that will be used to predict the in-service behavior and operating performance of the current nuclear-graphite grades for HTR designs. Specific emphasis is placed on data that account for the life-limiting effects of irradiation creep on graphite components and the effects creep may have on key irradiated material properties of several candidate graphite grades for use in an HTR design.

The critical component of the experiment is the irradiation test series, which irradiates the graphite specimens after pre-irradiation examination characterization has been completed. Six planned irradiation test trains to be irradiated in ATR in a large flux trap comprise the AGC test series, as described in the graphite technology-development plan. The test series exposes test specimens of select nuclear-graphite grades to temperatures and the initial range of the expected lifetime irradiation dose that are expected within an HTR design. Specifically, graphite specimens will be exposed to a fast-neutron dose ranging from 1 to 15 dpa at temperatures of 600 and 800°C. The first and second AGC capsules, AGC-1 and AGC-2, were designed to be irradiated within ATR's south flux trap. All other AGC capsules are to be irradiated within ATR's east flux trap. Generally, irradiations within the south flux trap require approximately 175 effective full-power days to provide a nominal fast-neutron dose range (in graphite) of approximately 0.5 to 3.5 dpa. For those capsules requiring a large dose range of approximately 3.5 to 7.0 dpa, the capsule is irradiated for twice as long, approximately 350 effective full-power days. For those specimens subjected to a maximum of 15 dpa select specimens from AGC-1 through AGC-4 will be re-irradiated for an additional 400 effective full-power days. These irradiations will be performed within the high-dose graphite (HDG) Capsules -1 and -2, with irradiation temperatures of 600°C (HDG-1) and 800°C (HDG-2).

In addition to determining irradiation-induced changes to the material properties of selected nuclear graphite grades, the AGC experiment dedicates a significant amount of scope to determining rates of irradiation-induced creep for different nuclear graphite grades. The traditional method for measuring irradiation-induced creep is to apply a significant mechanical load (inducing a mechanical stress within the graphite) to half the specimens during irradiation while leaving the remaining half of the specimens unloaded (i.e., unstressed) (Brown 1969) (Gray 1973). The resulting difference in dimensional change between the loaded and unloaded specimens (assuming that temperature and dose levels are the same) provides the amount of irradiation-induced strain for each "matched pair" of graphite specimens. From this strain level, a creep rate for each graphite grade can be calculated as a function of dose if both specimens were irradiated at the same constant temperature and similar dose level. Thus, each capsule is designed to be irradiated at a constant temperature, allowing only the dose and applied mechanical load to vary within the test train of each test-series capsule. With all graphite specimens at a constant temperature, only the applied stress level and dose will affect the calculated creep rate of each graphite grade within a test-series capsule.

The AGC experiment is designed to measure the constant creep-strain rate (secondary creep) of the various grades. The experiment assumes that the induced creep strain for all specimens is within the secondary creep regime and therefore behaves linearly with respect to received neutron dose (Windes 2010). This assumption is valid provided the specimens do not go beyond their turnaround dose at which creep strain can no longer be expected to be linear with irradiation dose (i.e., the onset of tertiary creep). Once the specimens begin to reach turnaround, the creep-strain response becomes non-linear with received dose.

While the effects from applied mechanical stresses and neutron dose can be determined within each irradiation capsule, the temperature dependency of any irradiation-induced material-property changes within the graphite grades is determined by comparing the measured values of the specimens between irradiation capsules. Because each test train is irradiated at a constant temperature (600 or 800°C), the temperature-induced and enhanced material-property changes must be determined by comparing specimens in different capsules exposed to similar doses and applied mechanical loads. All AGC capsules are designed to have the same specimen stacking patterns. Thus, if specimens of identical graphite grades are located in similar positions within each capsule, a similar dose and load level will be imposed on a consistent grade of graphite. Maintaining consistent specimen positions for each grade within the six different capsules will allow for the determination of temperature-induced changes for irradiation creep and material properties across the AGC experiment.

2.2 AGC Graphite Grades and Specimen Dimensions

The AGC experiment is designed to ascertain the irradiation behavior of currently available nuclear-graphite grades within the anticipated operating parameters of an HTR design. By exposing a variety of nuclear-graphite grades representing the range of fabrication parameters (e.g., grain size, fabrication processes, and raw source material) to the expected operating conditions for a moderate HTR design (600 to 800°C and 1 to 15 dpa maximum dose), a comprehensive understanding of the irradiation response and behavior of graphite components in general can be achieved. This will limit the need for additional research in the future if the current graphite grades are altered (i.e., new raw-material sources are used) or new grades are used in future reactors.

The AGC experiment uses a variety of current graphite grades to envelope the major fabrication parameters believed to be responsible for the irradiation behavior of nuclear graphite. This range of fabrication parameters is represented by AGC major grades that were deemed to be production ready and could be used in current or future HTR designs. Major graphite grades are one type of sample within the AGC irradiation capsule. In addition, four other sample types are designated within the AGC experiment. The five AGC sample types are categorized as follows:

1. Major grades (irradiation creep and control specimens). These graphite grades are current reactor candidates for the core structures of an HTR design. Historical or reference grades are considered major grades as well. Due to their fabrication maturity and consistency, HTR core components are most likely to be formed from these major grades. They are thus expected to receive reasonably large neutron doses in their lifetimes. Only major-grade specimens were used to determine the critical irradiation-induced creep-strain rate.
2. Minor grades (6 mm tall, button-shaped piggyback specimens). These grades are HTR-relevant grades that are not yet production ready or are most likely to be used in low-neutron-dose regions of the core (e.g., the permanent structure of the prismatic-block HTR design).
3. Alternate grades (piggyback specimens). Grades that current HTR vendors have identified as being of interest as alternate graphite grades for certain components within the reactor.
4. Experimental grades (piggyback specimens). These graphite grades are included in AGC to assess the viability of new graphite grades, the manufacturing processes and raw materials of which are such that they may offer superior irradiation stability. Additionally, other carbonaceous materials such as fuel-compact-matrix materials, carbon-carbon composites, silicon-carbide composites, or other experimental materials that could offer superior performance within the extreme environment of an HTR core are included.
5. Single-crystal graphite (piggyback specimens). Samples of highly ordered pyrolytic graphite (HOPG) are included in all AGC capsules to assess the fundamental irradiation response of single crystal graphite. These specimens offer specific dimensional-change behavior of graphite, which is particularly significant to the behavior of polycrystalline (polygranular) graphite grades.

To provide all necessary material property tests in the AGC experiment, each test-series capsule contains two primary specimens: (1) “creep” specimens, providing irradiation creep-rate value as well as mechanical properties, and (2) “piggyback” specimens, providing thermal material-property changes to the graphite. Creep specimens are fabricated only from major-grade graphite types. Piggyback specimens are fabricated from major-, minor-, and experimental-grade graphite types. The piggyback specimens are not mechanically loaded and are subjected only to neutron irradiation at high operating temperatures to assess the effects of a reactor environment on the specific graphite grade.

All specimens are 12.4 mm in diameter, with the larger creep specimens having a nominal length of 25.4 mm and the piggyback specimens having a nominal length of 6.3 mm. Small graphite containers that are 12.4 mm in diameter by 6 mm long contain the thin-wafer HOPG specimens. The large creep specimens provide a means to acquire dimensional and volume change, elastic modulus, thermal expansion, and electrical-resistivity measurements. However, these creep specimens are not suitable for thermal-diffusivity measurements because of their length. The small piggyback specimens permitted only dimensional measurements, density, and thermal-diffusivity testing to be performed. Together, both types of specimens provide the changes in material properties for stressed and unstressed graphite grades.

2.3 General AGC Test Train Design

All AGC test trains and irradiation capsules have the same general physical configuration to provide consistent dose and applied mechanical stresses on specimens of similar graphite grades. While there are key machining and structural differences between capsules to change the irradiation temperature for the different capsules, the majority of the AGC design is identical for all capsules. A schematic of the AGC-4 test train is shown in Figure 1.

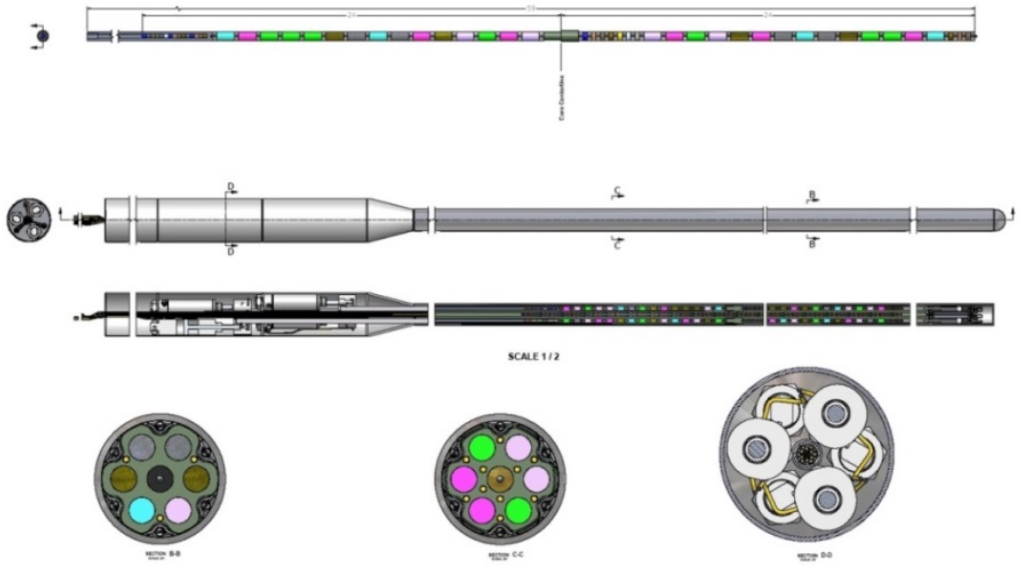

Figure 1.The AGC-4 creep capsule.

All irradiation capsules have six channels located on the outer perimeter of the graphite specimen-holder body and a center channel. All channels are 12.9 mm in diameter and are designed to hold all types of AGC specimens. The upper (top) half the outer channels have mechanical loads applied to the specimens. However, the lower (bottom) half for these channels have no mechanical load applied to the specimens in these locations. Due to the neutron flux profile in ATR, matched pairs with similar neutron fluence and temperatures are achieved by pre-ordering the specimen axial locations. Specimens in the upper half of the channels were stressed by the applied mechanical load while their matched pairs received a similar dose in an unstressed state. Three stress levels—13.8, 17.2, and 20.7 MPa nominal—are applied in all AGC capsules to provide a known stress upon the graphite specimens during irradiation. These induced stress levels are high enough to produce irradiation-induced creep strain with the graphite specimens.

Temperature values within all AGC capsules are calculated based upon thermocouple readings at select positions within the capsule. Specimen temperature is calculated with a finite-element model that has been calibrated to predict the known thermocouple readings in the capsule. Dose levels are calculated using Monte Carlo N-Particle Transport Code models and operating conditions in the ATR core and are corroborated from flux wire data.

2.4 Establishing Specimen Dose

To achieve the desired irradiation-dose levels and applied mechanical loads to specific specimens, an exact specimen-loading order is critical. Because irradiation creep is usually determined by the difference in dimensional change occurring within specimens that have an applied load and those that do not, these matched-pair specimens are assumed to have the same irradiation dose and irradiation temperature values. The AGC test-train designs use the symmetric flux profile generated within ATR to achieve these similar irradiation conditions for matched pairs.

Other considerations that went into the capsule design included the size of each creep specimen, need for periodically placed spacers containing flux wires, and space requirements in the top of the stacks for the pneumatic push rods. The core flux mid-plane, in relation to the capsule arrangement, was established so that the reactor neutron-flux field could be correlated to the physical elevations and positions in the capsule to yield accurate matched-pair irradiation dose levels (see Figure 2).

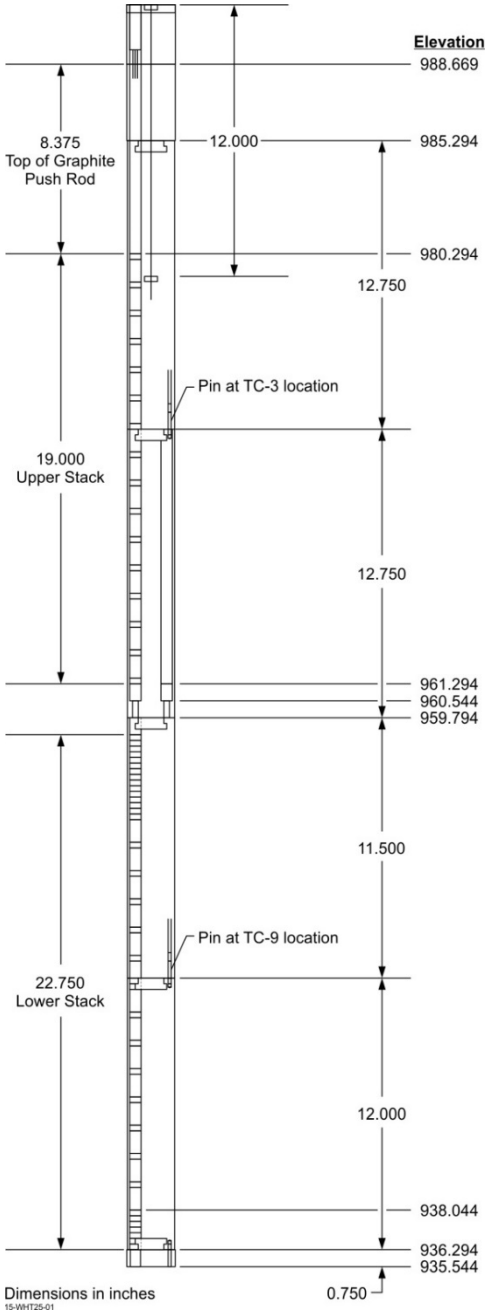

Figure 2. Elevation sketch of the AGC capsule.

Irradiation dose values, as a function of distance from the reactor core centerline, are calculated from the total calculated fluence using standard conversion factors for carbon in a fast-neutron irradiation field (E >0.1 MeV). There is a neutron-flux gradient across the capsule thickness, requiring the capsule to be rotated 180 degrees at the irradiation duration mid-point. This rotation results in a uniform neutron-fluence profile for all stacks, regardless of their position within the capsule.

As described in previous reports (Burchell T. 2005), the ATR neutron-flux profile is not completely symmetrical along the vertical axis. Thus, to produce matched-pair specimens that have similar dose profiles both above and below the core mid-plane, an offset position from the mid-plane is required. It was determined that an offset distance of 1.25 in. from the core mid-plane for the bottom creep specimens produces the closest dose matches between specimens.

2.5 Physical Positions of Creep Specimens in the Stacks

Once the specimen-position offset is established for the bottom half of the specimens, the number of total creep specimens for each grade of graphite is determined. It should be noted that the specimen-stacking order for subsequent AGC irradiation capsules was changed from that initially established for the AGC-1 test train. In the initial AGC capsule design, AGC-1 used 0.25-in.-long NBG-25 graphite spacers between all creep specimens to separate them from each other. It was determined that this was not necessary, and the 0.25-in.-long NBG-25 graphite spacers were eliminated. Eliminating the spacers increased the total number of creep specimens in the AGC capsules.

Because any two opposing stacks are at similar applied-stress levels, the specimen loading order can be shifted between the two stacks, allowing the same grade of graphite to be mechanically loaded over a broader neutron-dose range, as shown in Figure 3. Assuming both stacks will have the same applied stress level, receive similar dose levels per position, and have a constant temperature allows this shifting of the specimens and, consequently, a more-uniform, smoother dose profile for each graphite grade.

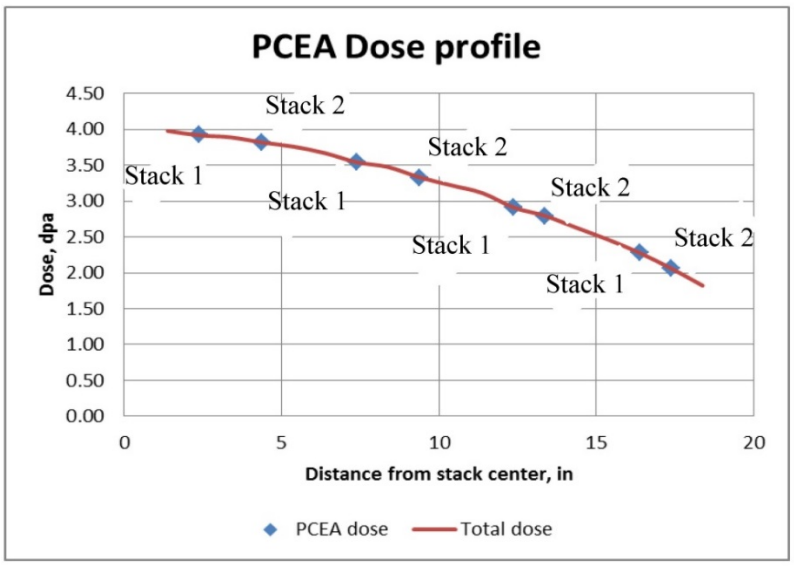

Figure 3. A typical dose profile for creep-graphite specimens using similar applied stress levels in matched stacks.

A final consideration when establishing the specimen-loading positions is the grain orientation of the specimens. For extruded-graphite grades, the against-grain (AG) and with-grain (WG) directions are obviously perpendicular and parallel to the extrusion direction, respectively. Isomolded grades have little to no grain direction, but these specimens were nonetheless machined at two distinct orientations. However, in the case of the vibration-molded graphite (i.e., NBG-17 and NBG-18), there are actually two WG directions and one AG direction as a consequence of the fabrication process. The total number of WG and AG specimens is dependent upon the particular AGC capsule pair (i.e., AGC-1 and AGC-2 have the same number of specimens with similar orientation).

Once these considerations are accounted for, the dose-level profiles are determined for each graphite grade within each channel stack. It should be noted that due to the elimination of the majority of the NBG-25 spacers from the AGC-1 design, the dose-level profiles for each graphite grade have been altered for the succeeding AGC capsules. However, the changes are modest, allowing nearly direct comparison between AGC-1 and the subsequent AGC capsules.

3. AGC-4 TEST TRAIN CAPSULE

Activities for AGC-4 began with the pre-irradiation characterization of all graphite samples to be inserted into the AGC-4 capsule. Following characterization, the samples were loaded into the AGC-4 capsule in the summer of 2009. The completed AGC-4 capsule was then inserted into the ATR east flux trap. The experiment was irradiated during ATR Cycles 157D, 158A, 162A, 162B, 164A, 164B, 166A, and 166B. ECAR-5345, "As-Run Physics Analysis for the AGC-4 Experiment Irradiated in the ATR," derived a cumulative received dose of approximately 8 dpa (Davenport 2019). The desired experiment average temperatures of 800°C were exceeded by at least 100°C during the second cycle of irradiation. It is presumed that the temperature excursion was due to unexpectedly high flux resulting from the insertion of the KiJang Research Reactor experiment in the northeast flux trap during the same irradiation cycle as AGC-4. After irradiation was completed, the capsule was removed from the ATR and transferred to the Materials and Fuels Complex Hot Fuels Examination Facility (HFEF) on May 15, 2020. The experiment was unloaded from the shipping cask into the HFEF decon cell through Penetration 2D on February 26, 2021. It was moved to the HFEF main cell Window 3M for disassembly on March 15, 2021. Disassembly and specimen extraction began March 18, 2021, and packaging of the graphite specimens into transfer tubes to be loaded into the shielded shipping drum was completed April 16, 2021. During preparations for shipping the samples to the INL Carbon Laboratory, it was observed that radiological dose rates of the packaged samples exceeded those measured for previous experiments by at least an order of magnitude.

3.1 AGC-4 Graphite Grades and Dimensions

The piggyback specimens in the AGC-4 capsule are smaller, button-size specimens that are approximately 12.5 mm × 6 mm. They are made of all the major grades of graphite. There were also two graphite-container-type specimens. One is 12.5 mm tall and the other is 6 mm tall. The 6 mm tall containers each held one HOPG specimen. The 12.5 mm tall containers each held a silicon-carbide-coated graphite hemisphere specimen fabricated at SIGRI GmbH Great Lakes to test for irradiation performance of SiC-coated graphite). Similar to the previous AGC-1, AGC-2 and AGC-3 experimental designs, most of the piggyback graphite specimens were irradiated in the unloaded center stack of AGC-4. All major-, piggyback-, and experimental-graphite grades are listed in Table 1.

Table 1. Graphite grades and grain orientations within AGC-4 capsule.

Grade	Specimen Type	Dimension	WG/AG
2114	Creep	Ø12.5 × 25.4 mm	48 WG/ 0 AG
NBG-17	Creep	Ø12.5 × 25.4 mm	18 WG/18 AG
NBG-18	Creep	Ø12.5 × 25.4 mm	24 WG/24 AG
IG-110	Creep	Ø12.5 × 25.4 mm	30 WG/12 AG
PCEA	Creep	Ø12.5 × 25.4 mm	36 WG/12 AG
2114	Piggyback	Ø12.5 × 6.3 mm	26 WG/0 AG
NBG-17	Piggyback	Ø12.5 × 6.3 mm	20 WG/6 AG
NBG-18	Piggyback	Ø12.5 × 6.3 mm	15 WG/11 AG
IG-110	Piggyback	Ø12.5 × 6.3 mm	16 WG/10 AG
PCEA	Piggyback	Ø12.5 × 6.3 mm	13 WG/10 AG
IG-430	Piggyback	Ø12.5 × 6.3 mm	9 WG/0 AG
NBG-25	Piggyback	Ø12.5 × 6.3 mm	22
A3 Matrix	Piggyback	Ø12.5 × 6.3 mm	18

3.2 AGC-4 Specimen Stack Positions

The final loading configuration for the outer channel and stacks was determined for each graphite grade to optimize the number of specimens for each grade, create a smooth irradiation profile for the creep and piggyback specimens, and assure the proper position of creep specimens to create the matched pairs. Table 2 lists the total number of specimens irradiated per major graphite grade.

The final loading configuration for the AGC-4 capsule is shown in Table 2 through Table 4. These tables also include the specimens' accumulated elevation within the capsule, channel number, and nominal load imposed on the specimens.

Table 2. Stack 1–3 loading order.

Stack 1			
Orient	ID#	Graphite	Height
AP	AP4801	NBG-17	19.500
	57	FLUX Wire	18.875
DW	DW4801	PCEA	18.250
BW	BW4301	NBG-18	17.250
EW	EW4801	IG-110	16.250
TW	TW4001	2114	15.250
DW	DW4803	PCEA	14.250
	A1	FLUX Wire	13.625
BP	BP4605	NBG-18	13.000
TW	TW4002	2114	12.000
EW	EW4802	IG-110	11.000
DW	DW4804	PCEA	10.000
BW	BW4302	NBG-18	9.000
TW	TW4003	2114	8.000
	1H	FLUX Wire	7.375
AP	AP4802	NBG-17	6.750
EW	EW4803	IG-110	5.750
DW	DW4901	PCEA	4.750
BL	BL3801	NBG-18	3.750
TW	TW4004	2114	2.750
	1R	FLUX Wire	2.125
AW	AW4801	NBG-17	1.500
SHUTTLE PISTON			0.000
Bottom of shuttle piston			-1.000
Bottom of 0.5" space			-1.500
TW	TW4005	2114 CRP	-2.000
FW	FW1707	IG-430 PB	-2.625
AW	AW4802	NBG-17	-3.250
	7J	FLUX Wire	-3.875
TW	TW4006	2114	-4.500
BL	BL3802	NBG-18	-5.500
DW	DW4902	PCEA	-6.500
EW	EW4804	IG-110	-7.500
AP	AP4803	NBG-17	-8.500
M	M0401	NBG-25 PB	-9.125
TW	TW4007	2114	-9.750
BW	BW4303	NBG-18	-10.750
DW	DW4903	PCEA	-11.750
EW	EW4901	IG-110	-12.750
TW	TW4008	2114	-13.750
BP	BP4202	NBG-18	-14.750
	7I	FLUX Wire	-15.375
DW	DW4904	PCEA	-16.000
TW	TW4009	2114	-17.000
EW	EW4902	IG-110	-18.000
BW	BW4401	NBG-18	-19.000
DW	DW5001	PCEA	-20.000
	8A	FLUX Wire	-20.625
AP	AP4804	NBG-17	-21.250
TW	TW4010	2114 CRP	-22.250
FW	FW1701	IG-430 PB	-22.875
	CAN121 -A	SIC-G	-23.250

Stack 2			
Orient	ID#	Graphite	Height
AP	AP4901	NBG-17	19.500
M	M0402	NBG-25 PB	18.875
DW	DW5002	PCEA	18.250
BW	BW4402	NBG-18	17.250
EW	EW4903	IG-110	16.250
TW	TW4101	2114	15.250
DW	DW5003	PCEA	14.250
	1I	FLUX Wire	13.625
BP	BP4203	NBG-18	13.000
TW	TW4102	2114	12.000
EW	EW4904	IG-110	11.000
DW	DW5004	PCEA	10.000
BW	BW4403	NBG-18	9.000
TW	TW4103	2114	8.000
M	M0403	NBG-25 PB	7.375
AP	AP4902	NBG-17	6.750
EW	EW5001	IG-110	5.750
DW	DW5101	PCEA	4.750
BL	BL3803	NBG-18	3.750
TW	TW4104	2114	2.750
	5Z	FLUX Wire	2.125
AW	AW4803	NBG-17	1.500
SHUTTLE PISTON			0.000
Bottom of shuttle piston			-1.000
Bottom of 0.5" space			-1.500
TW	TW4105	2114 CRP	-2.000
FW	FW1708	IG-430 PB	-2.625
AW	AW4804	NBG-17	-3.250
	M0404	NBG-25 PB	-3.875
TW	TW4106	2114	-4.500
BL	BL3804	NBG-18	-5.500
DW	DW5102	PCEA	-6.500
EW	EW5002	IG-110	-7.500
AP	AP4903	NBG-17	-8.500
M	M0405	NBG-25 PB	-9.125
TW	TW4107	2114	-9.750
BW	BW4501	NBG-18	-10.750
DW	DW5103	PCEA	-11.750
EW	EW5003	IG-110	-12.750
TW	TW4108	2114	-13.750
BP	BP4204	NBG-18	-14.750
	9E	FLUX Wire	-15.375
DW	DW5104	PCEA	-16.000
TW	TW4109	2114	-17.000
EW	EW5004	IG-110	-18.000
BW	BW4603	NBG-18	-19.000
DW	DW5201	PCEA	-20.000
M	M0406	NBG-25 PB	-20.625
AP	AP4904	NBG-17	-21.250
TW	TW4110	2114 CRP	-22.250
FW	FW1702	IG-430 PB	-22.875
	CAN122 -A	SIC-G	-23.250

Stack 3			
Orient	ID#	Graphite	Height
AP	AP5001	NBG-17	19.500
M	M0407	NBG-25 PB	18.875
DW	DW5202	PCEA	18.250
BW	BW4502	NBG-18	17.250
EW	EW5101	IG-110	16.250
TW	TW4201	2114	15.250
DW	DW5203	PCEA	14.250
	1B	FLUX Wire	13.625
BP	BP4205	NBG-18	13.000
TW	TW4202	2114	12.000
EW	EW5102	IG-110	11.000
DW	DW5204	PCEA	10.000
BW	BW4503	NBG-18	9.000
TW	TW4203	2114	8.000
M	M0408	NBG-25 PB	7.375
AP	AP5002	NBG-17	6.750
EW	EW5103	IG-110	5.750
DW	DW5301	PCEA	4.750
BL	BL3805	NBG-18	3.750
TW	TW4204	2114	2.750
	1Z	FLUX Wire	2.125
AW	AW4901	NBG-17	1.500
SHUTTLE PISTON			0.000
Bottom of shuttle piston			-1.000
Bottom of 0.5" space			-1.500
TW	TW4205	2114 CRP	-2.000
FW	FW1709	IG-430 PB	-2.625
AW	AW4902	NBG-17	-3.250
M	M0409	NBG-25 PB	-3.875
TW	TW4206	2114	-4.500
BL	BL3901	NBG-18	-5.500
DW	DW5302	PCEA	-6.500
EW	EW5104	IG-110	-7.500
AP	AP5003	NBG-17	-8.500
	8Y	FLUX Wire	-9.125
TW	TW4207	2114	-9.750
BW	BW4601	NBG-18	-10.750
DW	DW5303	PCEA	-11.750
EW	EW5201	IG-110	-12.750
TW	TW4208	2114	-13.750
BP	BP4301	NBG-18	-14.750
M	M0410	NBG-25 PB	-15.375
DW	DW5304	PCEA	-16.000
TW	TW4209	2114	-17.000
EW	EW5202	IG-110	-18.000
BW	BW4602	NBG-18	-19.000
DW	DW5401	PCEA	-20.000
M	M0411	NBG-25 PB	-20.625
AP	AP5004	NBG-17	-21.250
TW	TW4210	2114 CRP	-22.250
FW	FW1703	IG-430 PB	-22.875
	CAN123 -AG	SIC-G	-23.250

Table 3. Stack 4–6 loading order.

	Stack 4		
Orient	ID#	Graphite	Height
EW	EW5203	IG-110	19.500
	1E	FLUX Wire	18.875
TW	TW4301	2114	18.250
DA	DA3801	PCEA	17.250
BP	BP4302	NBG-18	16.250
AL	AL4801	NBG-17	15.250
EW	EW5204	IG-110	14.250
	8B	FLUX Wire	13.625
DW	DW5402	PCEA	13.000
BL	BL3902	NBG-18	12.000
TW	TW4302	2114	11.000
AW	AW4903	NBG-17	10.000
EA	EA4801	IG-110	9.000
DA	DA3802	PCEA	8.000
	8R	FLUX Wire	7.375
BP	BP4604	NBG-18	6.750
TW	TW4303	2114	5.750
AP	AP5101	NBG-17	4.750
EA	EA4802	IG-110	3.750
DW	DW5403	PCEA	2.750
	5L	FLUX Wire	2.125
BP	BP4303	NBG-18	1.500
SHUTTLE PISTON			0.000
Bottom of shuttle piston			-1.000
Bottom of 0.5" space			-1.500
AW	AW5801	NBG-17 PB	-1.625
EW	EW6301	IG-110 PB	-1.875
TW	TW4701	2114 PB	-2.125
BP	BP3910	NBG-18 PB	-2.375
FW	FW1704	IG-430 PB	-2.625
BP	BP4304	NBG-18	-3.250
	9F	FLUX Wire	-3.875
DW	DW5404	PCEA	-4.500
EA	EA5004	IG-110	-5.500
AP	AP5102	NBG-17	-6.500
TW	TW4304	2114	-7.500
BP	BP4305	NBG-18	-8.500
M	M0412	NBG-25 PB	-9.125
DA	DA3803	PCEA	-9.750
EA	EA4803	IG-110	-10.750
AW	AW4904	NBG-17	-11.750
TW	TW4305	2114	-12.750
BL	BL3903	NBG-18	-13.750
DW	DW5501	PCEA	-14.750
	5R	FLUX Wire	-15.375
EW	EW5302	IG-110	-16.000
AL	AL4802	NBG-17	-17.000
BP	BP4401	NBG-18	-18.000
DA	DA3804	PCEA	-19.000
TW	TW4306	2114	-20.000
	2A	FLUX Wire	-20.625
EW	EW5303	IG-110	-21.250
BL	BL4601	NBG-18 PB	-21.875
AL	AL5801	NBG-17 PB	-22.125
EW	EW6302	IG-110 PB	-22.375
TW	TW4702	2114 PB	-22.625
DW	DW6201	PCEA PB	-22.875
	CAN124 -A0	SIC-G	-23.250

	Stack 5		
Orient	ID#	Graphite	Height
EW	EW5304	IG-110	19.500
M	M0301	NBG-25 PB	18.875
TW	TW4307	2114	18.250
DA	DA3901	PCEA	17.250
BP	BP4402	NBG-18	16.250
AL	AL4803	NBG-17	15.250
EW	EW5401	IG-110	14.250
	10	FLUX Wire	13.625
DW	DW5502	PCEA	13.000
BL	BL3904	NBG-18	12.000
TW	TW4308	2114	11.000
AW	AW5001	NBG-17	10.000
EA	EA4804	IG-110	9.000
DA	DA3902	PCEA	8.000
M	M0302	NBG-25 PB	7.375
BP	BP4403	NBG-18	6.750
TW	TW4309	2114	5.750
AP	AP5103	NBG-17	4.750
EA	EA4901	IG-110	3.750
DW	DW5503	PCEA	2.750
	7F	FLUX Wire	2.125
BP	BP4404	NBG-18	1.500
SHUTTLE PISTON			0.000
Bottom of shuttle piston			-1.000
Bottom of 0.5" space			-1.500
AW	AW5802	NBG-17 PB	-1.625
EW	EW6303	IG-110 PB	-1.875
TW	TW4703	2114 PB	-2.125
BP	BP3911	NBG-18 PB	-2.375
FW	FW1705	IG-430 PB	-2.625
BP	BP4405	NBG-18	-3.250
M	M0303	NBG-25 PB	-3.875
DW	DW5504	PCEA	-4.500
EA	EA4902	IG-110	-5.500
AP	AP5104	NBG-17	-6.500
TW	TW4310	2114	-7.500
BP	BP4501	NBG-18	-8.500
M	M0304	NBG-25 PB	-9.125
DA	DA3903	PCEA	-9.750
EA	EA4903	IG-110	-10.750
AW	AW5002	NBG-17	-11.750
TW	TW4401	2114	-12.750
BL	BL3905	NBG-18	-13.750
DW	DW5601	PCEA	-14.750
	7E	FLUX Wire	-15.375
EW	EW5402	IG-110	-16.000
AL	AL4804	NBG-17	-17.000
BP	BP4502	NBG-18	-18.000
DA	DA3904	PCEA	-19.000
TW	TW4402	2114	-20.000
M	M0305	NBG-25 PB	-20.625
EW	EW5403	IG-110	-21.250
BL	BL4602	NBG-18 PB	-21.875
AL	AL5802	NBG-17 PB	-22.125
EW	EW6304	IG-110 PB	-22.375
TW	TW4704	2114 PB	-22.625
DW	DW6202	PCEA PB	-22.875
	CAN125 -AG0	SIC-G	-23.250

	Stack 6		
Orient	ID#	Graphite	Height
EW	EW5404	IG-110	19.500
M	M0306	NBG-25 PB	18.875
TW	TW4403	2114	18.250
DA	DA4001	PCEA	17.250
BP	BP4503	NBG-18	16.250
AL	AL4901	NBG-17	15.250
EW	EW5501	IG-110	14.250
	2L	FLUX Wire	13.625
DW	DW5602	PCEA	13.000
BL	BL4001	NBG-18	12.000
TW	TW4404	2114	11.000
AW	AW5003	NBG-17	10.000
EA	EA4904	IG-110	9.000
DA	DA4002	PCEA	8.000
M	M0307	NBG-25 PB	7.375
BP	BP4504	NBG-18	6.750
TW	TW4405	2114	5.750
AP	AP5201	NBG-17	4.750
EA	EA5001	IG-110	3.750
DW	DW5603	PCEA	2.750
	8F	FLUX Wire	2.125
BP	BP4505	NBG-18	1.500
SHUTTLE PISTON			0.000
Bottom of shuttle piston			-1.000
Bottom of 0.5" space			-1.500
AW	AW5803	NBG-17 PB	-1.625
EW	EW6305	IG-110 PB	-1.875
TW	TW4705	2114 PB	-2.125
BP	BP3912	NBG-18 PB	-2.375
FW	FW1706	IG-430 PB	-2.625
BP	BP4601	NBG-18	-3.250
	M0308	NBG-25 PB	-3.875
DW	DW5604	PCEA	-4.500
EA	EA5002	IG-110	-5.500
AP	AP5202	NBG-17	-6.500
TW	TW4406	2114	-7.500
BP	BP4602	NBG-18	-8.500
	87	FLUX Wire	-9.125
DA	DA4003	PCEA	-9.750
EA	EA5003	IG-110	-10.750
AW	AW5004	NBG-17	-11.750
TW	TW4407	2114	-12.750
BL	BL4002	NBG-18	-13.750
DW	DW5701	PCEA	-14.750
M	M0309	NBG-25 PB	-15.375
EW	EW5502	IG-110	-16.000
AL	AL4902	NBG-17	-17.000
BP	BP4603	NBG-18	-18.000
DA	DA4004	PCEA	-19.000
TW	TW4408	2114	-20.000
M	M0310	NBG-25 PB	-20.625
EW	EW5503	IG-110	-21.250
BL	BL4603	NBG-18 PB	-21.875
AL	AL5803	NBG-17 PB	-22.125
EW	EW6306	IG-110 PB	-22.375
TW	TW4706	2114 PB	-22.625
DW	DW6203	PCEA PB	-22.875
	CAN126 -AGC4	SIC-G	-23.250

Table 4. Center-stack loading order.

Center Channel		
Orient	ID#	Height
SIC-G	CAN127 -AGC4	
SIC-G	CAN128 -AGC4	
NBG-18-A	BP3901	
NBG-17-A	AL5804	
IG-110-A	EA6301	
2114-A	TW4707	2
PCEA-A	DA4801	
HOPG	CAN101 -AGC4	
C/C	CAN131 -AGC4	3
NBG-18-W	BW5701	
NBG-17-W	AW5804	
IG-110-W	EW6405	
2114-W	TW4708	4
PCEA-W	DW6301	
A3-27	Z-1	
HOPG	CAN102 -AGC4	
NBG-18-A	BP3902	5
NBG-17-A	AP5801	
IG-110-A	EA6303	
2114-A	TW4709	
PCEA-A	DA4803	6
A3-27	Z-2	
HOPG	CAN103 -AGC4	
C/C	CAN132 -AGC4	7
NBG-18-W	BW5702	
NBG-17-W	AW5805	
IG-110-W	EW6307	
2114-W	TW4710	8
PCEA-W	DW6204	
A3-27	Z-3	
HOPG	CAN104 -AGC4	
NBG-18-A	BW5703	9
NBG-17-A	AP5802	
IG-110-A	EA6304	
2114-A	TW4711	
PCEA-A	DA4804	10
A3-27	Z-4	
HOPG	CAN105 -AGC4	
C/C	CAN133 -AGC4	11
NBG-18-W	BW5803	
NBG-17-W	AP5803	
IG-110-W	EW6308	
2114-W	TW4712	12
PCEA-W	DW6205	
A3-27	Z-5	
HOPG	CAN106 -AGC4	
NBG-18-A	BP3904	13
NBG-17-A	AL5805	
IG-110-A	EA6305	
2114-A	TW4713	
PCEA-A	DA4805	14
A3-27	Z-6	
HOPG	CAN107 -AGC4	
C/C	CAN134 -AGC4	15
NBG-18-A	BW5704	
NBG-17-A	AP5804	
IG-110-A	EA6306	
2114-A	TW4714	16
PCEA-A	DA4806	
A3-27	Z-7	
HOPG	CAN108 -AGC4	
NBG-18-W	BW5705	17
NBG-17-W	AW5806	
IG-110-W	EW6309	
2114-W	TW4715	
PCEA-W	DW6206	18
A3-27	Z-8	
HOPG	CAN109 -AGC4	
C/C	CAN135 -AGC4	19
NBG-18-A	BP3905	
NBG-17-A	AW5807	
IG-110-A	EA6311	
2114-A	TW4716	20
PCEA-A	DA4807	
A3-27	Z-9	
HOPG	CAN110 -AGC4	
C/C	CAN136 -AGC4	21.25
NBG-18-W	BW5706	
NBG-17-W	AW5808	
IG-110-W	EW6311	
2114-W	TW4717	
PCEA-W	DW6207	
A3-27	Z-10	
HOPG	CAN111 -AGC4	
C/C	CAN137 -AGC4	23.5
NBG-18-A	BP3906	
NBG-17-A	AP5805	
IG-110-A	EA6307	
2114-A	TW4718	
PCEA-A	DA4808	
A3-27	Z-11	
HOPG	CAN112 -AGC4	
NBG-18-A	BP3907	25.5
NBG-17-A	AW5809	
IG-110-A	EA6308	
2114-A	TW4719	
PCEA-A	DA4809	
A3-27	Z-12	
HOPG	CAN113 -AGC4	
C/C	CAN138 -AGC4	27.5
NBG-18-W	BW5707	
NBG-17-W	AW5810	
IG-110-W	EW6312	
2114-W	TW4720	
PCEA-W	DW6208	
A3-27	Z-13	
HOPG	CAN114 -AGC4	
NBG-18-A	BP3908	29.5
NBG-17-A	AL5806	
IG-110-A	EA6309	
2114-A	TW4721	
PCEA-A	DA4810	
A3-27	Z-14	
HOPG	CAN115 -AGC4	
C/C	CAN139 -AGC4	31.5
NBG-18-W	BW5708	
NBG-17-W	AW5811	
IG-110-W	EW6401	
2114-W	TW4722	
PCEA-W	DW6209	
A3-27	Z-15	
HOPG	CAN116 -AGC4	
NBG-18-W	BP3909	33.5
NBG-17-W	AW5812	
IG-110-W	EW6402	
2114-W	TW4723	
PCEA-W	DW6210	
A3-27	Z-16	
HOPG	CAN117 -AGC4	
C/C	CAN140 -AGC4	35.5
NBG-18-W	BW5801	
NBG-17-W	AW5901	
IG-110-W	EW6403	
2114-W	TW4724	
PCEA-W	DW6211	
A3-27	Z-17	
HOPG	CAN118 -AGC4	
NBG-18-W	BW5802	37.5
NBG-17-W	AW5902	
IG-110-W	EW6404	
2114-W	TW4725	
PCEA-W	DW6212	
A3-27	Z-18	
HOPG	CAN119 -AGC4	
C/C	CAN141 -AGC4	39.5
NBG-18-A	BL4604	
NBG-17-A	AP5806	
IG-110-A	EA6310	
2114-A	TW4726	
PCEA-A	DA4812	
HOPG	CAN120 -AGC4	
C/C	CAN142 -AGC4	41.5
SIC-G	CAN129 -AGC4	
SIC-G	CAN130 -AGC4	42.5

4. TESTING

A significant level of preparation was needed to meet the NQA-1 quality requirements prior to actual material-property testing. An approved characterization plan was developed that was dependent upon the two graphite-specimen geometries and on the material properties to be measured. In general, all testing was performed through American Society for Testing and Materials (ASTM)-approved standards; however, due to the small size of the graphite specimens, some methods required modification and/or variation of the testing standards. Details of these testing-standard variations, along with equipment calibration, personnel training on testing methodology, and data acquisition, are specified in the characterization plans.

Electrical-resistivity, elastic-modulus, mass, and dimensional measurements have been performed on the AGC-4 irradiated specimens at this point. These measurements were performed per the AGC-4 graphite specimen post-irradiation characterization plan. This plan describes in detail the measurement techniques, equipment, and standards used to gather the data presented here.

Data gathered for the characterization of AGC-4 specimens are contained in the appendixes of this report. Appendix A, Data Plots, contains plots of the individual data points for each specimen. The upper and lower limits of the interquartile range (IQR) are shown by the dashed lines in each plot. These limits are established by either the least or greatest value in the data or by multiplying the IQR by 1.5 and adding or subtracting this value from the third and first quartile. Any datum value outside of these established limits is considered a suspected outlier of the established pattern and may indicate a mistaken measurement test or calculated value. Any sample exhibiting a measured data point outside of the established pattern is reassessed, including retesting the specific material-property value, to ascertain whether the sample was tested correctly. It is important to note that the analysis of these outlying values is not meant to determine the changes due to irradiation - i.e., variations resulting from different grades, received dose, temperature, orientation, and/or applied stress. A complete analysis addressing the irradiation conditions will be provided in a future data analysis report.

These outlying values are examined in the context of the entire data set, including pre-irradiation data. Other statistical parameters are calculated and presented in the tables of Appendix B, Statistical Tables. The mean, standard deviation, and coefficient of variance (COV) are all calculated for the various measurement data sets and graphite types. Upper and lower limits displayed in the tables of Appendix B are the IQR limits described above. Raw, tabulated data can be found in the Nuclear Data Management and Analysis System Database, including parameters specified by the applicable ASTM standard (e.g., dates, performer identifier, and laboratory conditions).

There are many ways to compare the data presented here. In doing so, the validity of the test data is exercised and scrutinized. First, the data sets are evaluated independently, using the statistical analysis described above. Additionally, a limited comparison of pre- and post-irradiation values is made for each graphite grade to show the effects of irradiation and applied stress (where applicable). Note that pre-irradiation properties were measured using the same techniques, equipment, and standards per PLN-4239, “AGC-4 Graphite Specimen Preirradiation Characterization Plan” (Matthews 2012). Pre-irradiation data for the AGC-4 specimens can be found in INL/EXT-16-38044, “AGC-4 Graphite Pre-Irradiation Data Analysis Report” (May 2016). These initial comparisons provide an initial examination of the data for trends and correlations that are intuitive and logical. In this way, the physical and thermal post-irradiation property measurements are vetted.

The data presented in this report include testing from all irradiated AGC-4 graphite specimens currently located at the INL Carbon Characterization Laboratory. Variables of irradiation, grain orientation, and temperature are not considered for any property measurement in Figure 5 through Figure 9 or for the figures in Appendix A. The data are presented simply to illustrate the measured material-property trends for the major-graphite grades in AGC-4. It should be noted that the averaged data show significant spread across all material-property measurements. This is expected because the data include measurements from all samples and do not differentiate between the effects of irradiation dose, temperature variations, graphite grades, orientation, or the other factors being tested in the AGC experiment. A more-detailed analysis, taking all test variables into consideration, will be reported in the subsequent AGC-4 data analysis reports.

4.1 Dimensions, Mass, and Density

Specimens are weighed and dimensionally measured at room temperature. Plots of the measured dimensions, mass, and densities for all AGC-4 irradiated specimens are shown in Appendix A, Figure A-1 through Figure A-48. Prior to irradiation, the freshly machined surfaces produced consistent dimensional measurements with a COV of less than 0.05% for all specimens. Following irradiation, the surfaces are more irregular and inconsistent. Figure 4 through Figure 11 show the dimensional measurements as well as mass and density of the irradiated specimens.

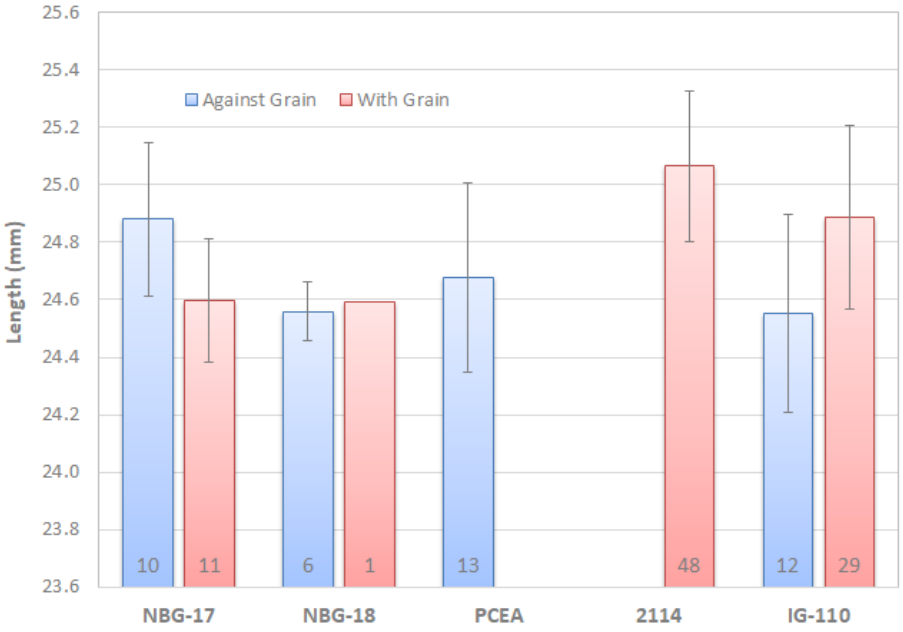

Figure 4. Creep-specimen-length averages.

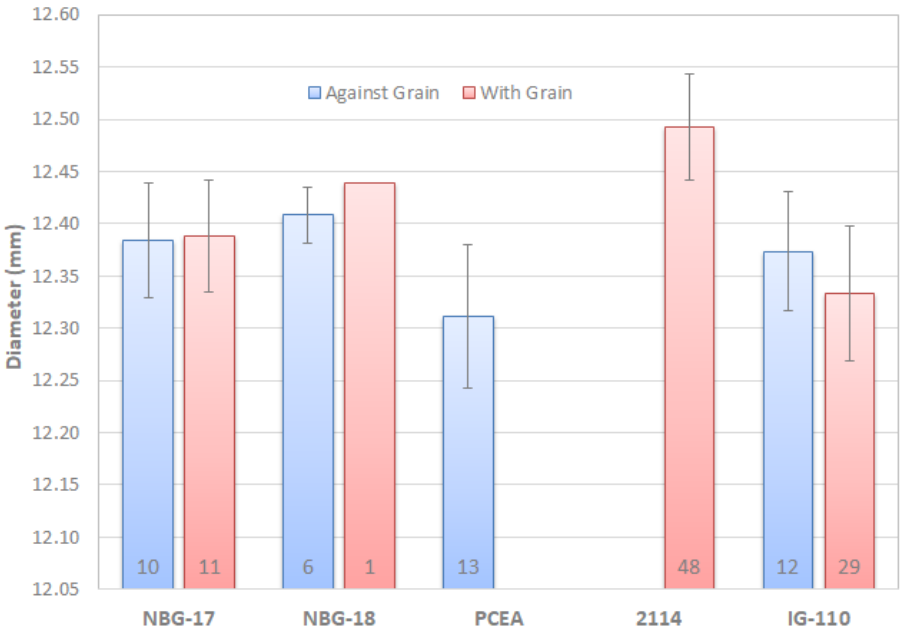

Figure 5. Creep-specimen-diameter averages.

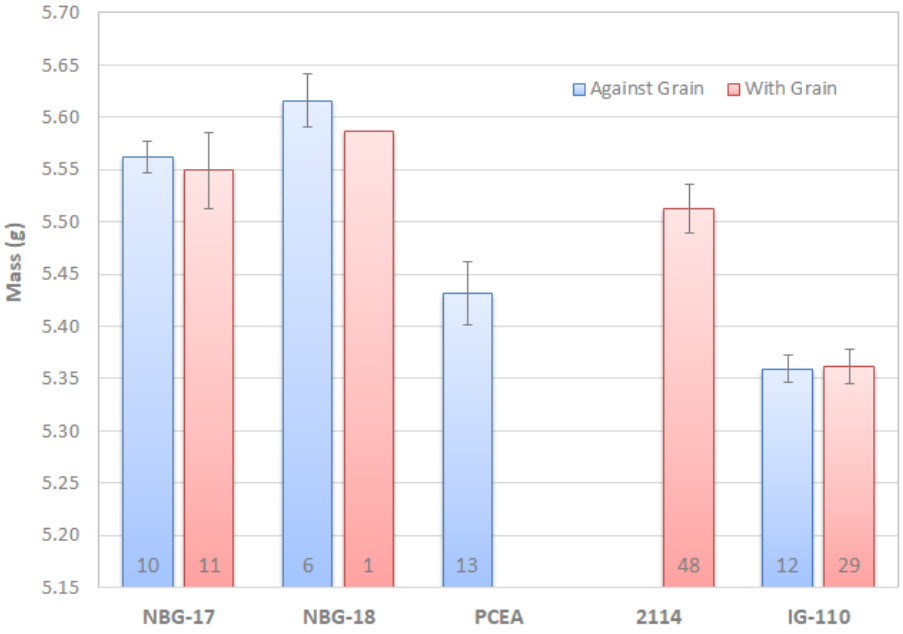

Figure 6. Creep specimen mass averages.

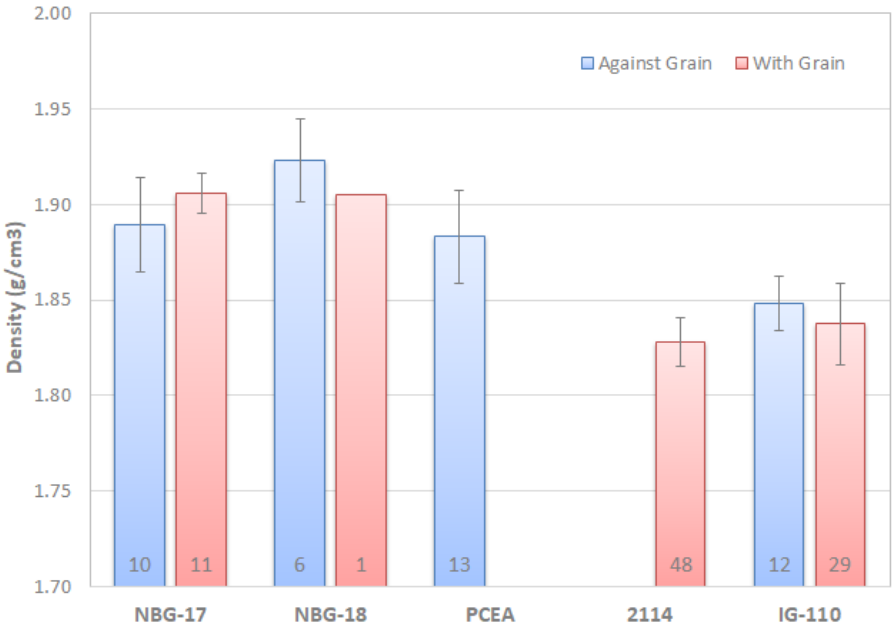

Figure 7. Creep-specimen-density averages.

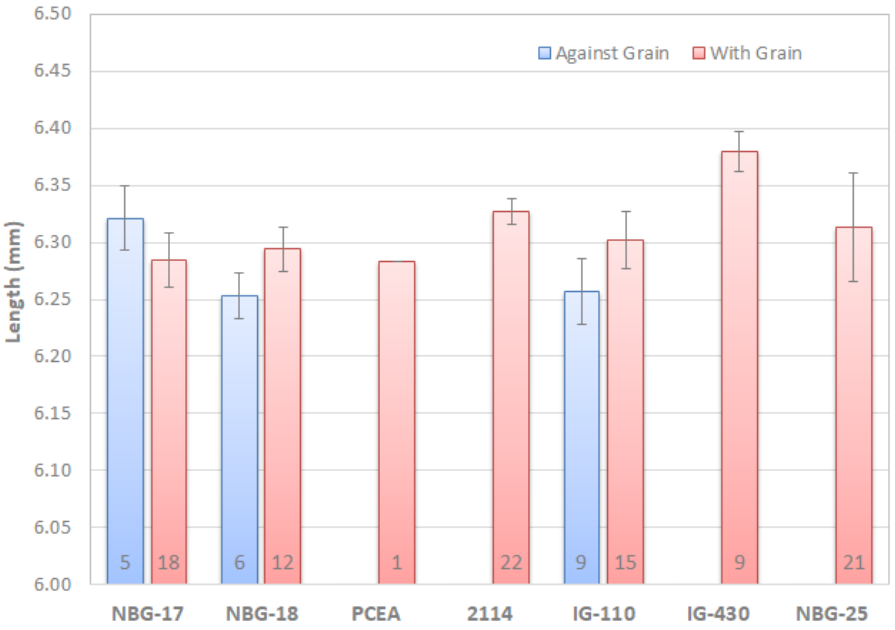

Figure 8. Piggyback-specimen-length averages.

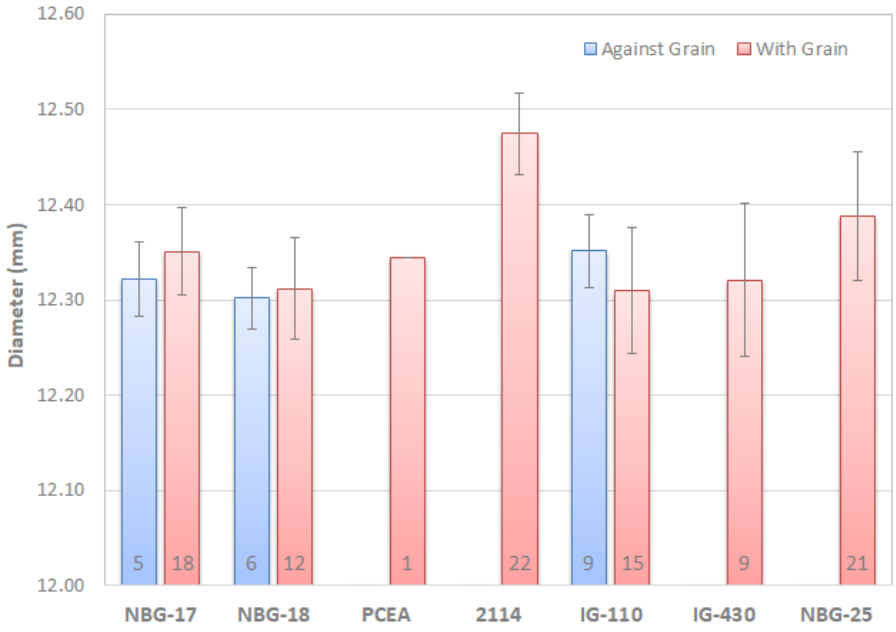

Figure 9. Piggyback-specimen-diameter averages.

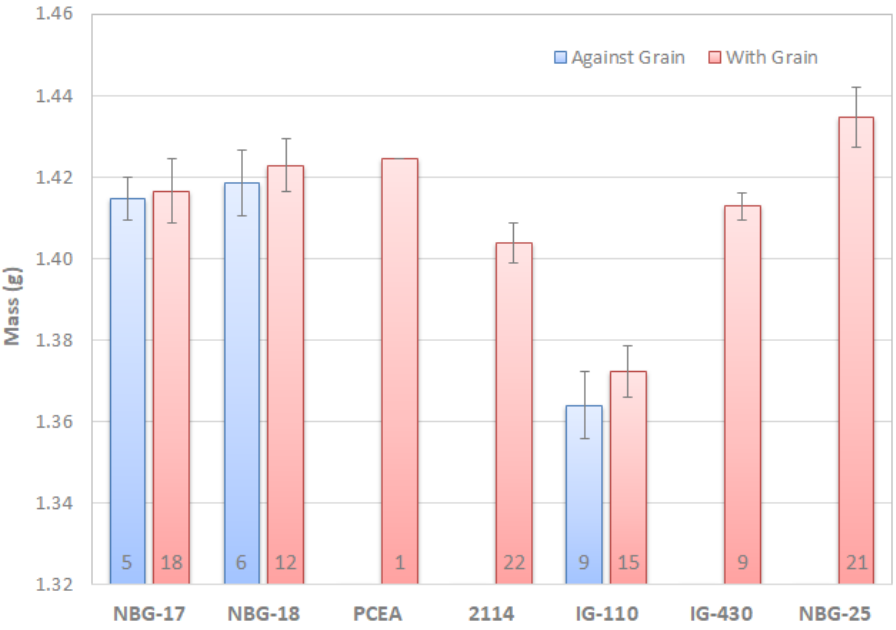

Figure 10. Piggyback-specimen-mass averages.

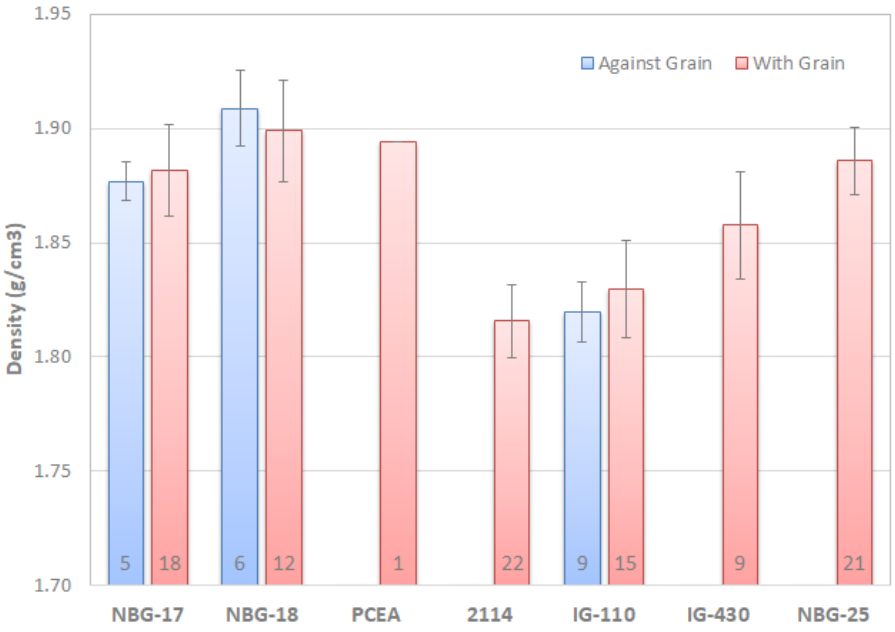

Figure 11. Piggyback-specimen-density averages.

4.2 Elastic Modulus

Elastic properties were measured with two dynamic nondestructive-testing techniques at room temperature (ASTM 2009) (ASTM 2005) (ASTM 2008) (ASTM 2010). In the fundamental-frequency testing technique, Young's modulus is derived from the natural frequency of the creep specimens oscilating in the flexural mode. Due to the geometry of the specimens, the shear modulus cannot be determined using this technique. However, both Young's modulus and shear modulus can be determined using the sonic-velocity technique. In this case, an ultrasonic longitudinal or shear wave is sent through the specimen. The time it takes for this wave to pass through the specimen and the length of the specimen are used to determine the sonic velocity. Young's modulus and shear modulus can then be calculated from this time-of-flight measurement.

Elastic and shear modulus, determined by measurement of fundamental frequency and sonic resonance, are plotted below in Figures 12 through 14 and the statistical data are contained in Appendix B Table B-5, Table B-7, and Table B-8.

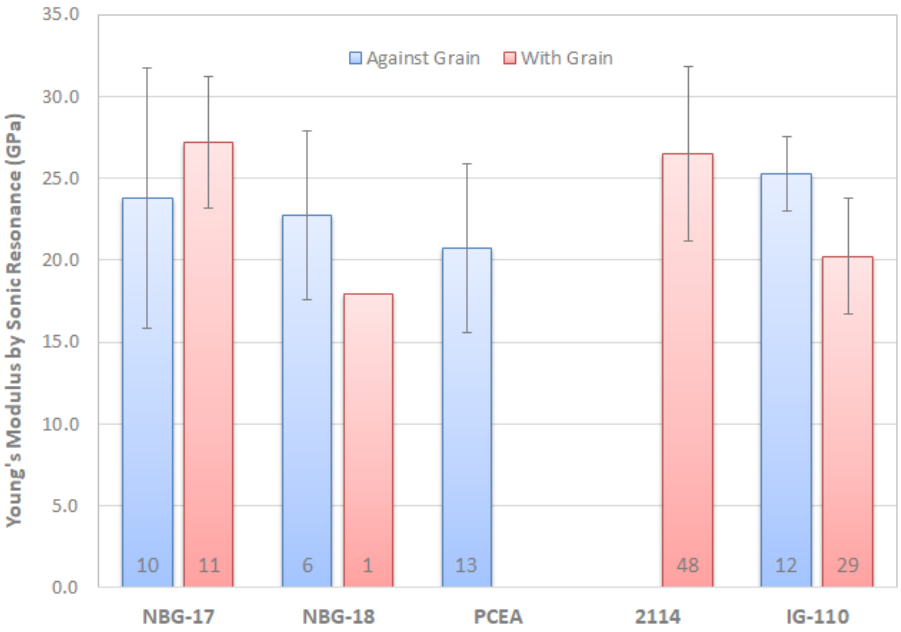

Figure 12. Creep-specimen Young's modulus by sonic resonance averages.

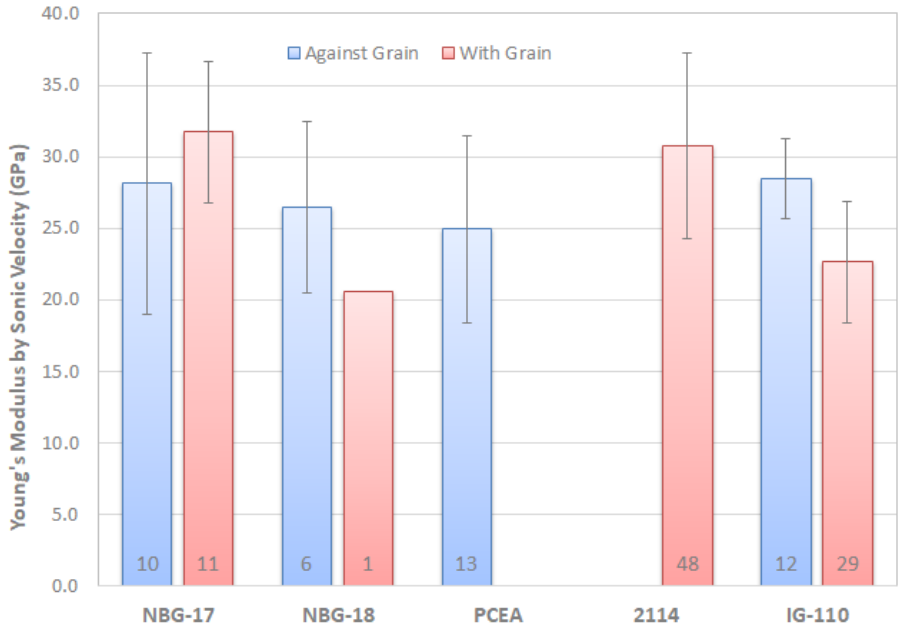

Figure 13. Creep-specimen Young's modulus by sonic velocity averages.

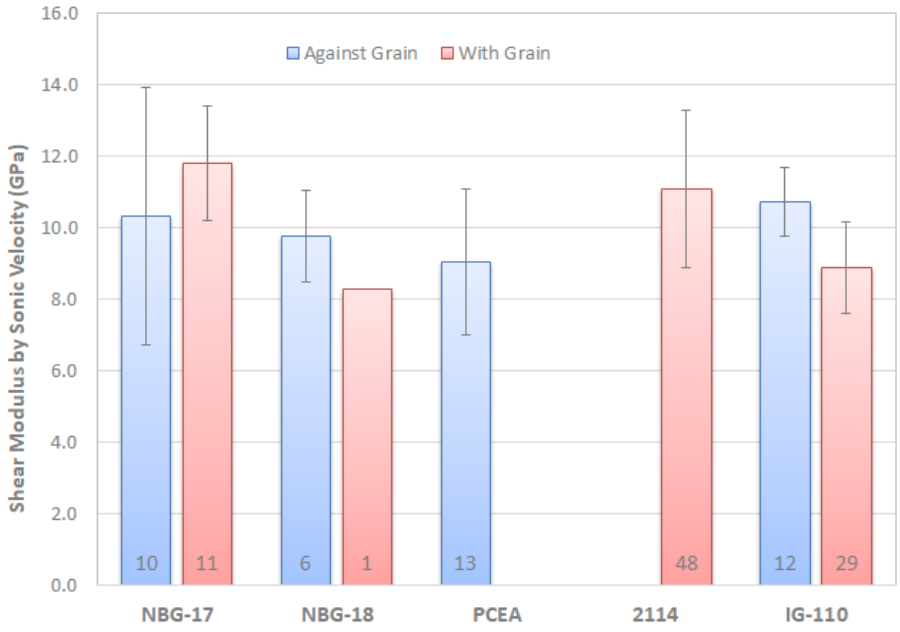

Figure 14. Creep-specimen shear modulus by sonic velocity averages.

4.3 Resistivity

Plots of electrical resistivity are shown in Appendix A, Figure A-54 through Figure A-58, for graphite grades of 2114, IG-110, NBG-17, NBG-18, and PCEA. Resistivity measurements were performed on the longer creep specimens only. Statistical parameters can be found in Appendix B, Table B-6. The resistivity data are well behaved, with only one 2114-specimen outlier and one PCEA-specimen outlier. A closer look at the resistance measurements showed that these specimens had consistent, but either high or low resistance values. Because these measurements were stable, the final resistivity values are included in the data.

Specimen resistivity is measured at room temperature using a four-point testing method. A constant current is passed through the long axis of the specimen, and the voltage is measured at a fixed distance along the specimen axis. Resistivity is calculated from these values and the specimen geometry. Figure 15 shows the average resistivity measurements Detailed electrical resistivity analysis, including irradiation dose and irradiation temperature effects, will be addressed in the subsequent AGC-4 data-analysis report.

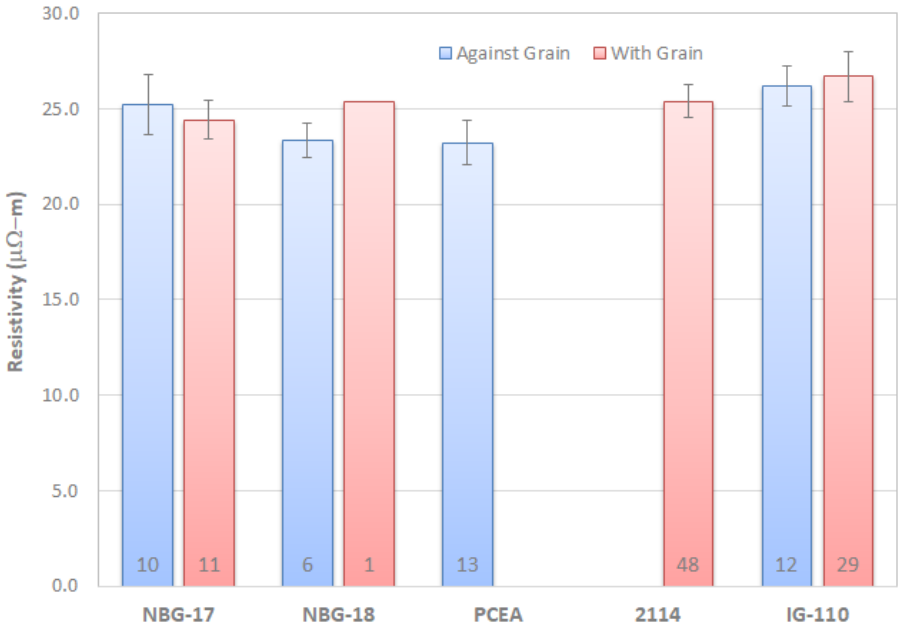

Figure 15. Creep-specimen resistivity averages.

5. REFERENCES

ASME. 2009. "Quality Assurance Requirements for Nuclear Facility Applications." NQA-1 2008/1a-2009. American Society of Mechanical Engineers.

ASTM. 2009. "Standard Test Method for Sonic Velocity in Manufactured Carbon and Graphite Materials for Use in Obtaining Young's Modulus." ASTM-769-09. American Society for Testing and Materials International. 2009.

ASTM 2005. "Standard Test Method for Sonic Velocity in Manufactured Carbon and Graphite Materials for Use in Obtaining Young's Modulus." ASTM-769-98. American Society for Testing and Materials International. 2005.

ASTM. 2008. "Dynamic Young's Modulus, Shear Modulus, and Poisson's Ratio for Advanced Ceramics by Impulse Excitation of Vibration." ASTM-C1259-08. American Society for Testing and Materials International. 2008.

ASTM. 2010. "Standard Test Method of Moduli of Elasticity and Fundamental Frequencies of Carbon and Graphite Materials by Sonic Resonance." ASTM-C747-93. American Society for Testing and Materials International. 2010.

Bratton, R. L. 2005. *NGNP Graphite Testing and Qualification Specimen Selection Strategy.* INL/EXT 05 00269, Idaho National Laboratory. May 2005.

Brown, B. J. 1969. "Constant stress irradiation creep experiments on graphite in Br 2." *Carbon* 7, no. 4. August 1969: 489–497.

Burchell, T. 2005. *Graphite Irradiation Creep Capsule AGC 1 Experimental Plan.* ORNL/TM 2005/505. Oak Ridge National Laboratory. 2005.

Burchell, T. 2007. *NGNP Graphite Selection and Acquisition Strategy.* ORLN/TM-2007/153. Oak Ridge National Laboratory. September 2007.

Davenport, M. 2019. "As-Run Physics Analysis for the AGC-4 Experiment Irradiated in the ATR." ECAR-5345. Idaho National Laboratory. November 2019.

Gray, W. J. 1973. "Constant stress irradiation-induced compressive creep of graphite at high fluences." *Carbon 11*, no. 4. August 1973: 387–392.

Matthews, A. 2012. “AGC-4 Graphite Specimen Preirradation Characterization Plan.” PLN-4239. Idaho National Laboratory. August 30, 2012.
Windes, W. 2010. “Graphite Technology Development Plan.” PLN-2497. Idaho National Laboratory. October 04, 2010.
Winston, P. 2023. *AGC-4 Disassembly Report.* INL/EXT-21-63591. Idaho National Laboratory.October 2023.

Page intentionally left blank

Appendix A

Data Plots

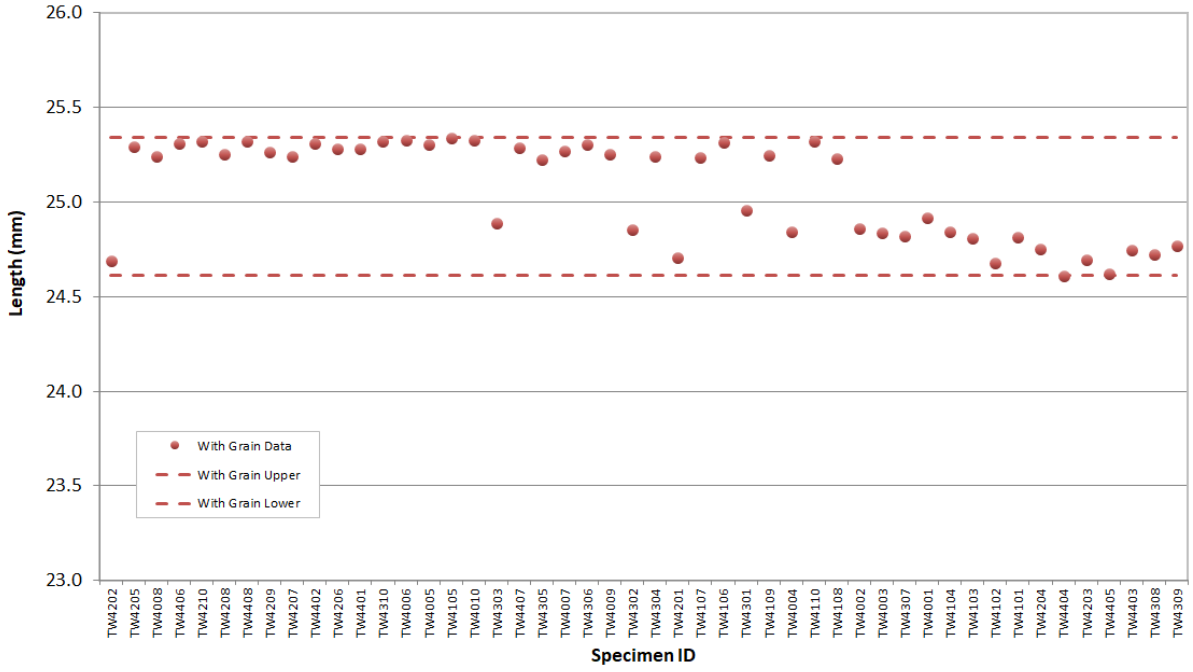

Figure A-1. 2114 creep length.

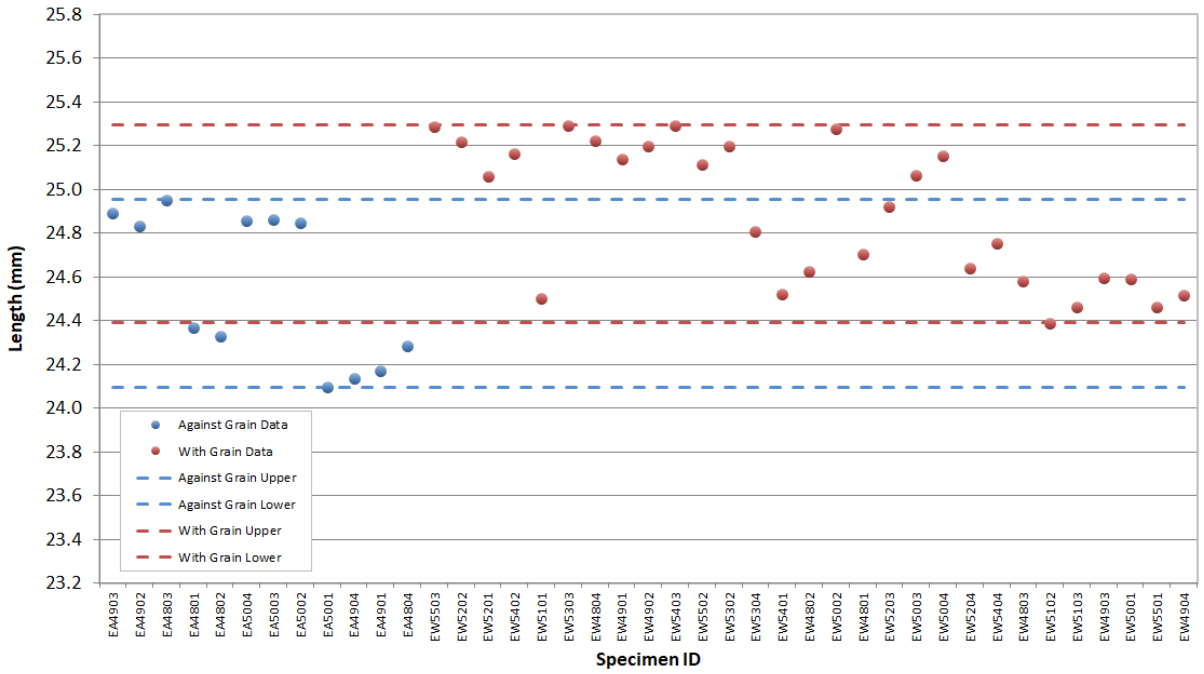

Figure A-2. IG-110 creep length.

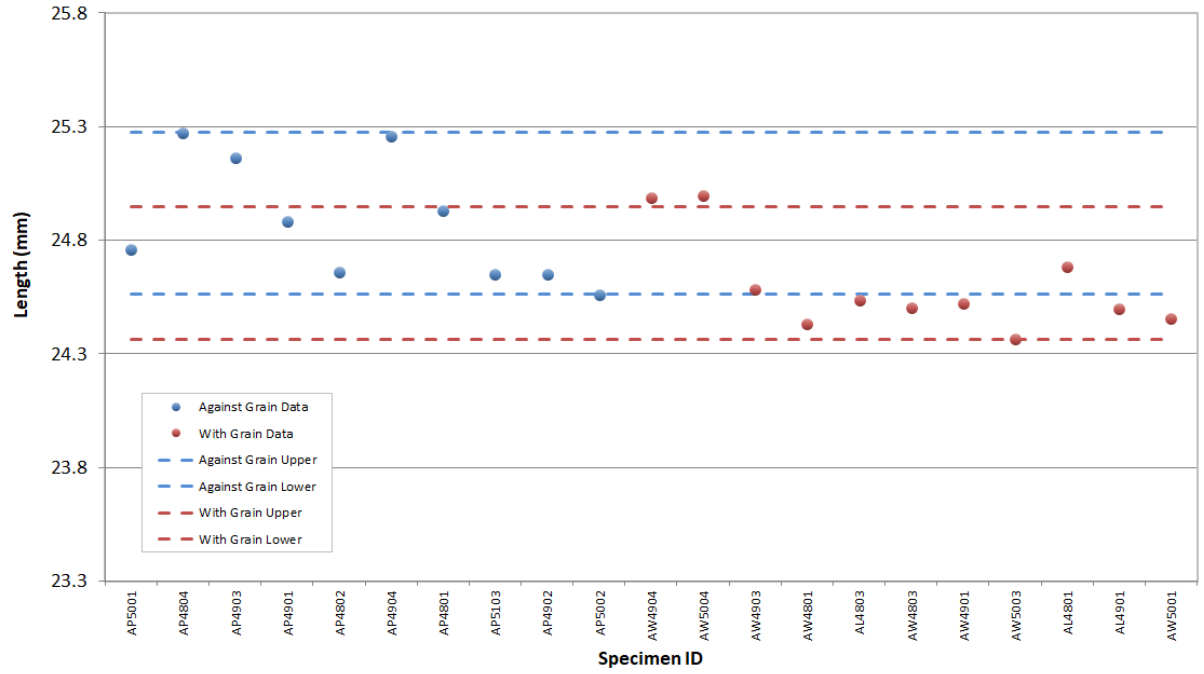

Figure A-3. NBG-17 creep length.

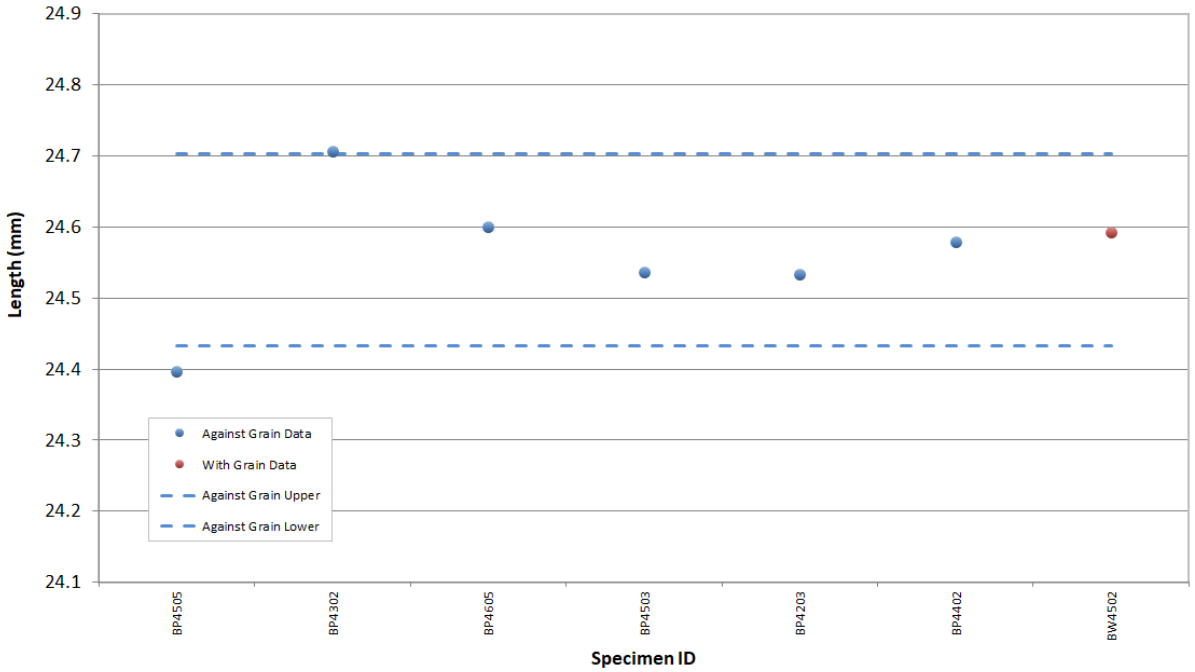

Figure A-4. NBG-18 creep length.

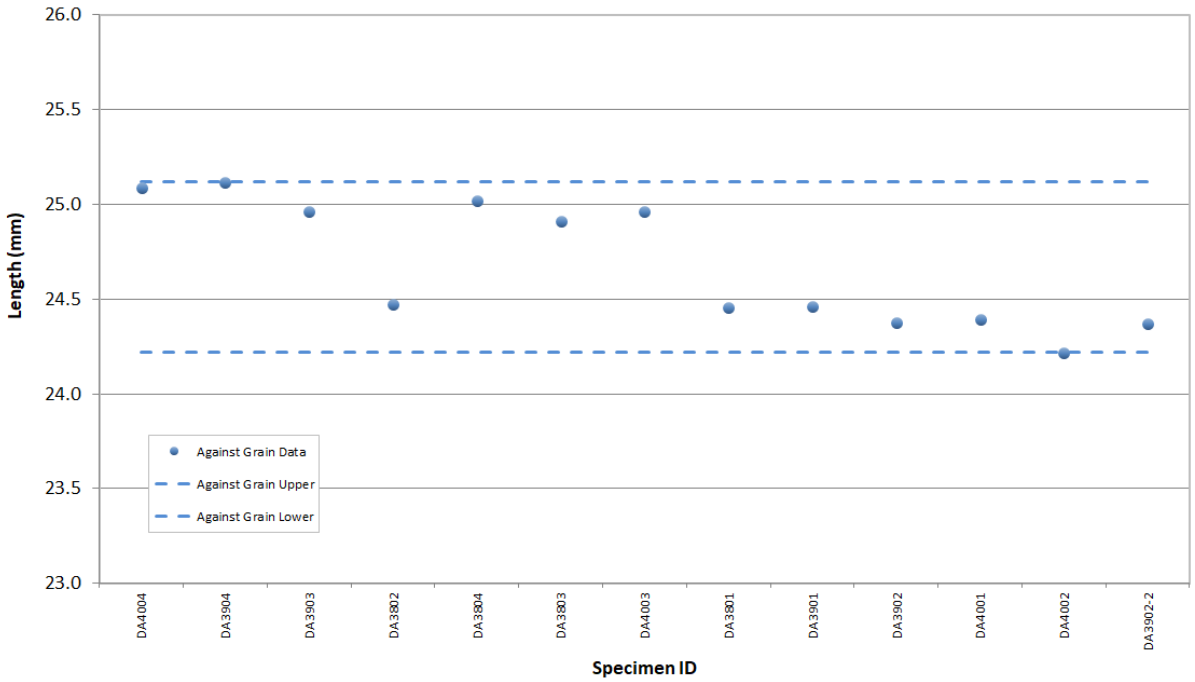

Figure A-5. PCEA creep length.

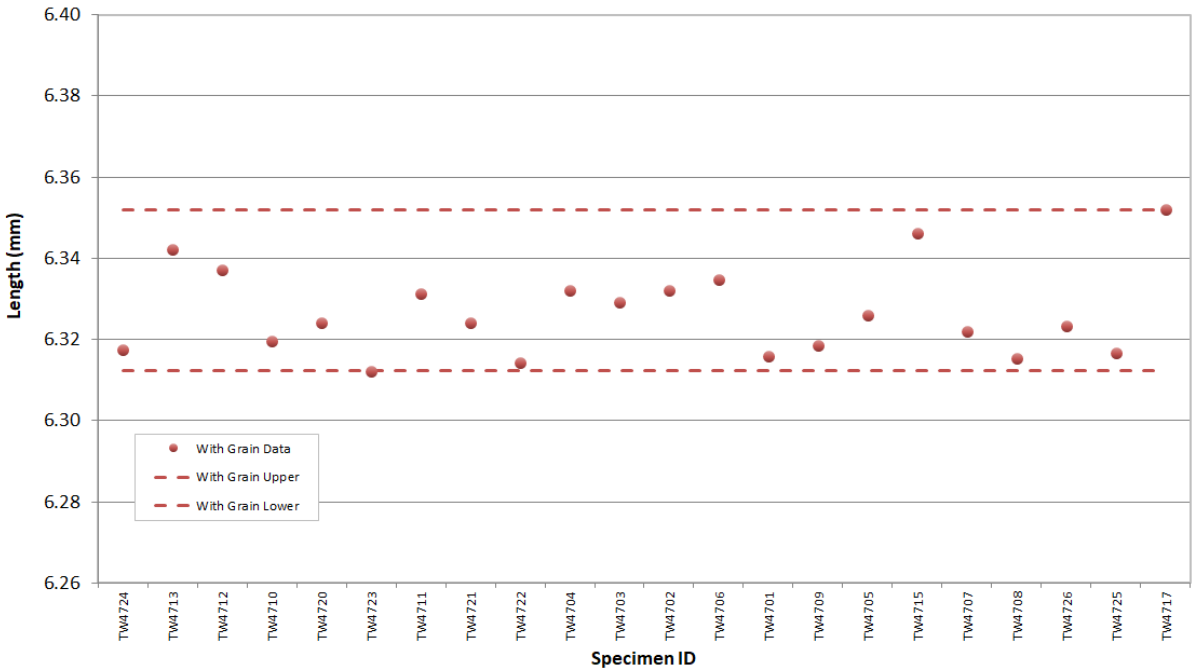

Figure A-6. 2114 piggyback length.

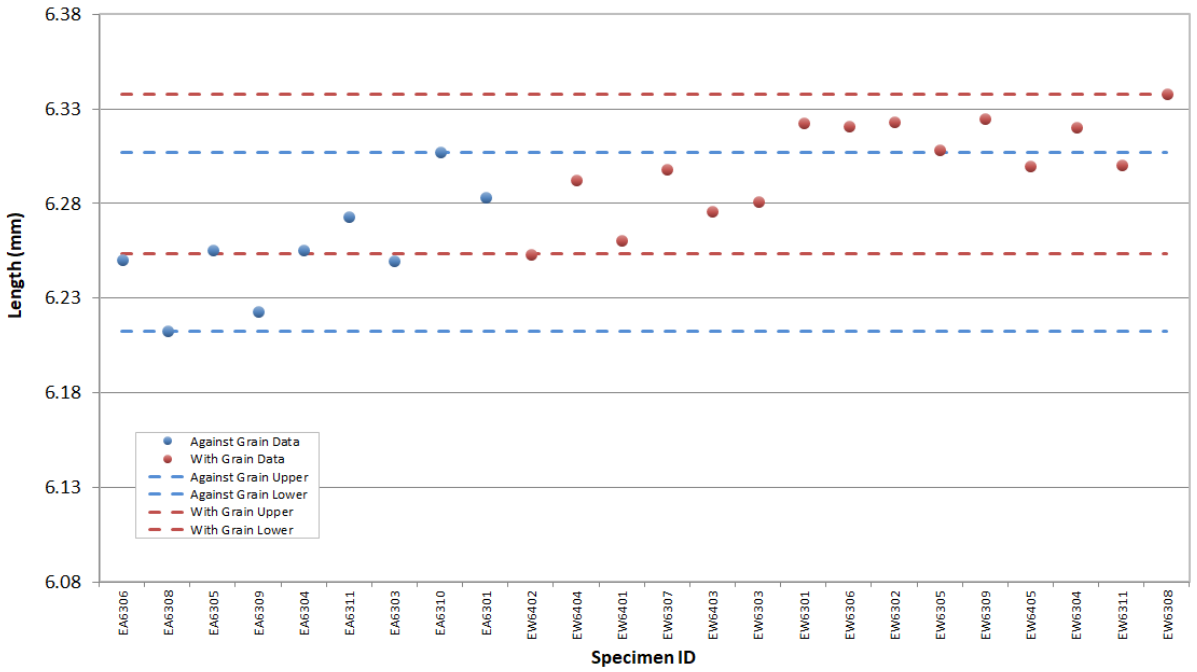

Figure A-7. IG-110 piggyback length.

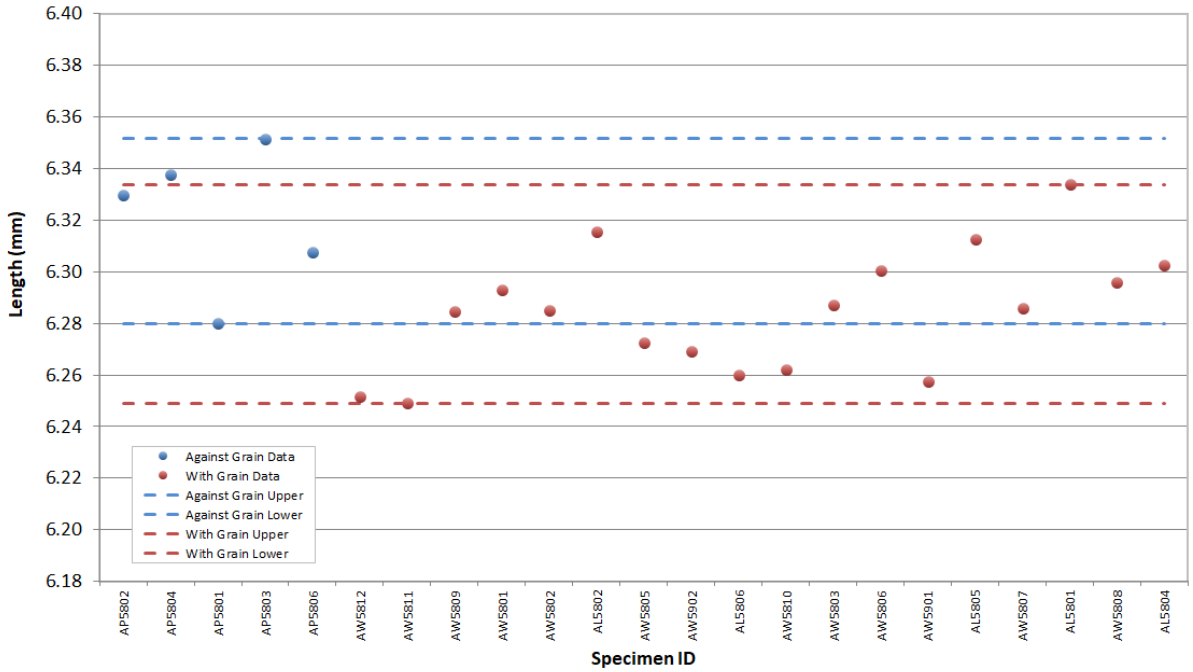

Figure A-8. NBG-17 piggyback length.

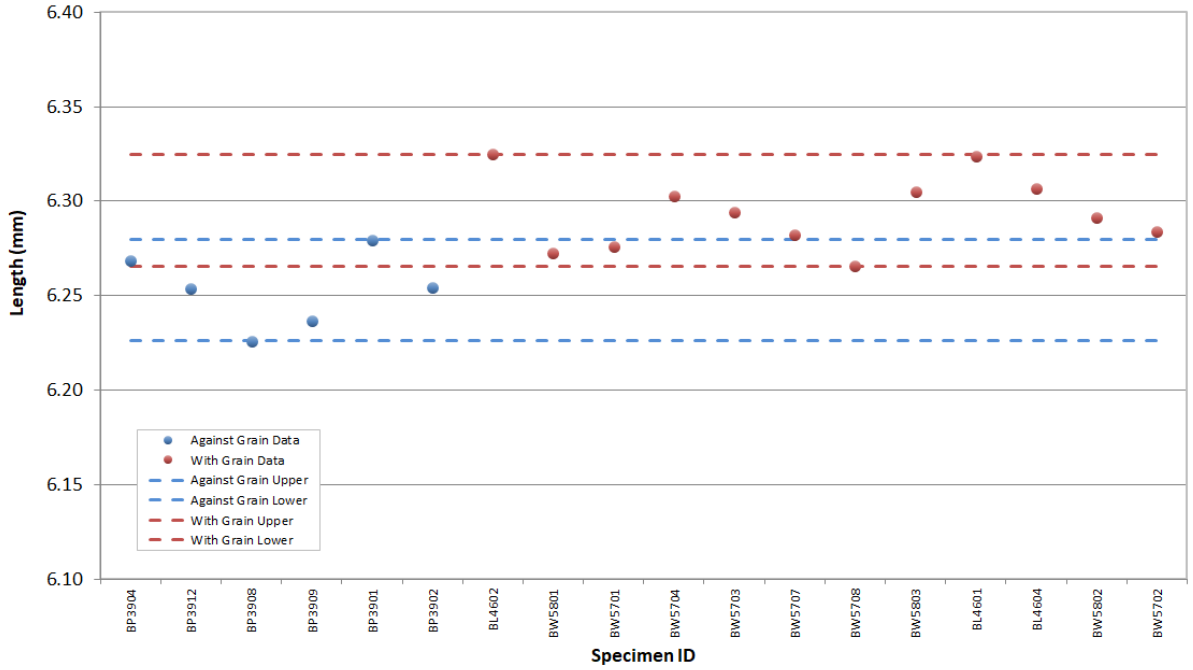

Figure A-9. NBG-18 piggyback length.

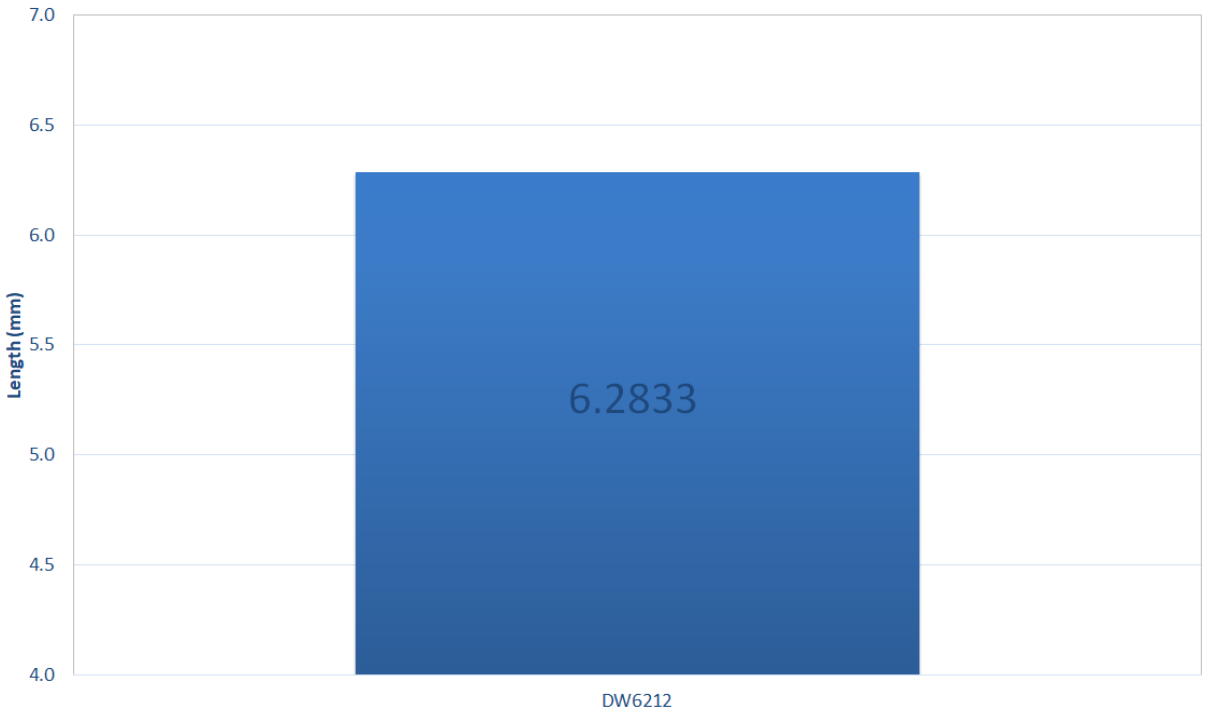

Figure A-10. PCEA piggyback length.

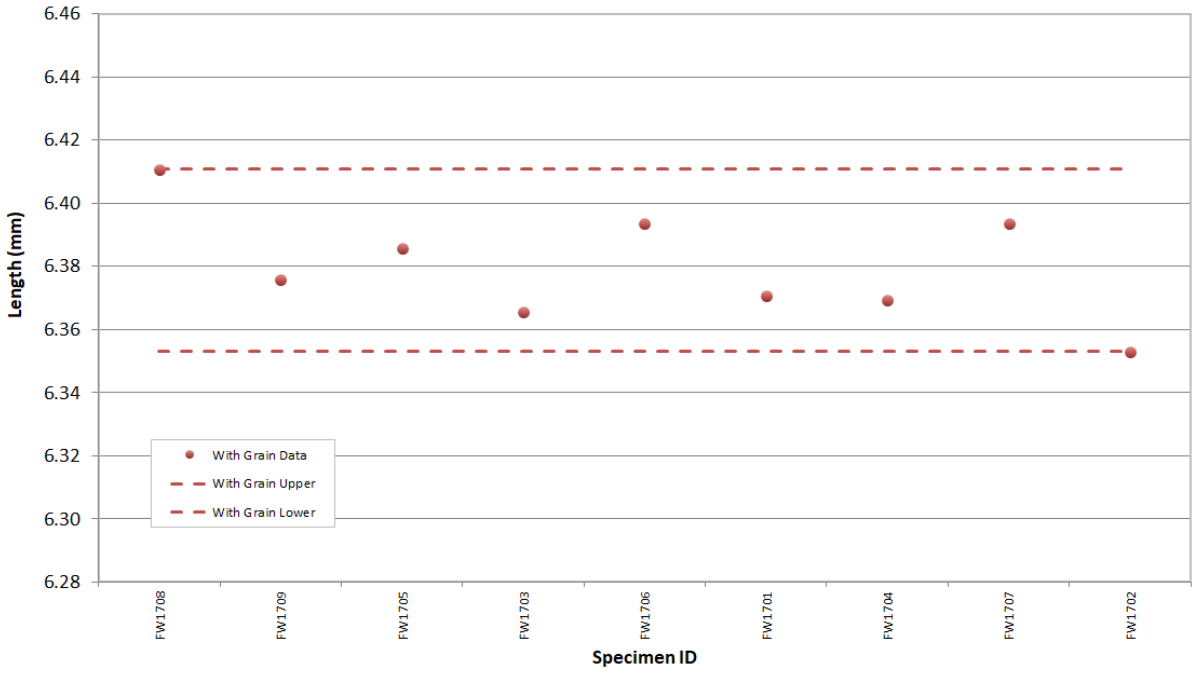

Figure A-11. IG-430 piggyback length.

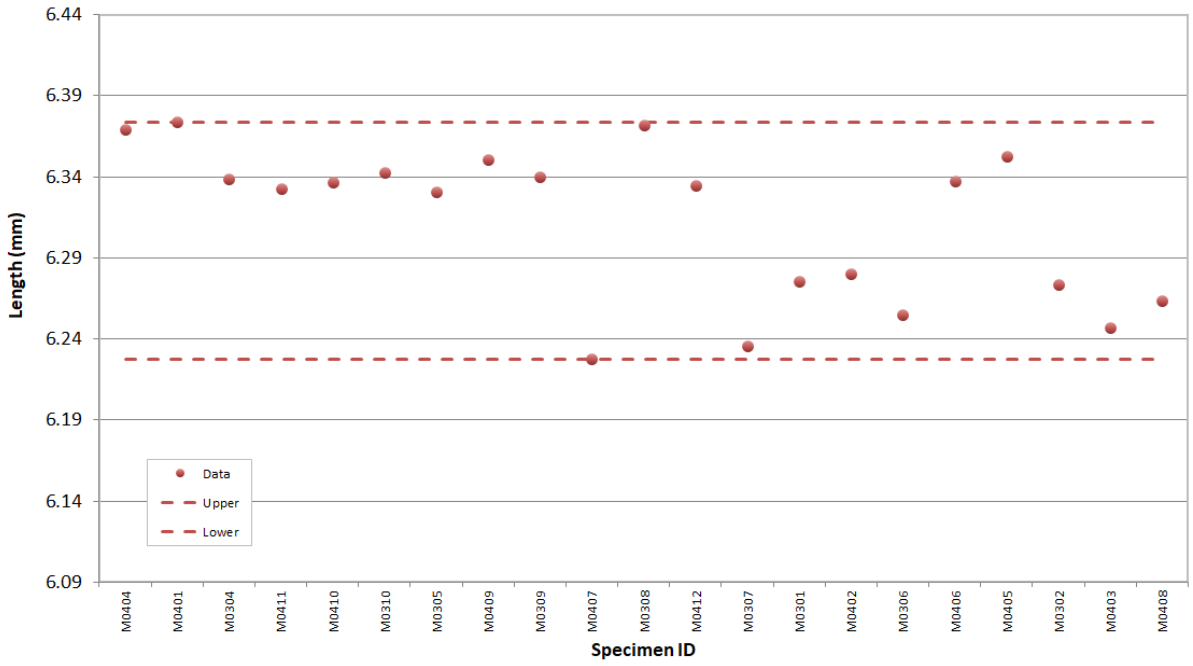

Figure A-12. NBG-25 piggyback length.

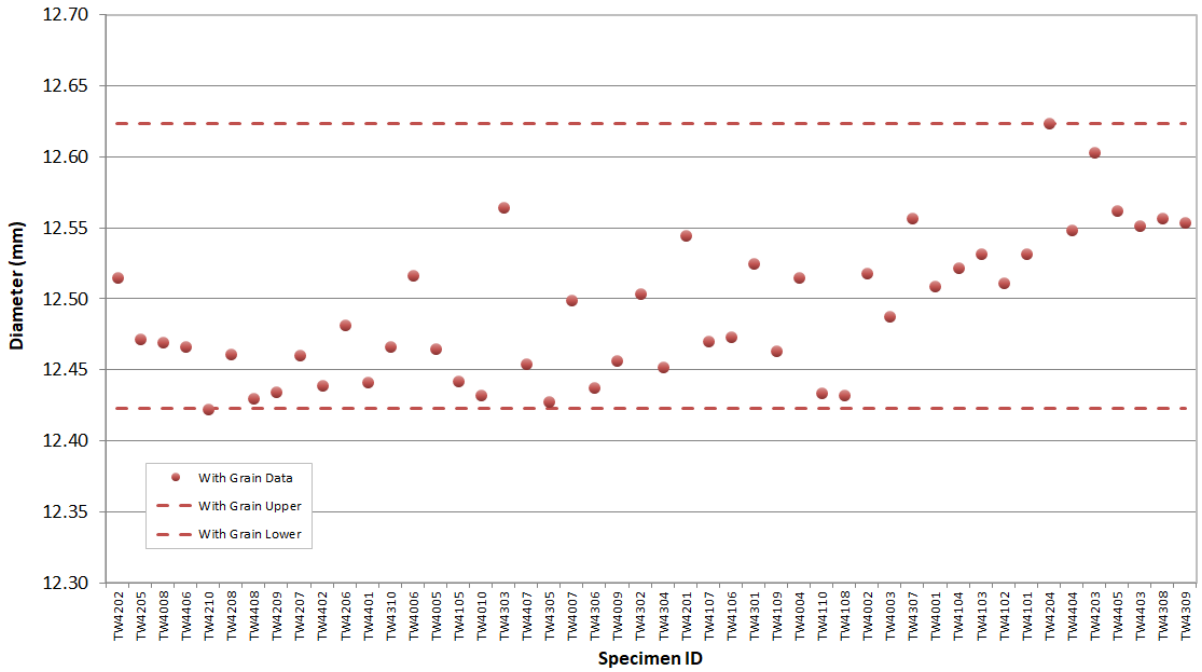

Figure A-13. 2114 creep diameter.

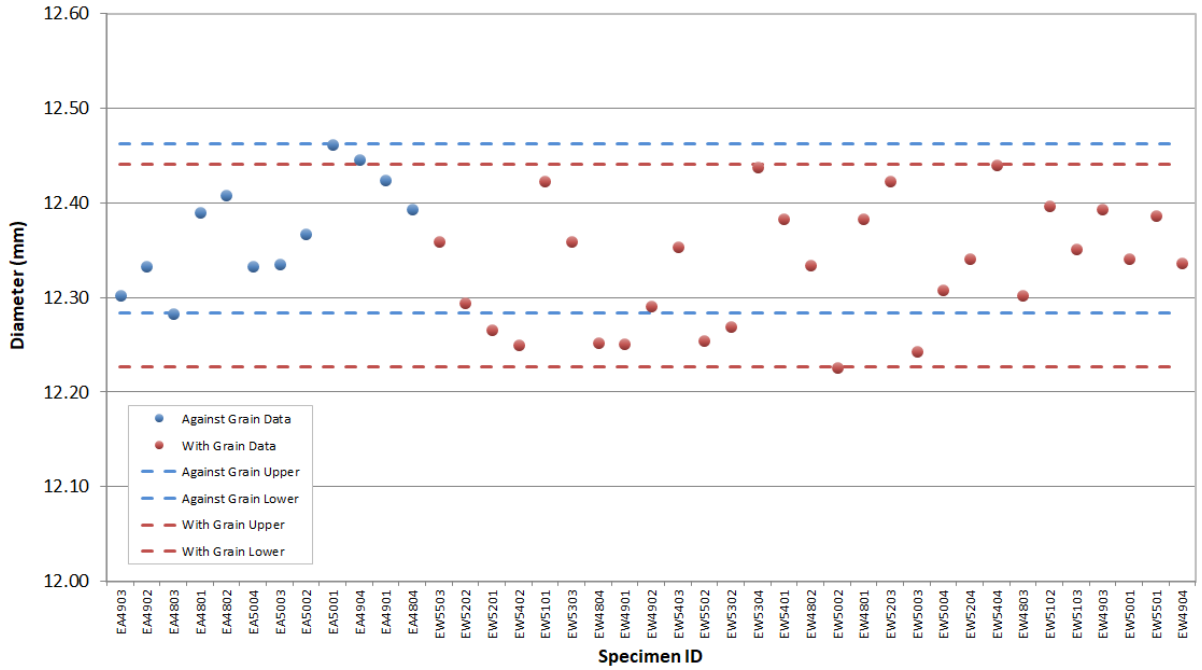

Figure A-14. IG-110 creep diameter.

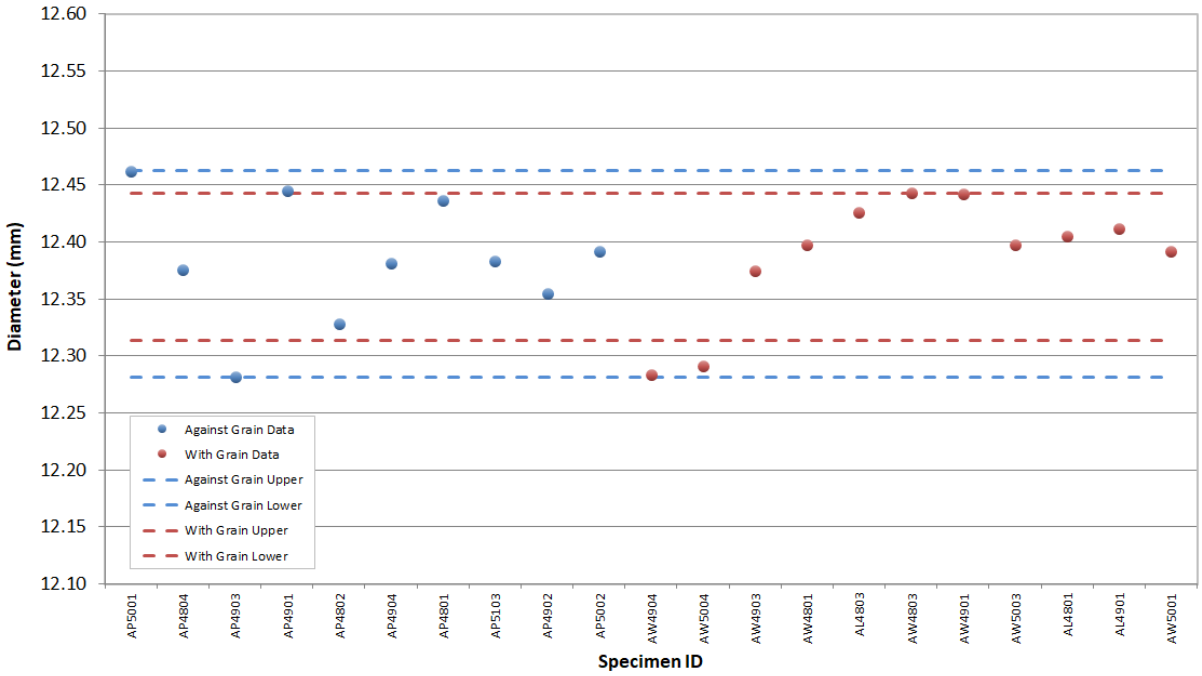

Figure A-15. NBG-17 creep diameter.

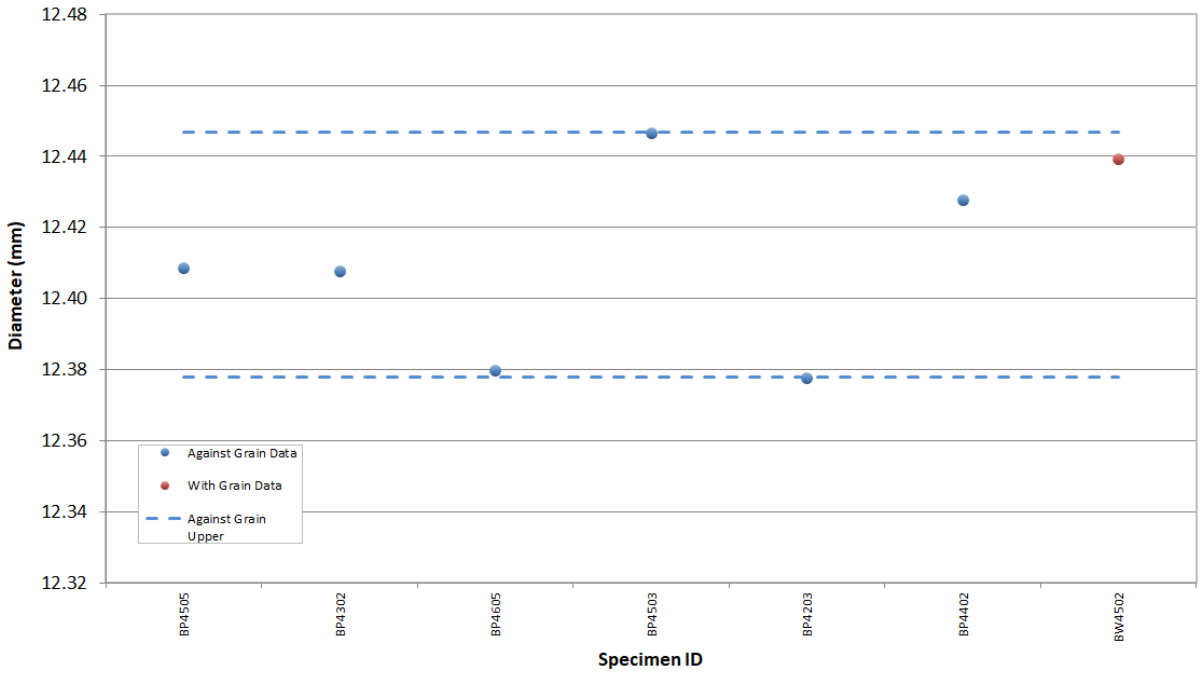

Figure A-16. NBG-18 creep diameter.

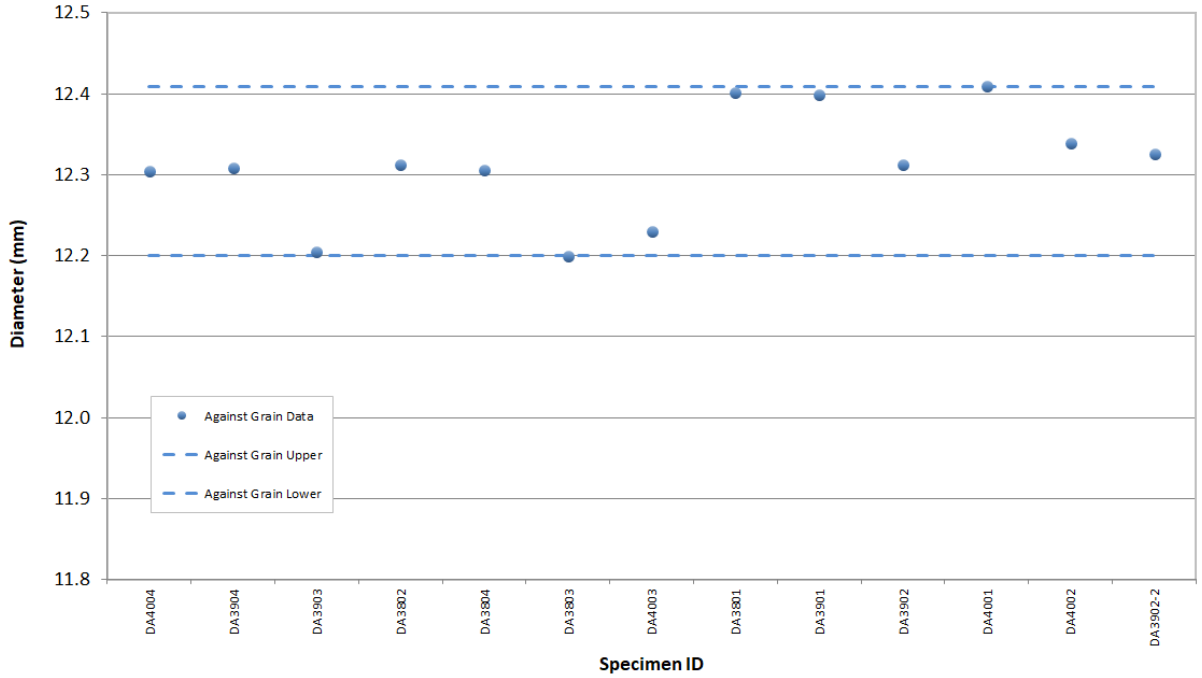

Figure A-17. PCEA creep diameter.

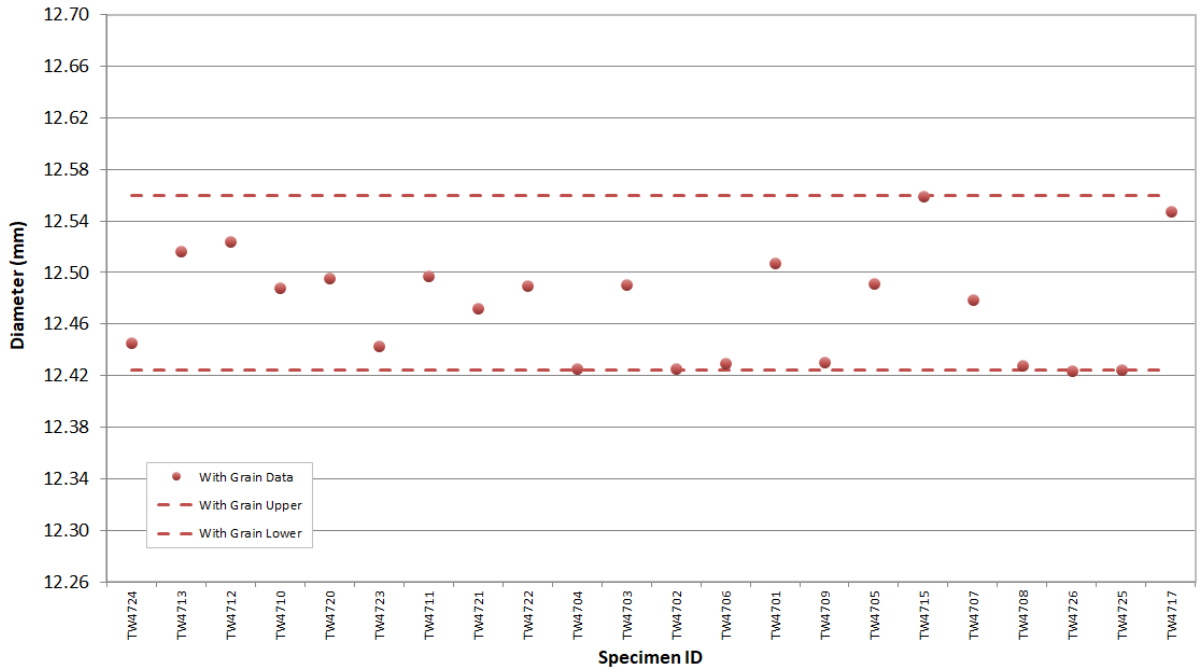

Figure A-18. 2114 piggyback diameter.

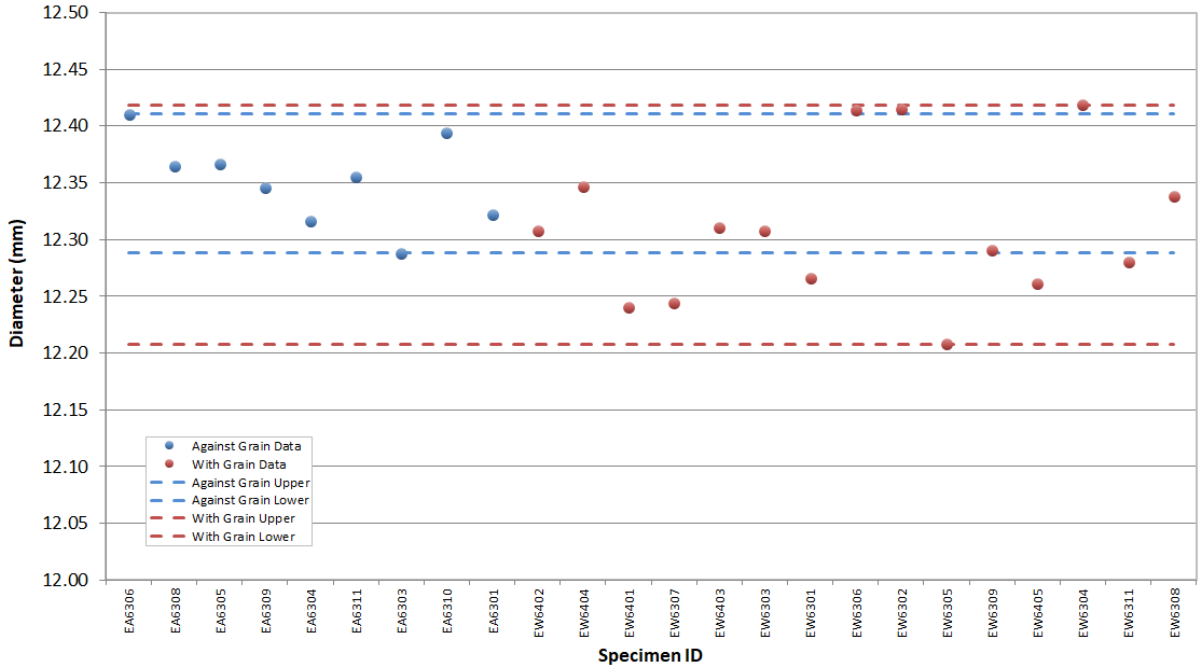

Figure A-19. IG-110 piggyback diameter.

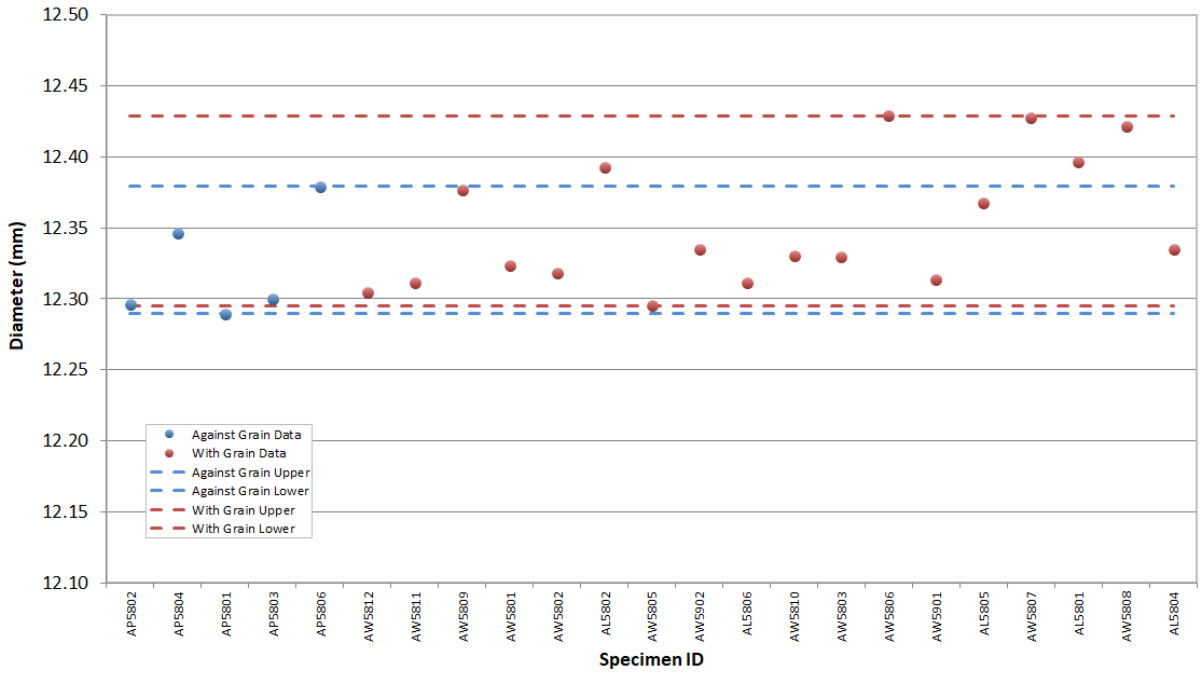

Figure A-20. NBG-17 piggyback diameter.

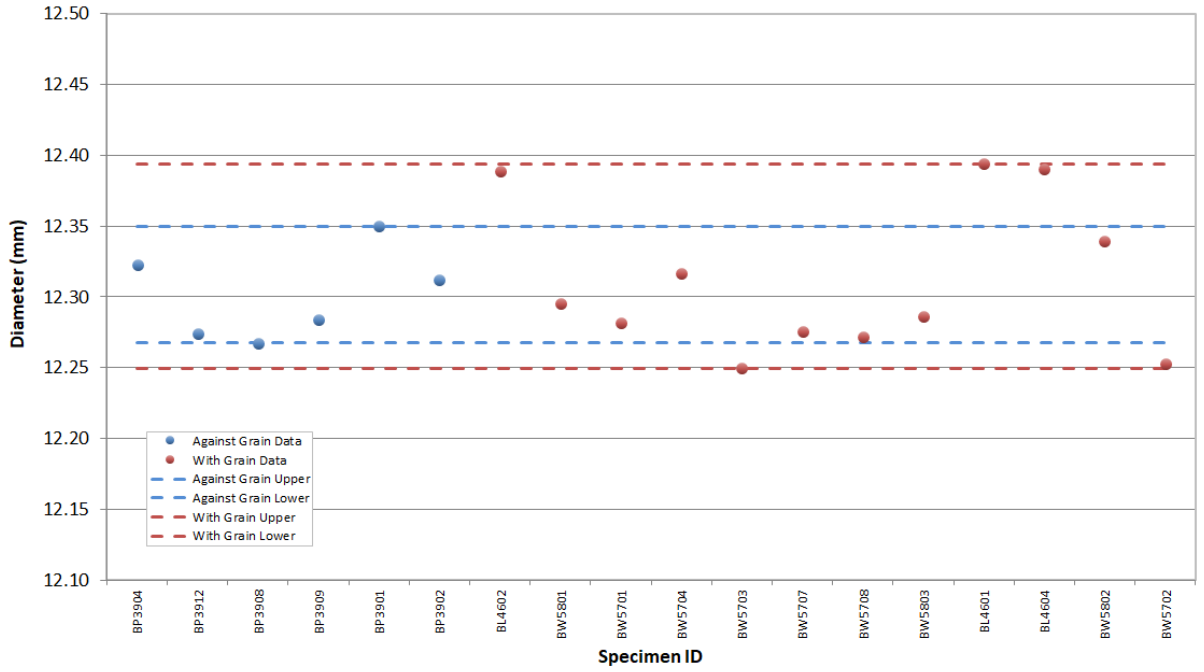

Figure A-21. NBG-18 piggyback diameter.

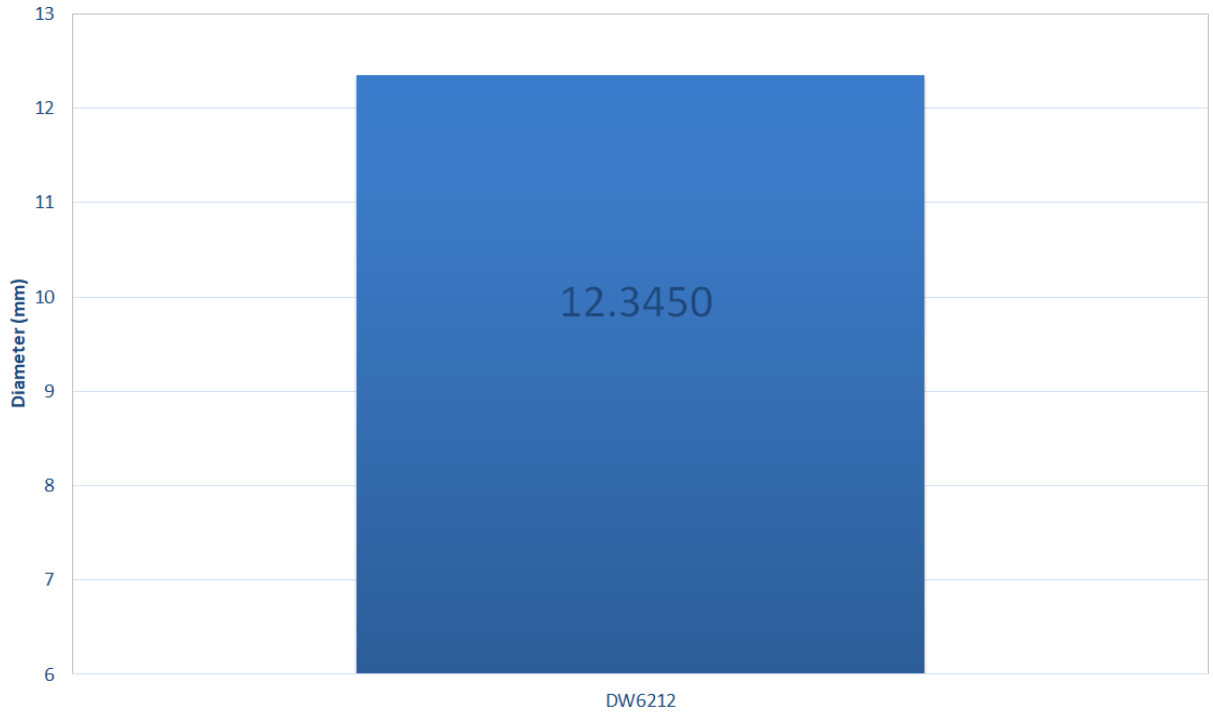

Figure A-22. PCEA piggyback diameter.

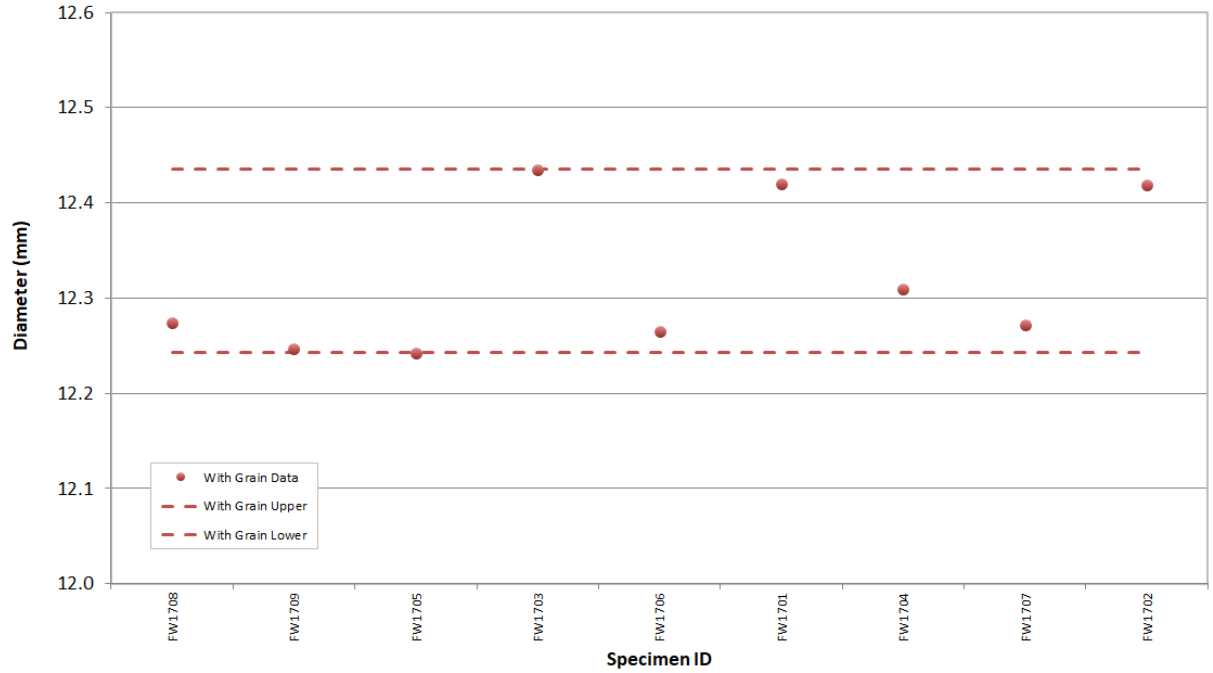

Figure A-23. IG-430 piggyback diameter.

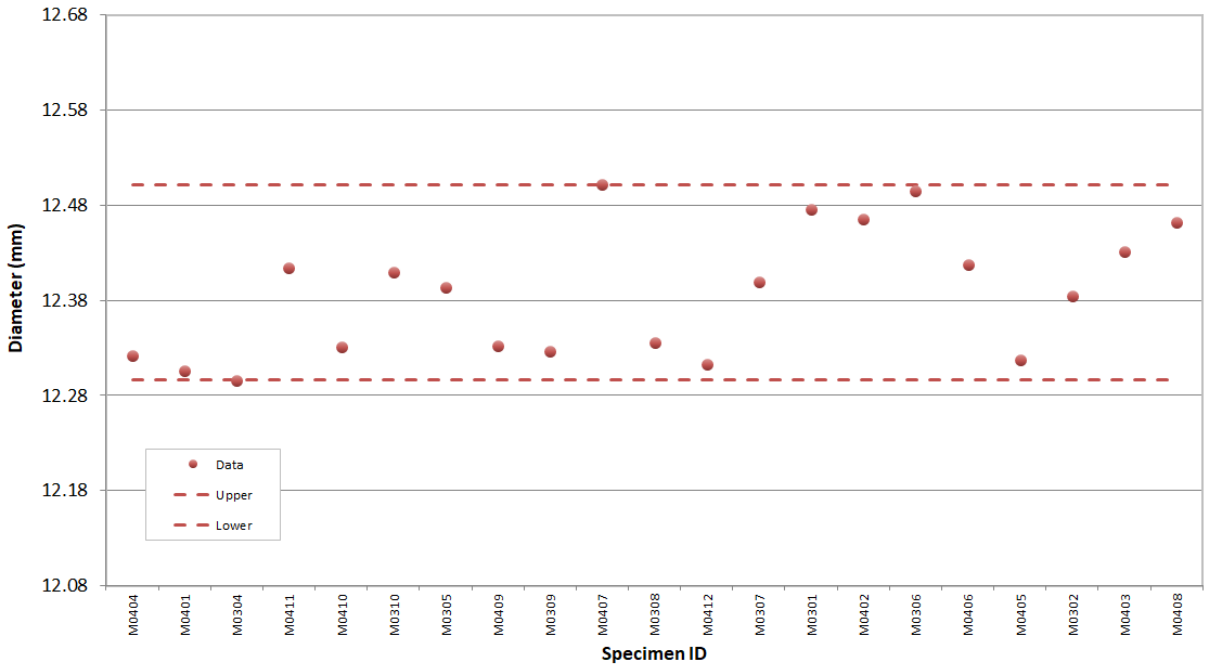

Figure A-24. NBG-25 piggyback diameter.

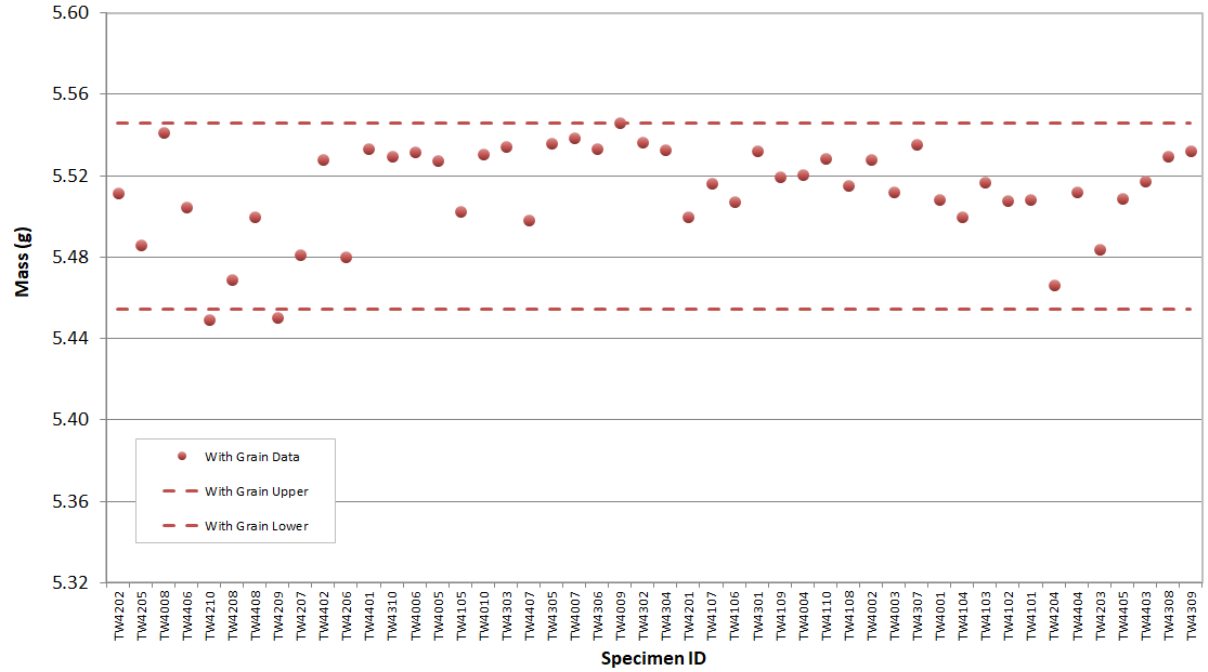

Figure A-25. 2114 creep mass.

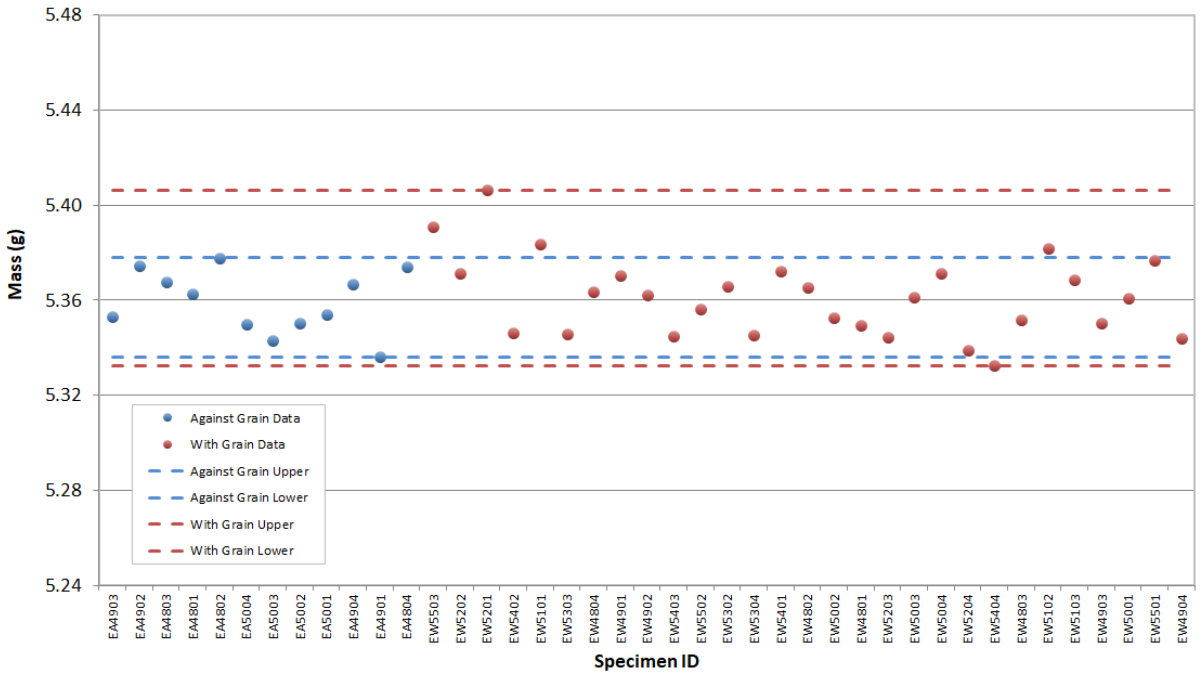

Figure A-26. IG-110 creep mass.

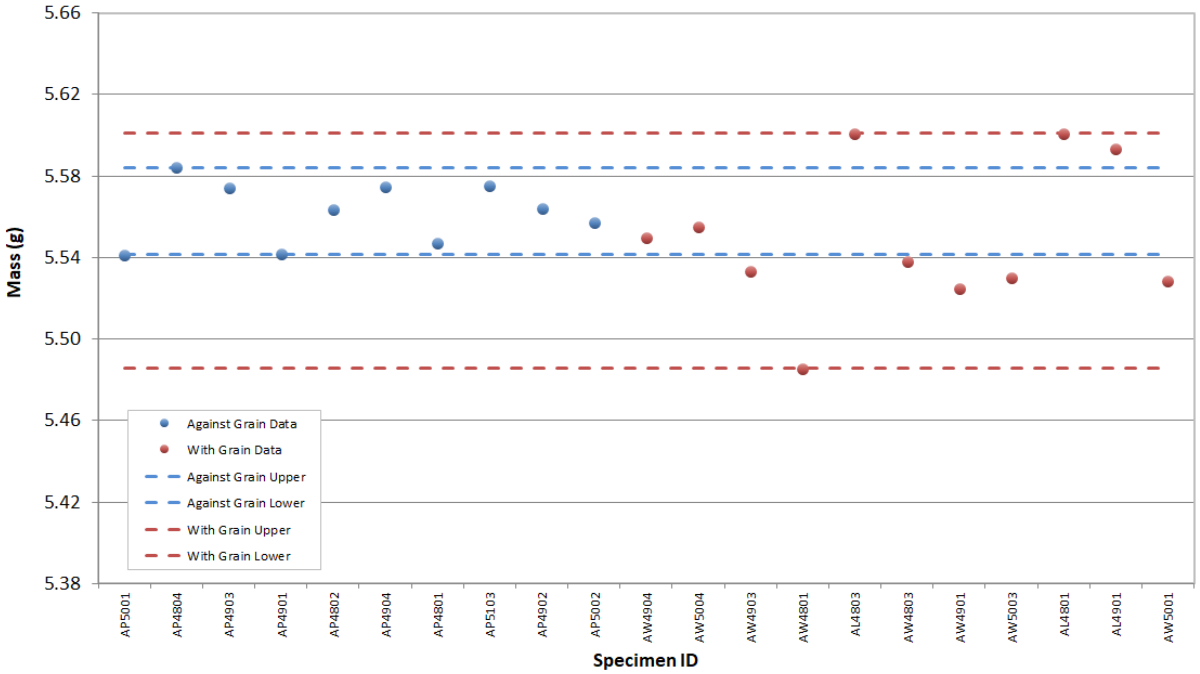

Figure A-27. NBG-17 creep mass.

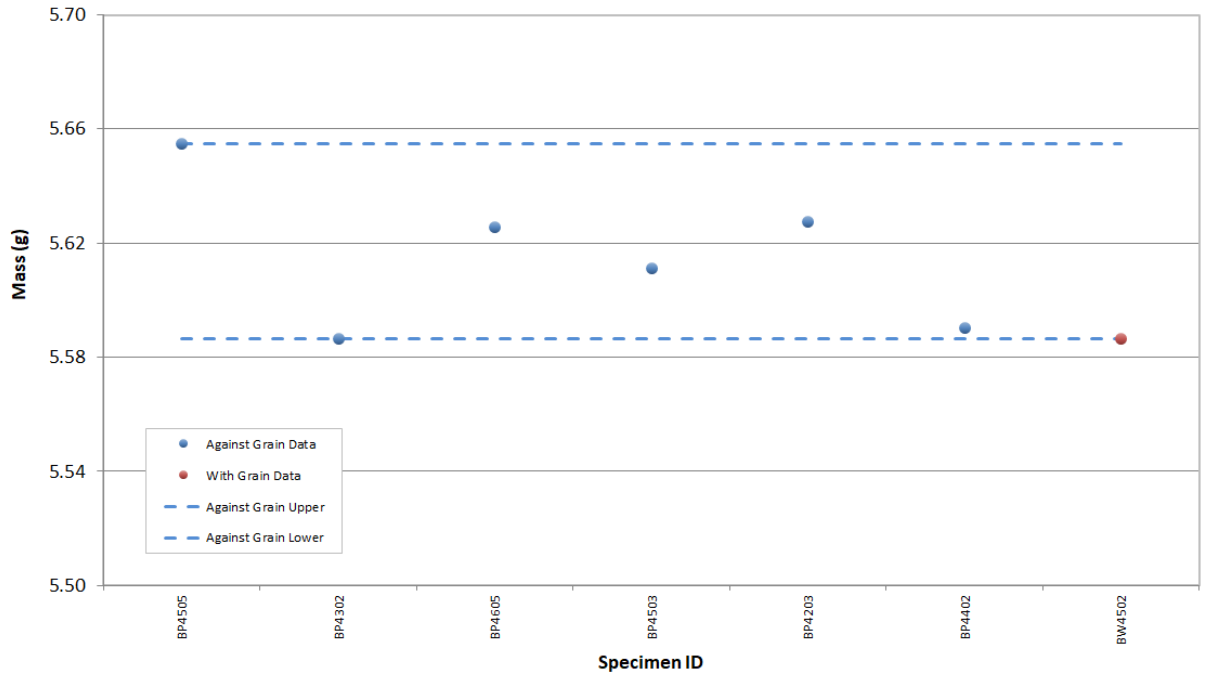

Figure A-28. NBG-18 creep mass.

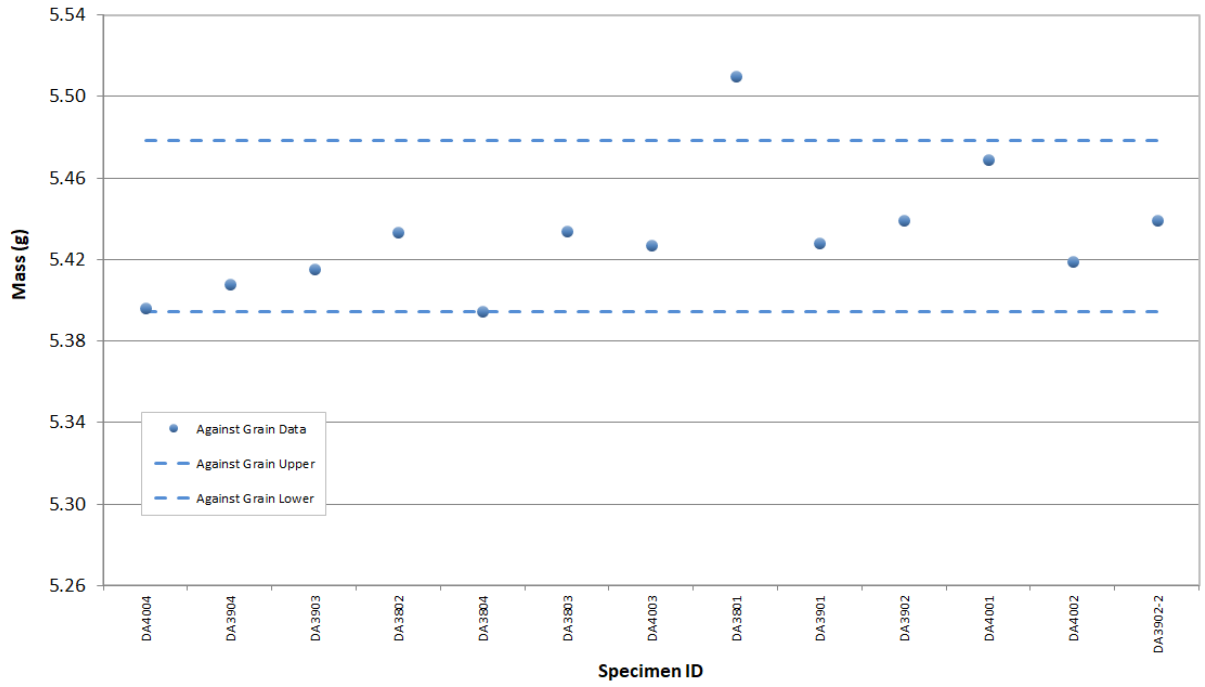

Figure A-29. PCEA creep mass.

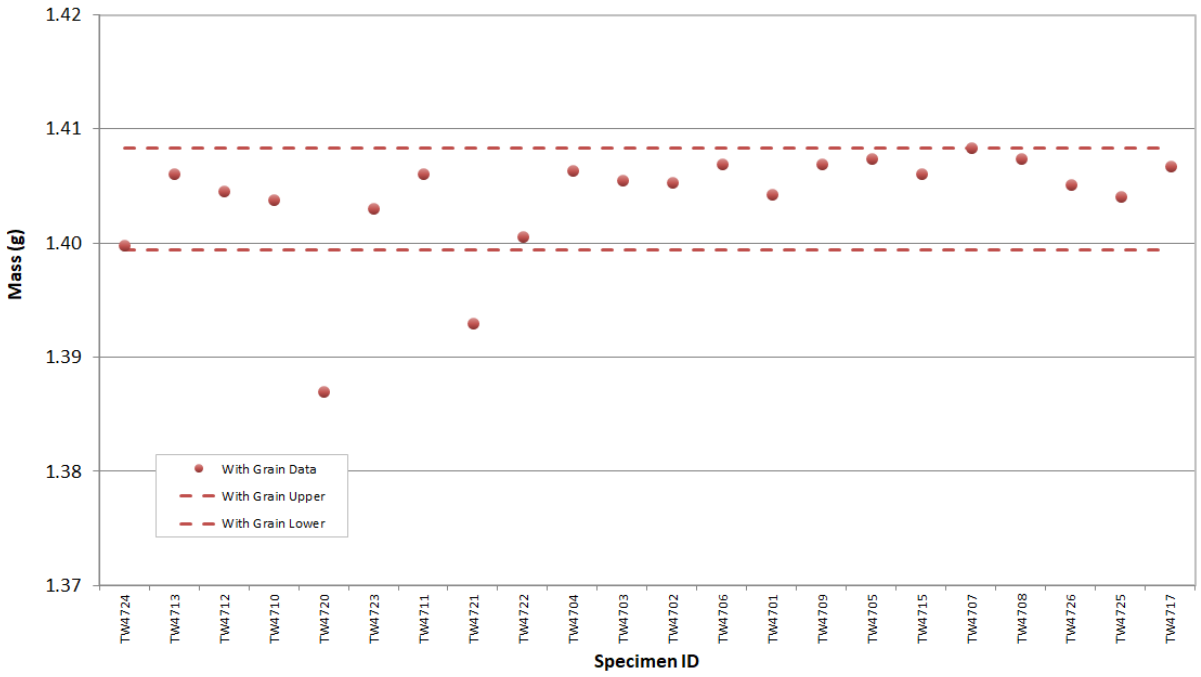

Figure A-30. 2114 piggyback mass.

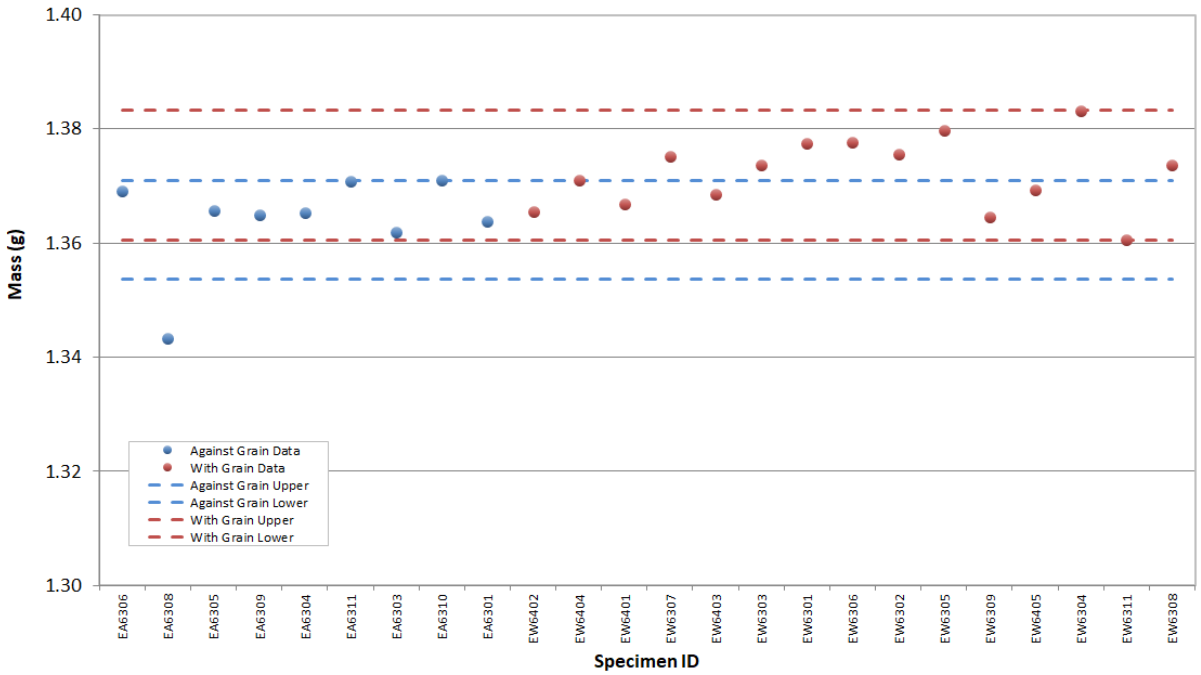

Figure A-31. IG-110 piggyback mass.

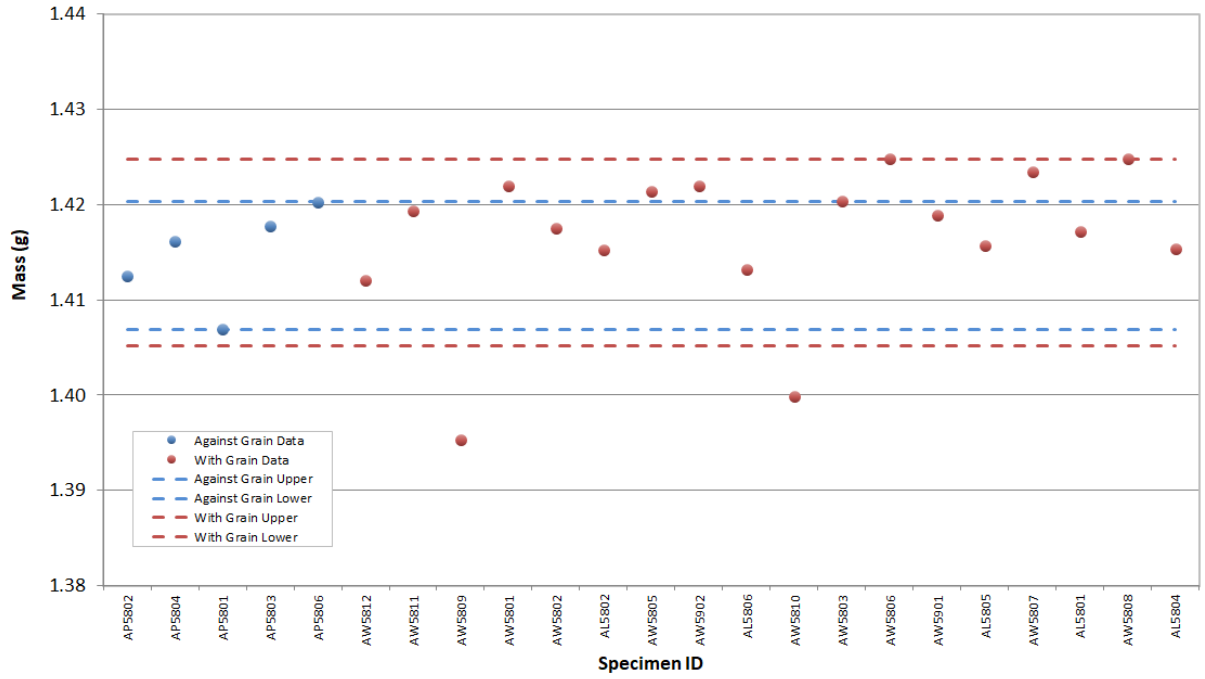

Figure A-32. NBG-17 piggyback mass.

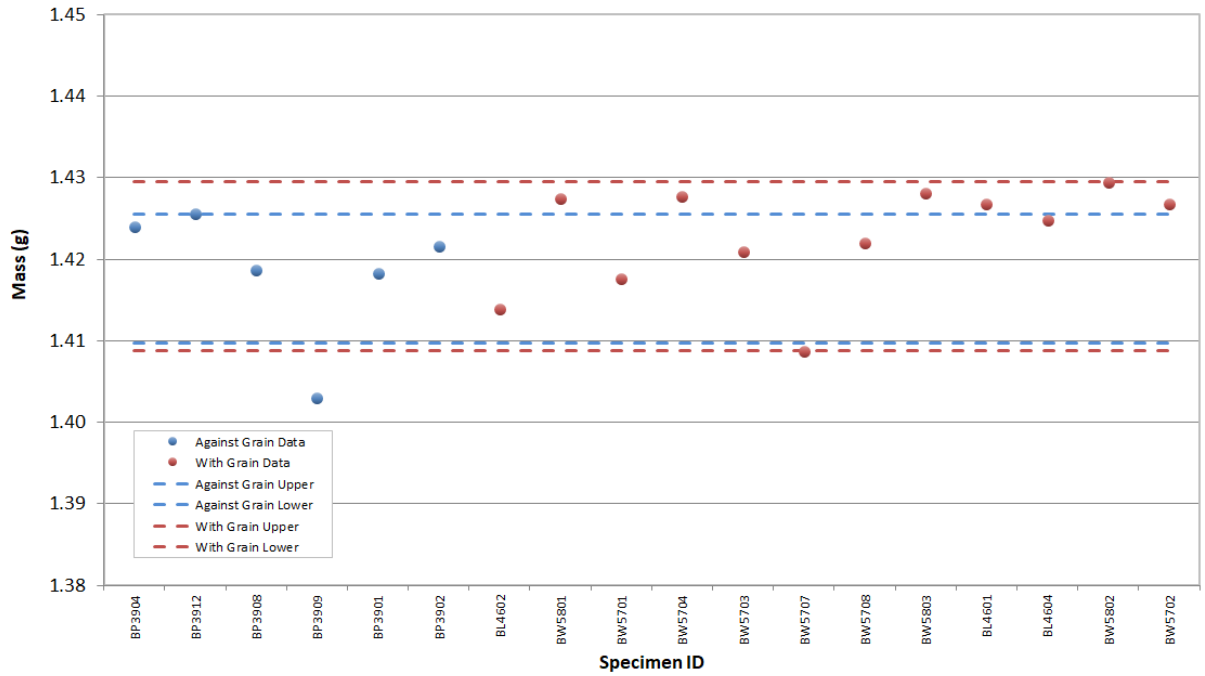

Figure A-33. NBG-18 piggyback mass.

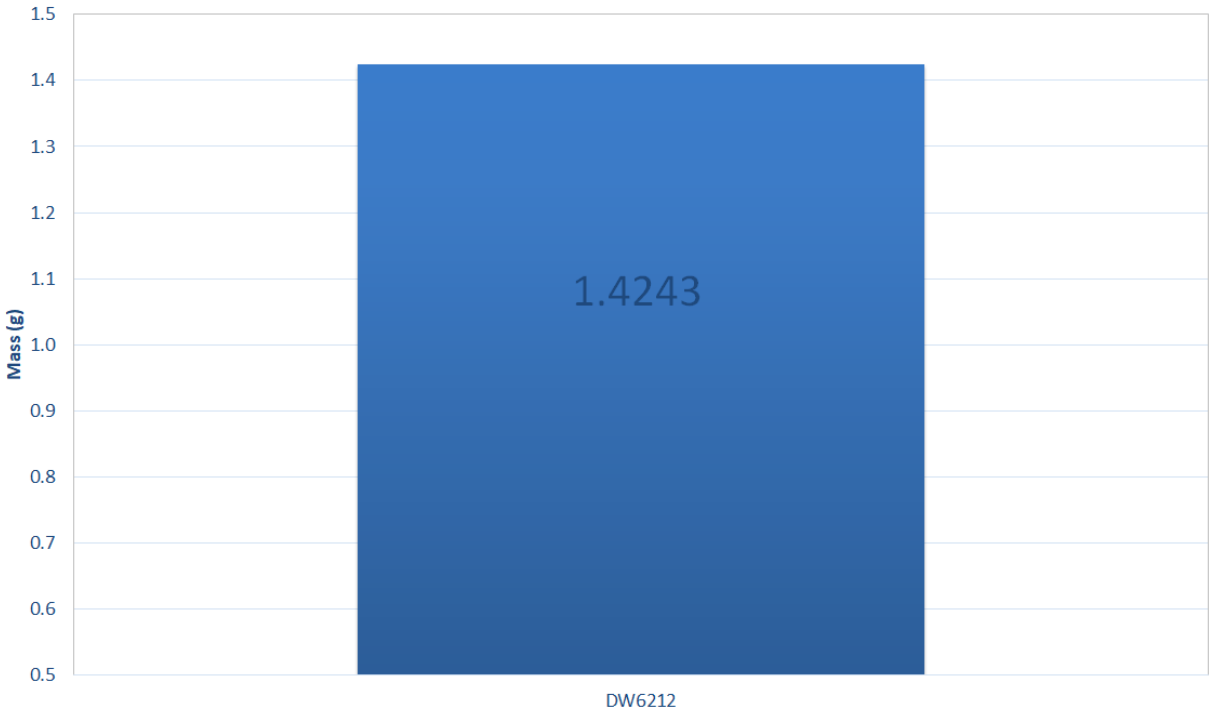

Figure A-34. PCEA piggyback mass.

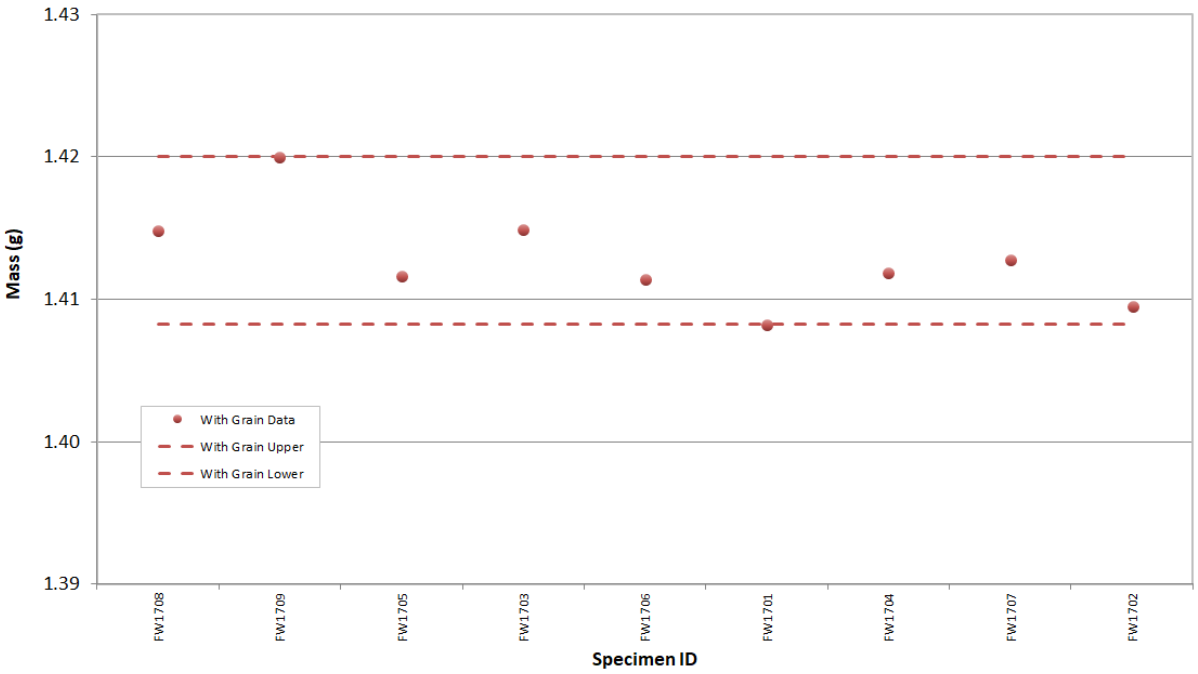

Figure A-35. IG-430 piggyback mass.

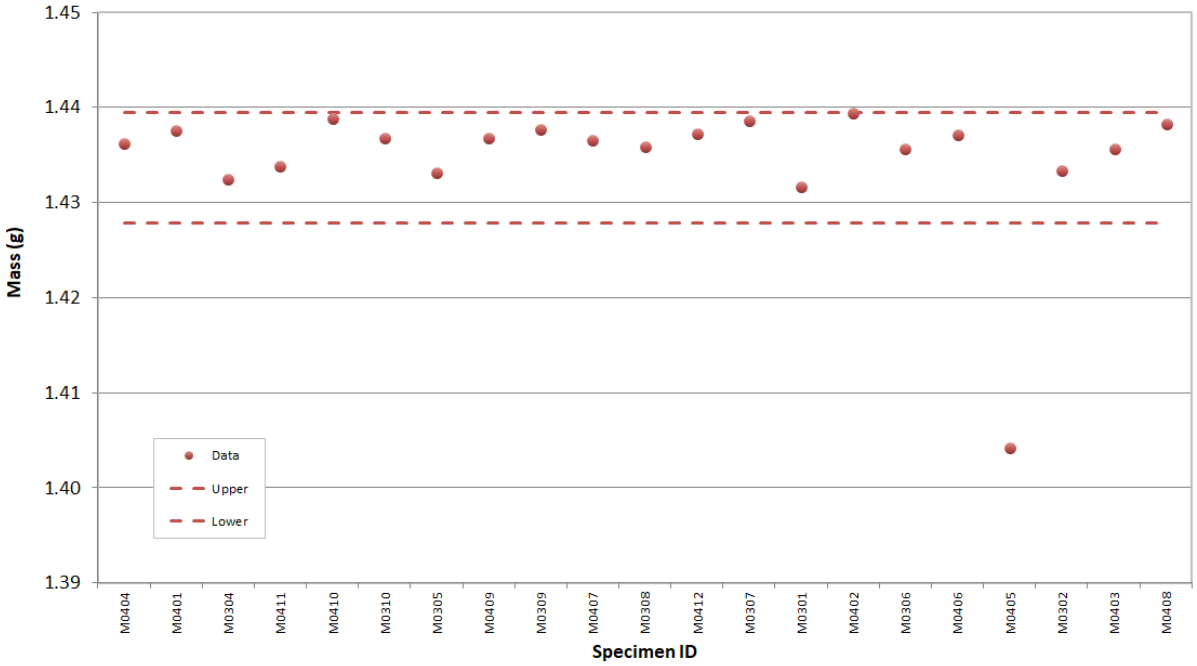

Figure A-36. NBG-25 piggyback mass.

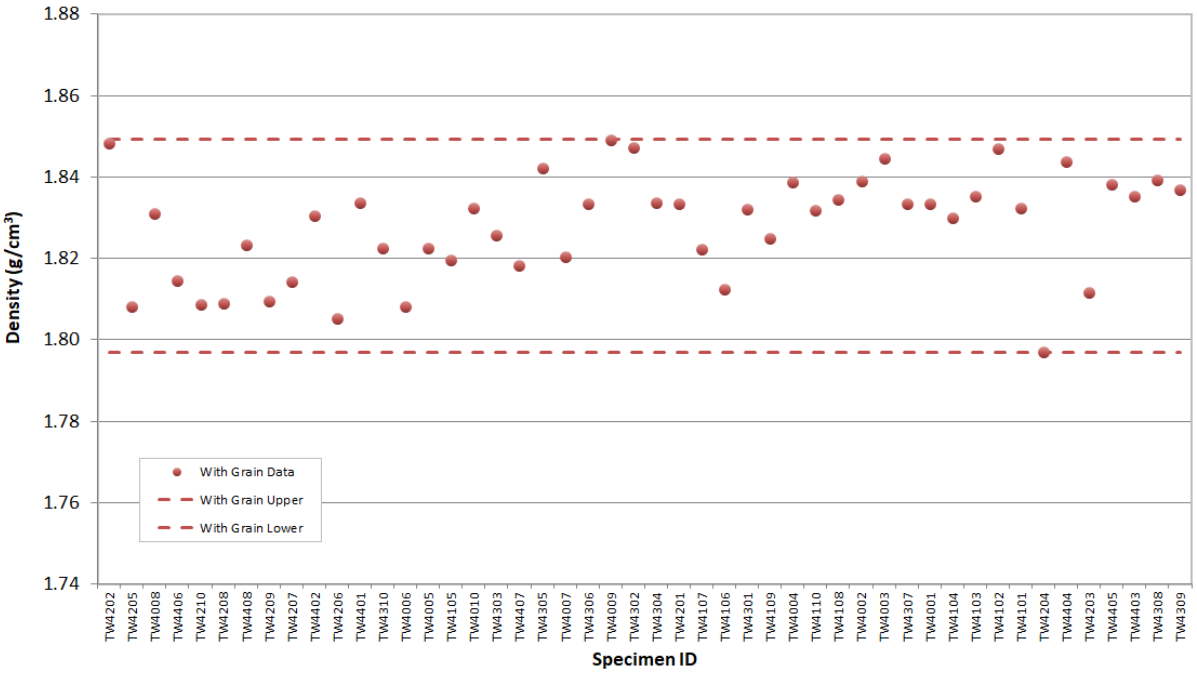

Figure A-37. 2114 creep density.

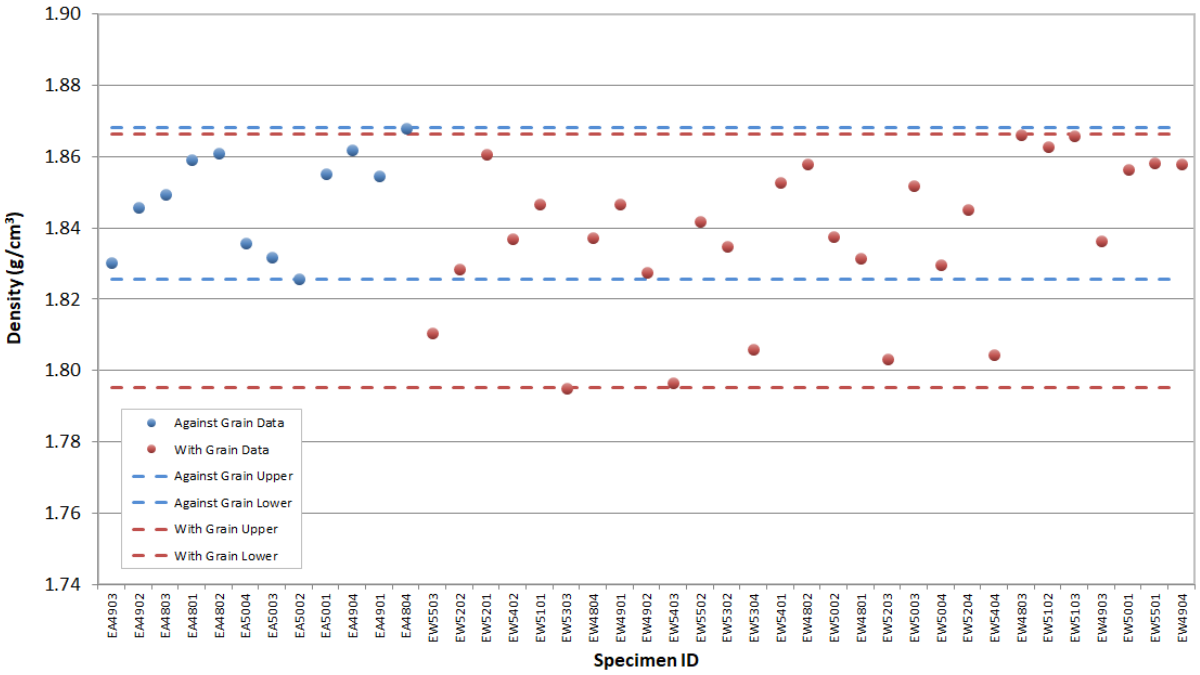

Figure A-38. IG-110 creep density.

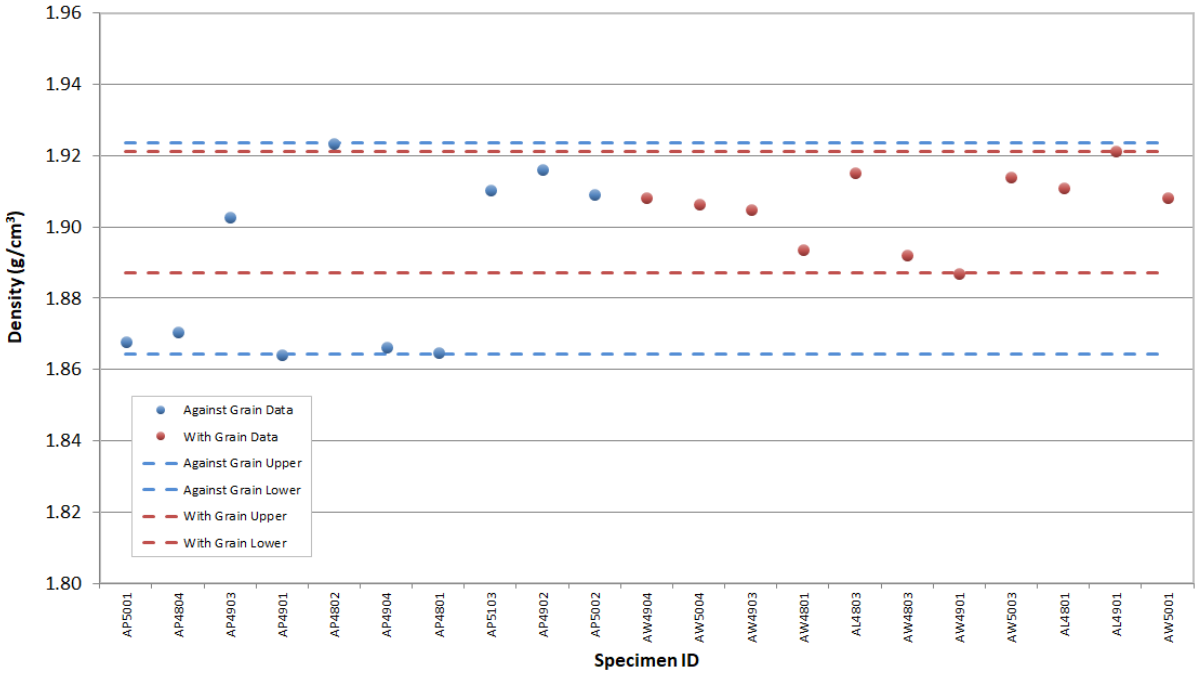

Figure A-39. NBG-17 creep density.

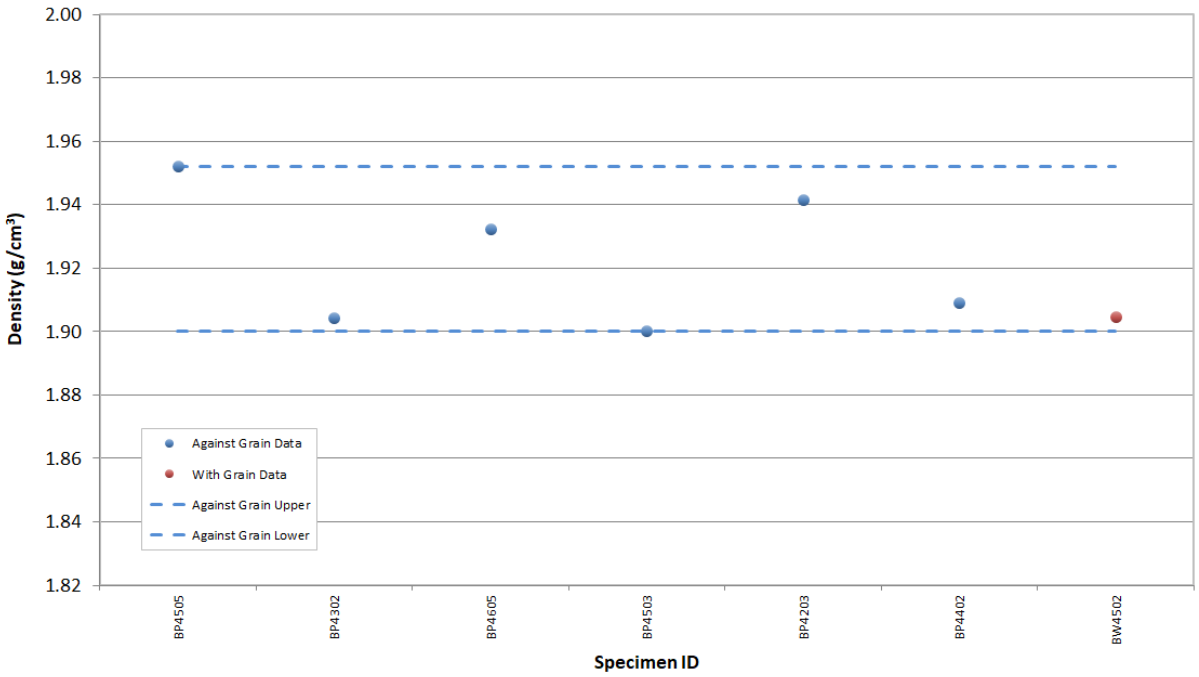

Figure A-40. NBG-18 creep density.

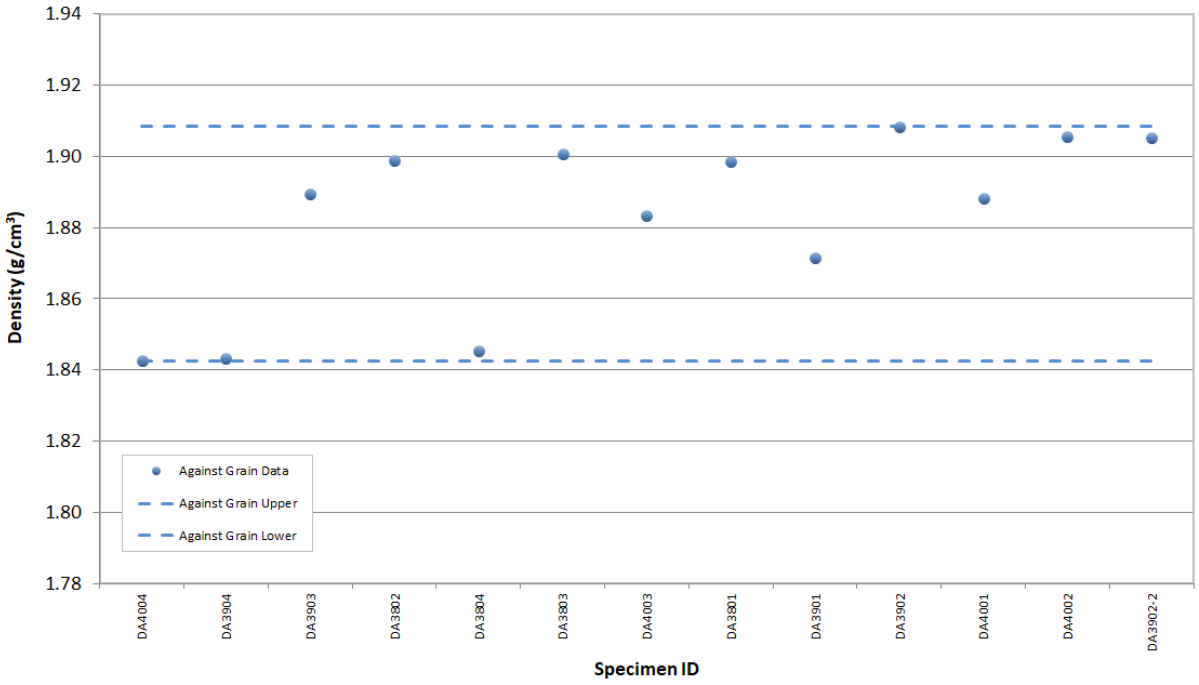

Figure A-41. PCEA creep density.

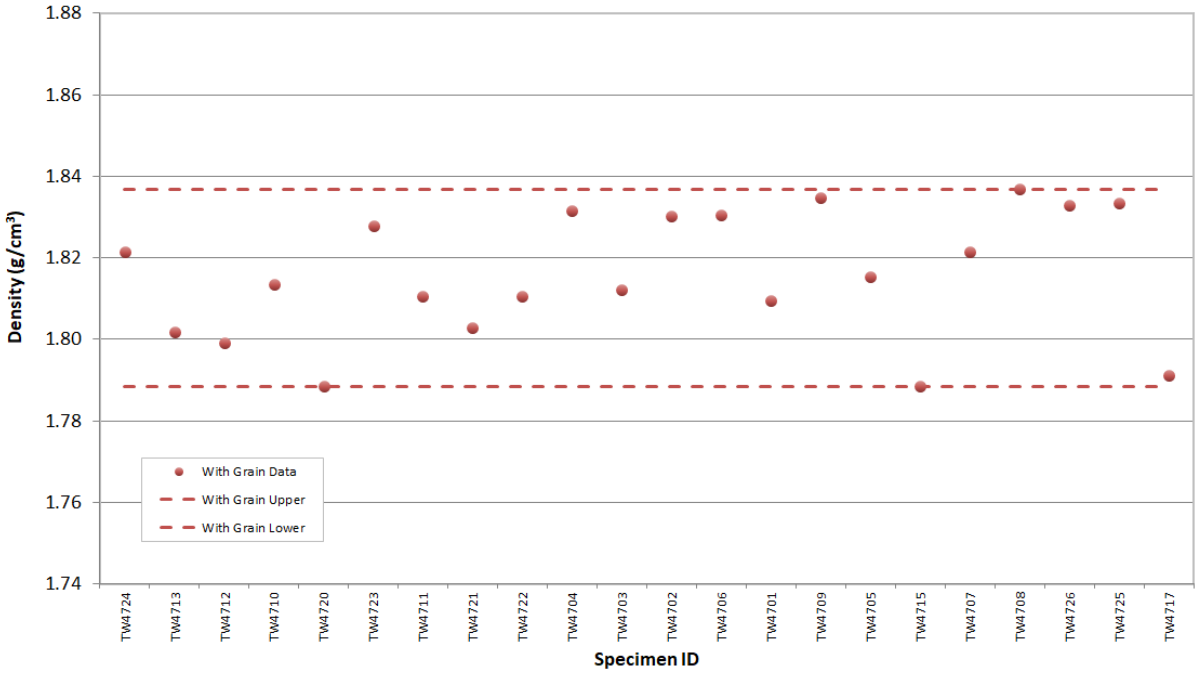

Figure A-42. 2114 piggyback density.

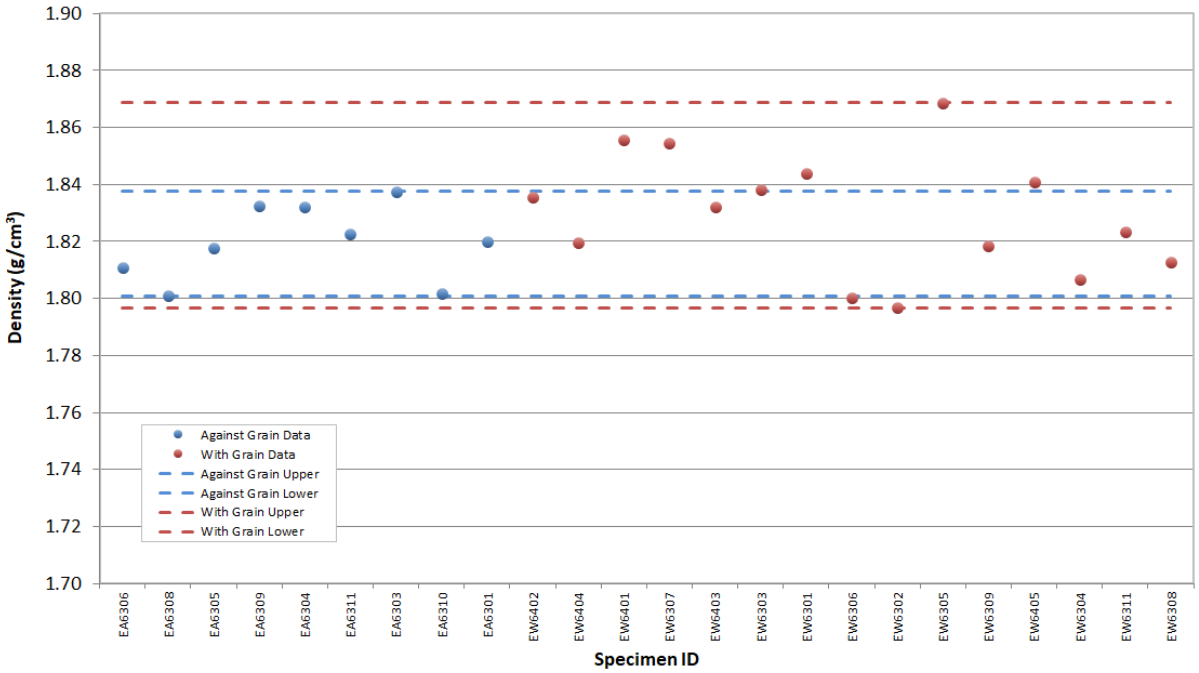

Figure A-43. IG-110 piggyback density.

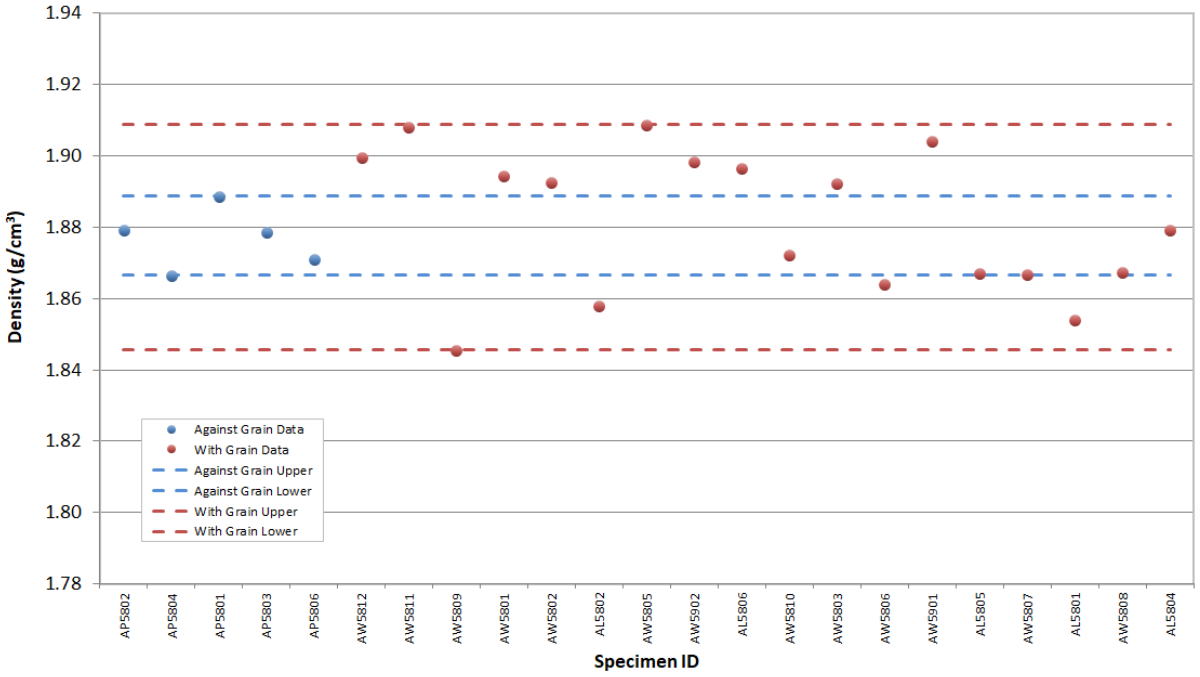

Figure A-44. NBG-17 piggyback density.

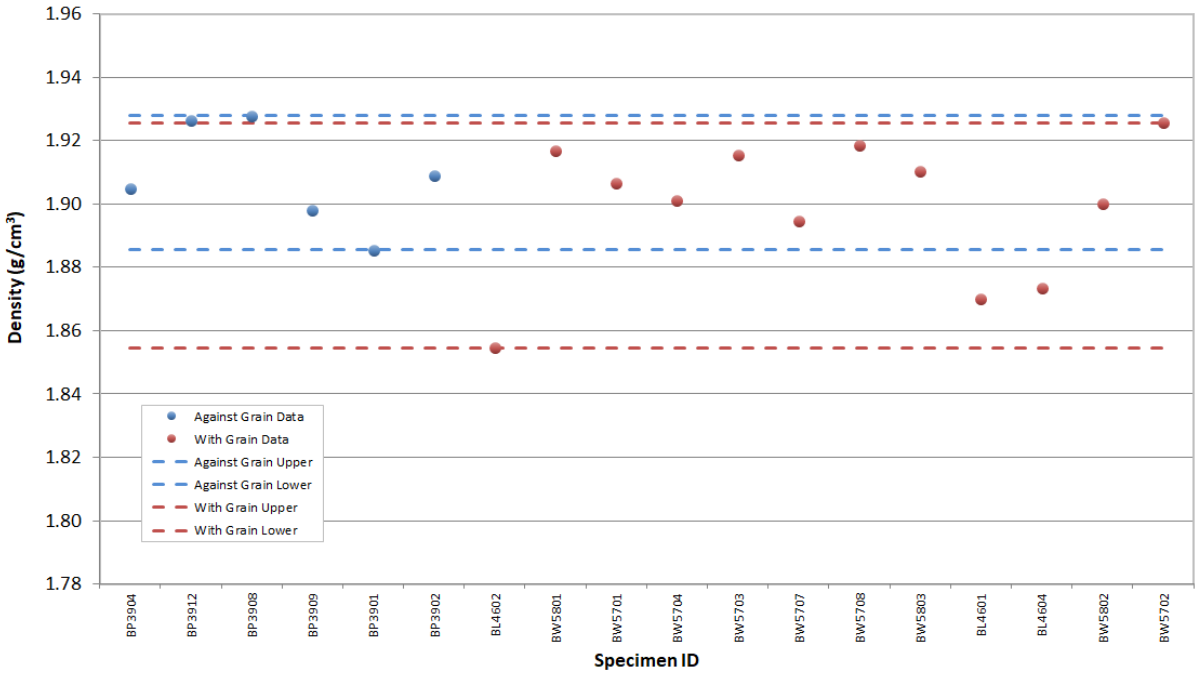

Figure A-45. NBG-18 piggyback density.

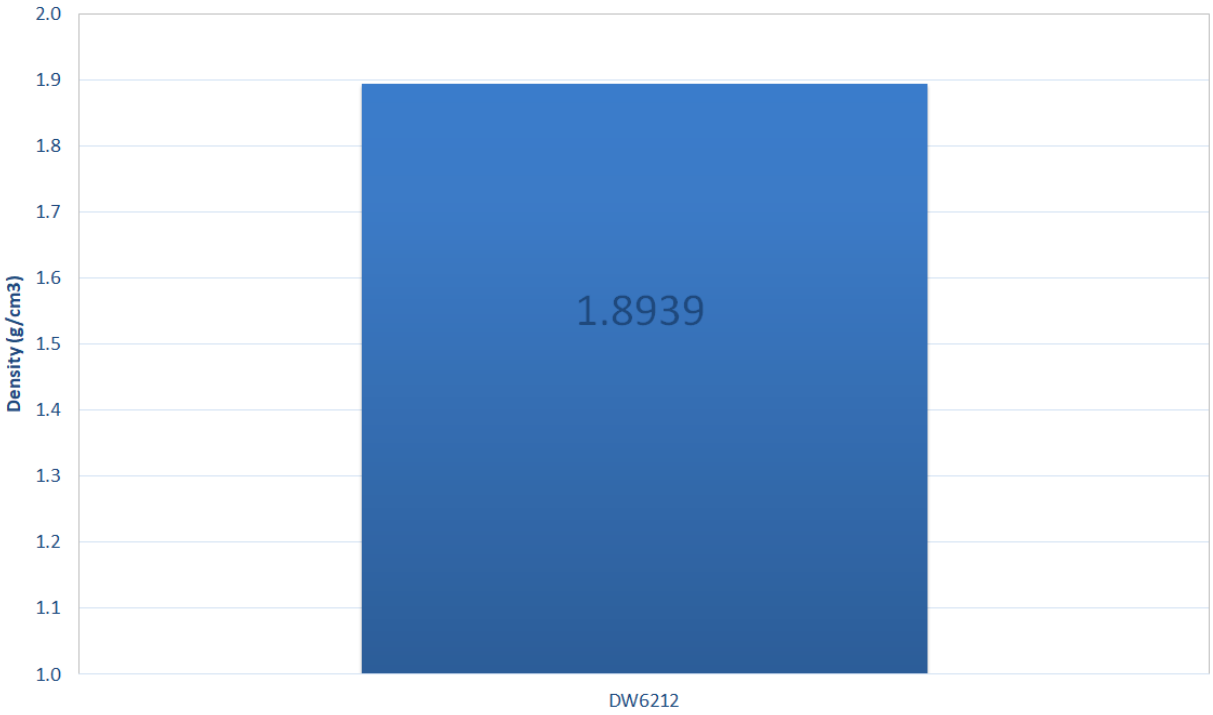

Figure A-46. PCEA piggyback density.

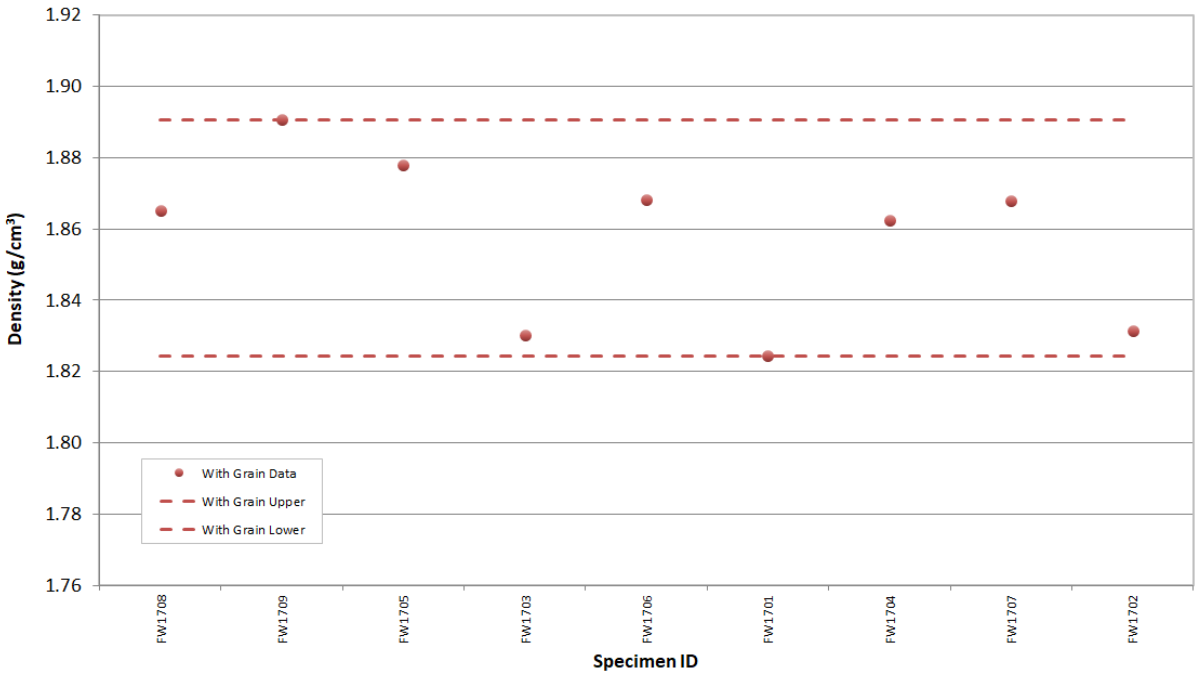

Figure A-47. IG-430 piggyback density.

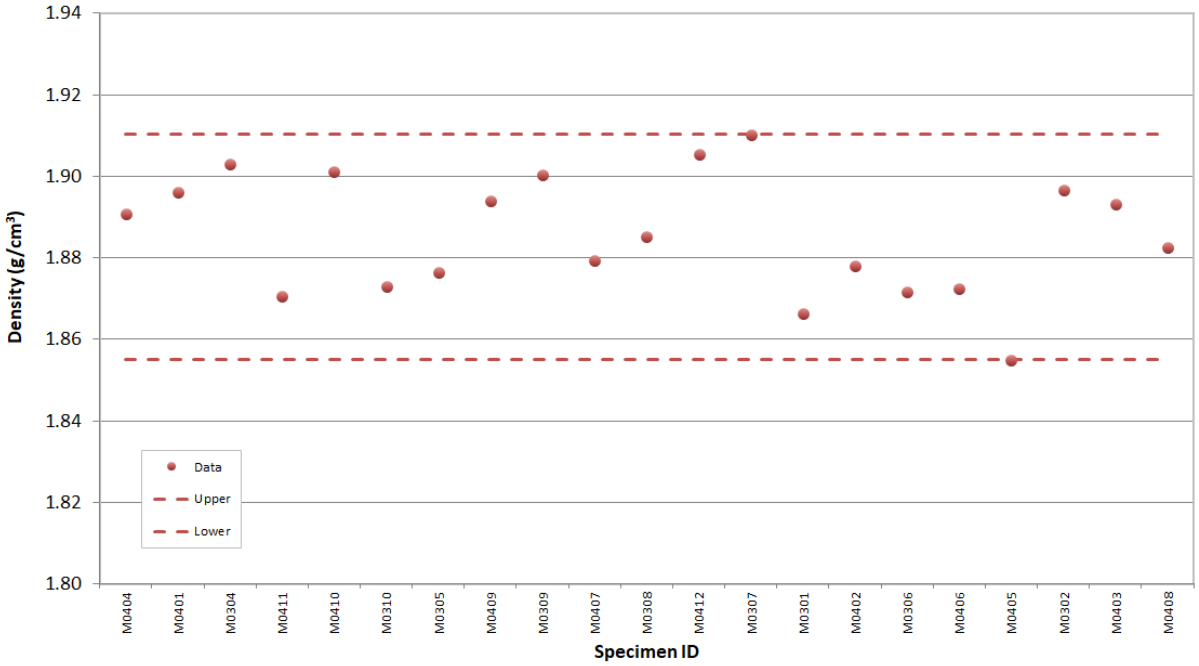

Figure A-48. NBG-25 piggyback density.

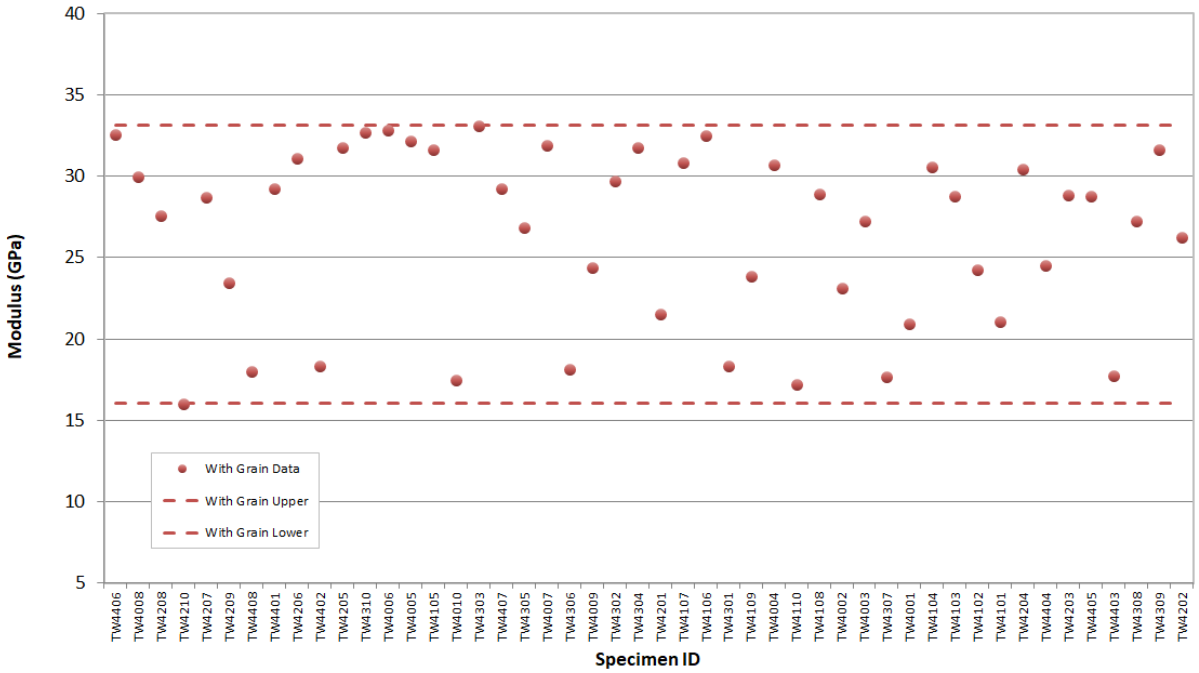

Figure A-49. 2114 creep modulus by resonant frequency.

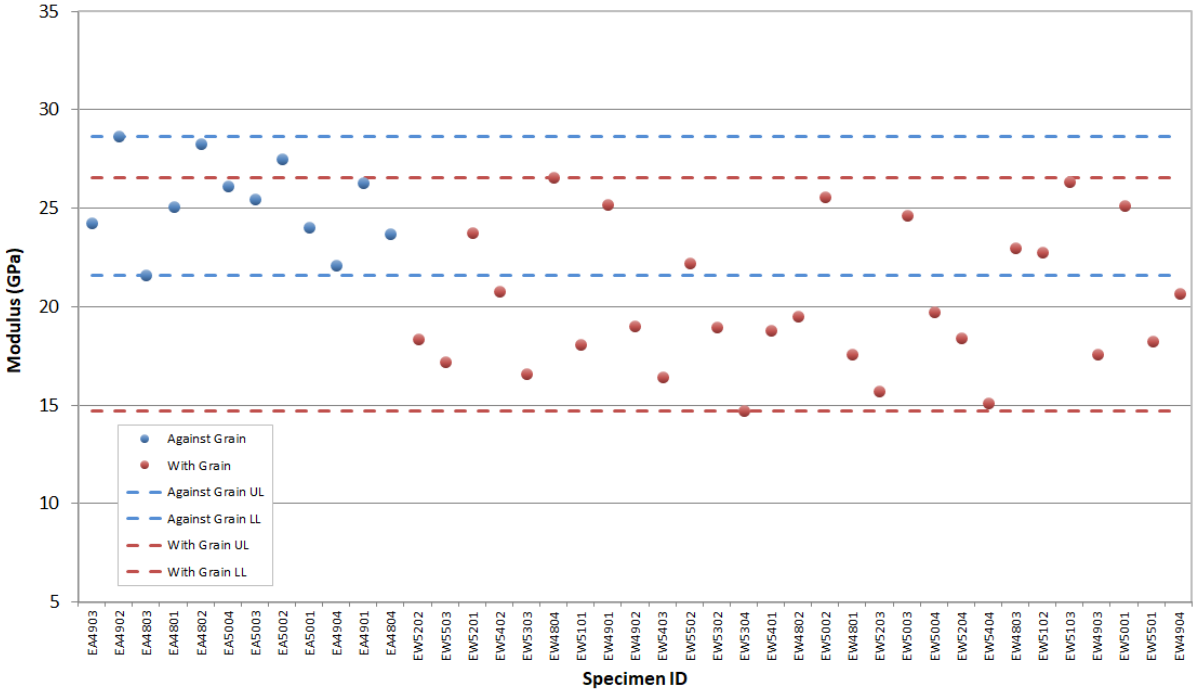

Figure A-50. IG-110 creep modulus by resonant frequency.

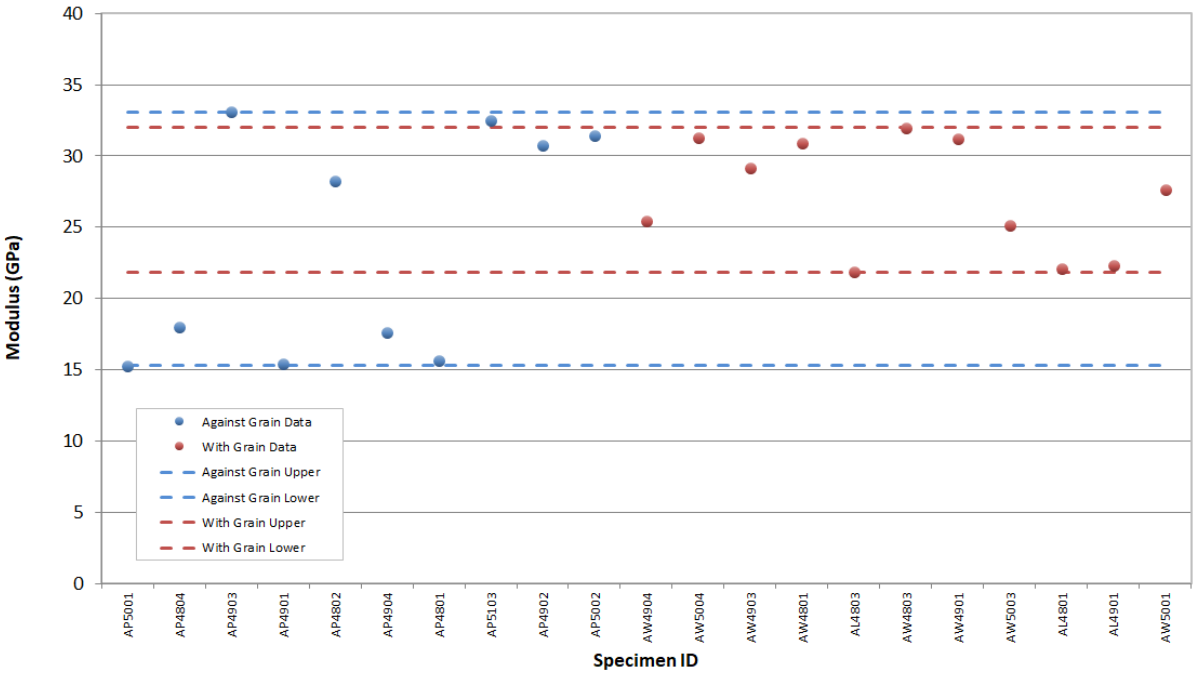

Figure A-51. NBG-17 creep modulus by resonant frequency.

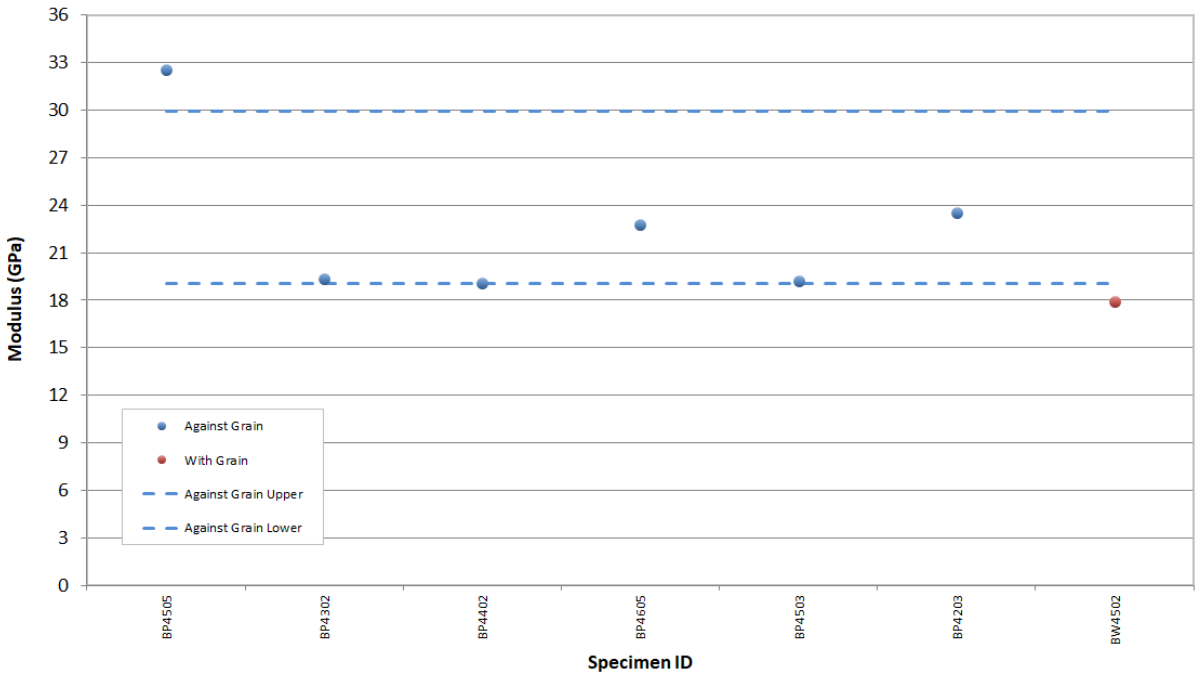

Figure A-52. NBG-18 creep modulus by resonant frequency.

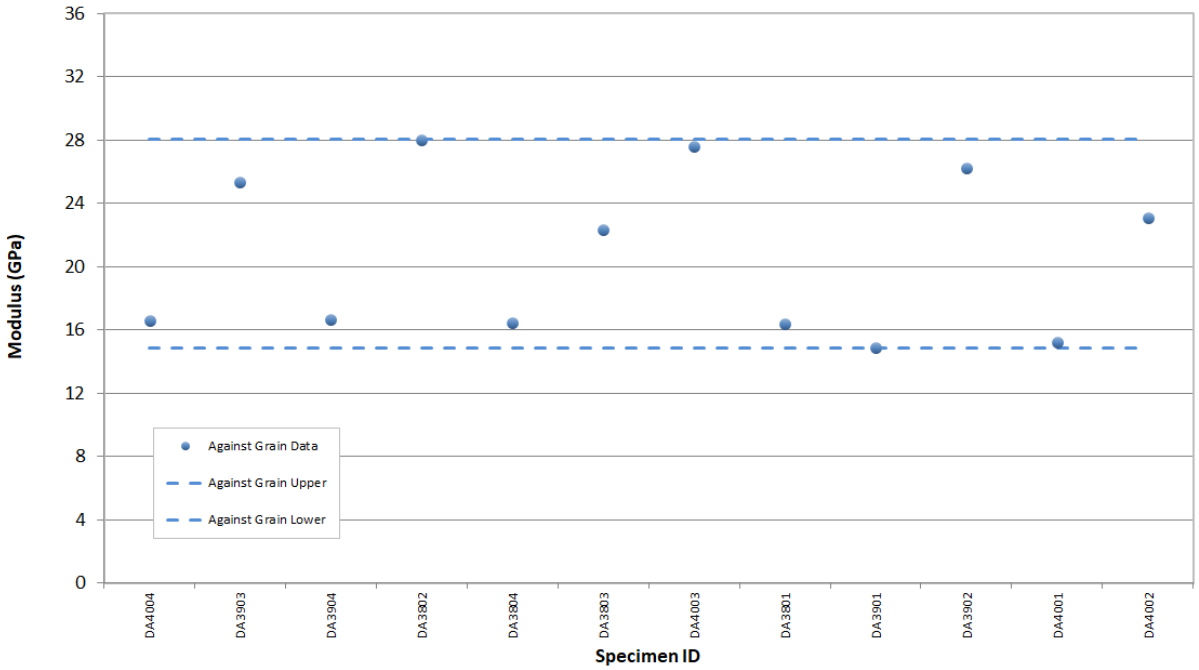

Figure A-53. PCEA creep modulus by resonant frequency.

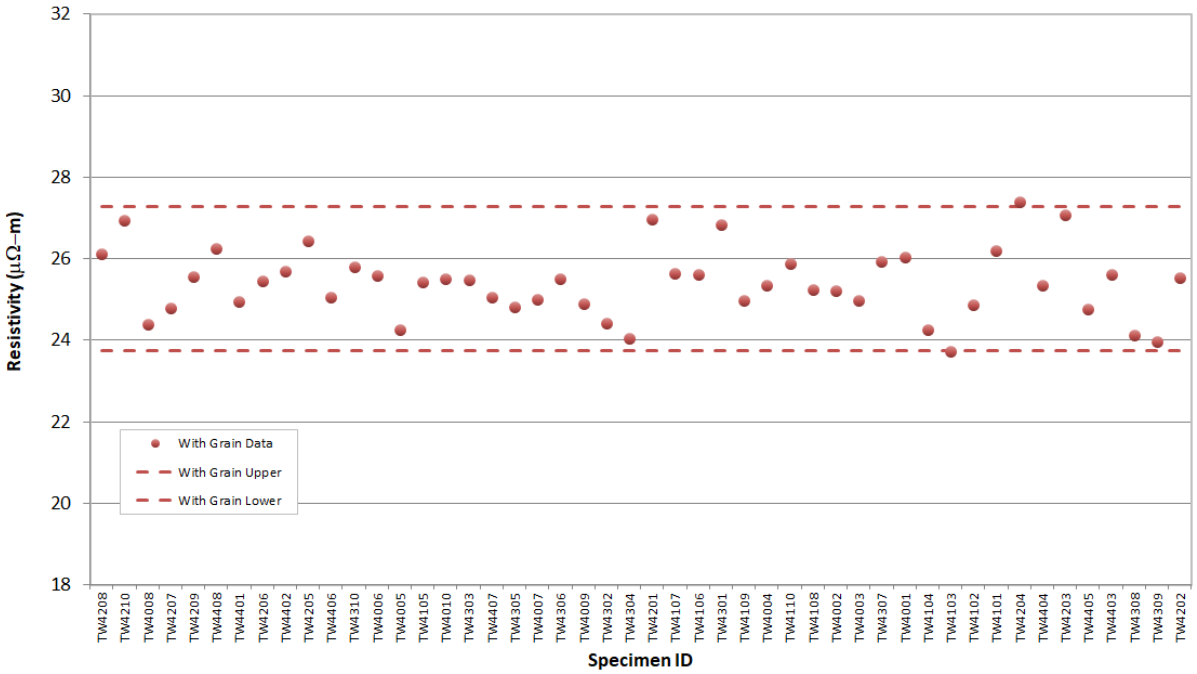

Figure A-54. 2114 creep resistivity.

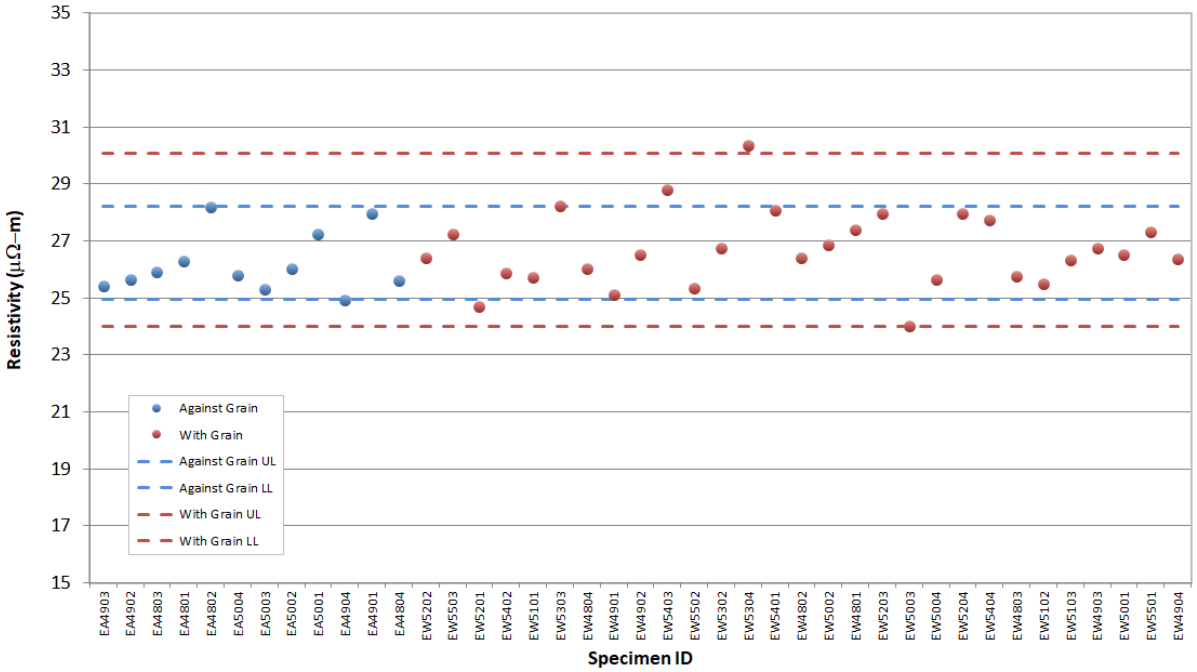

Figure A-55. IG-110 creep resistivity.

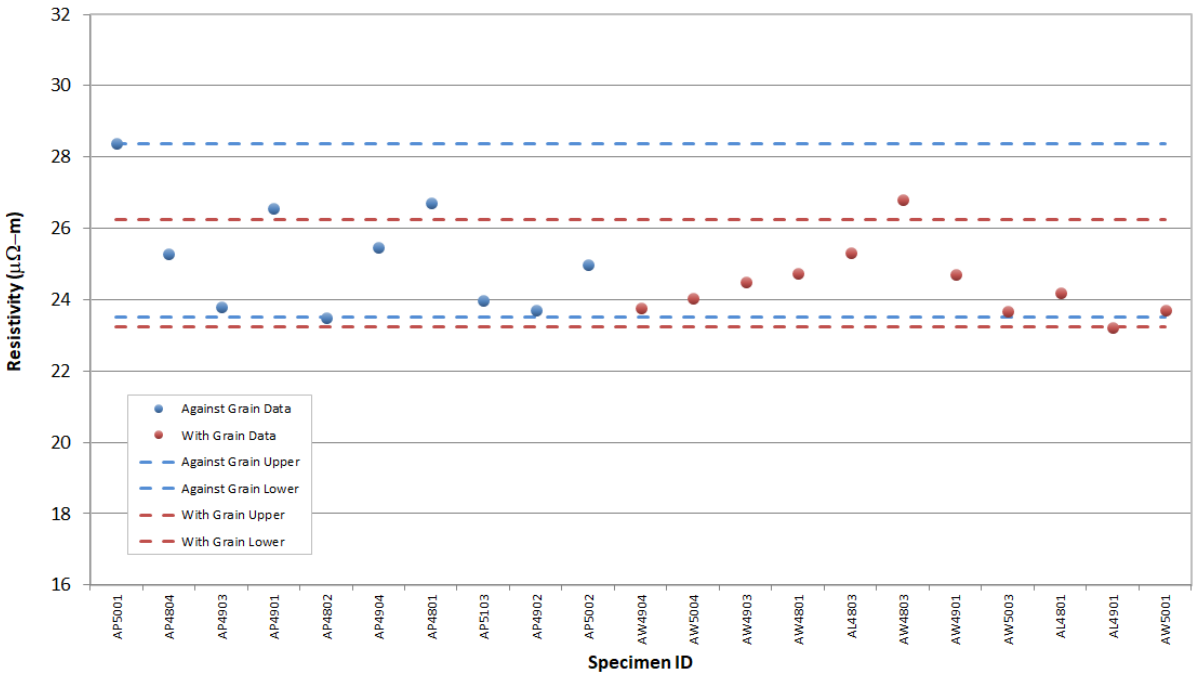

Figure A-56. NBG-17 creep resistivity.

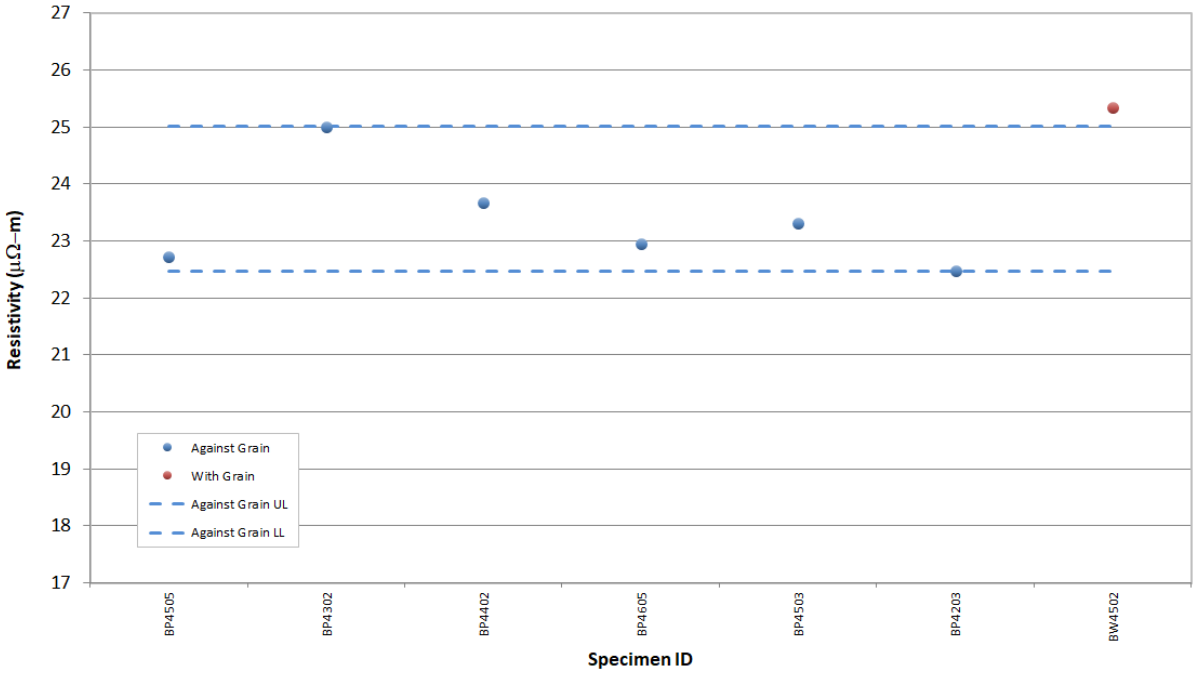

Figure A-57. NBG-18 creep resistivity.

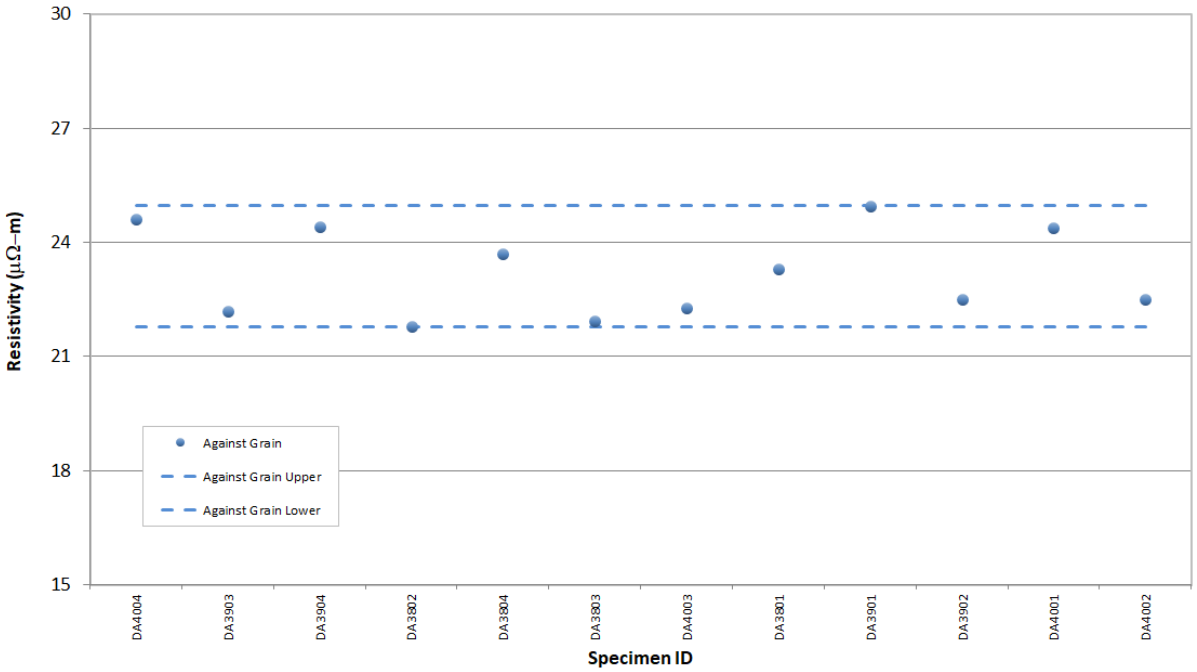

Figure A-58. PCEA creep resistivity.

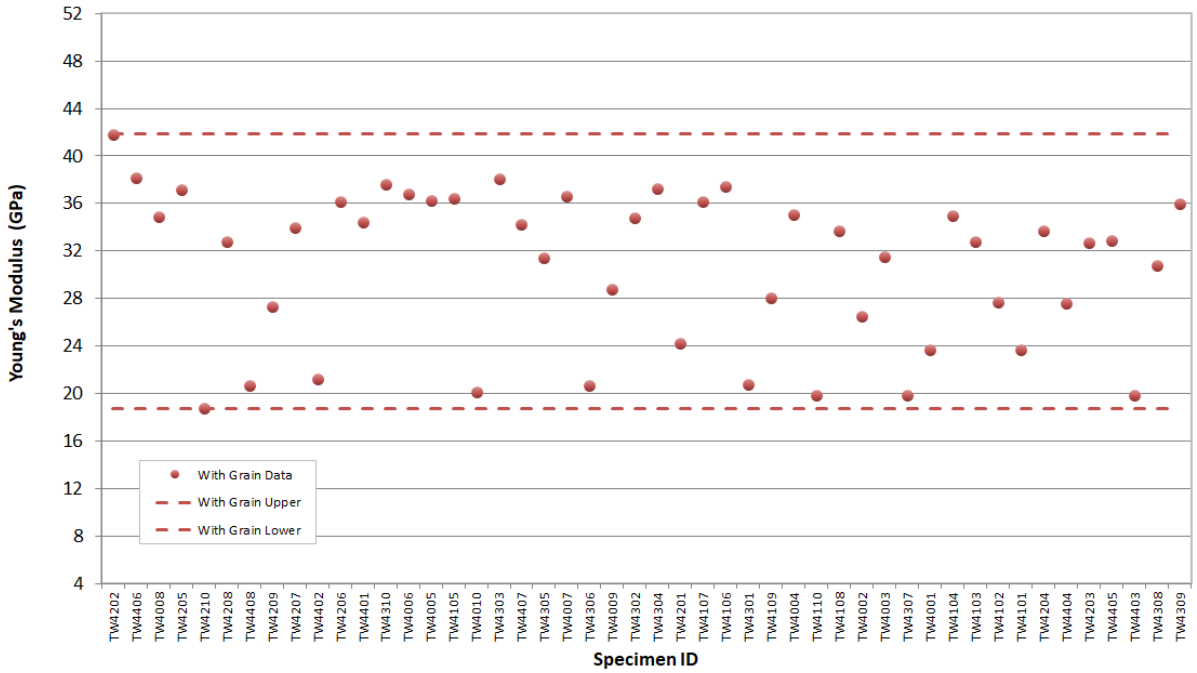

Figure A-59. 2114 creep modulus by sonic velocity.

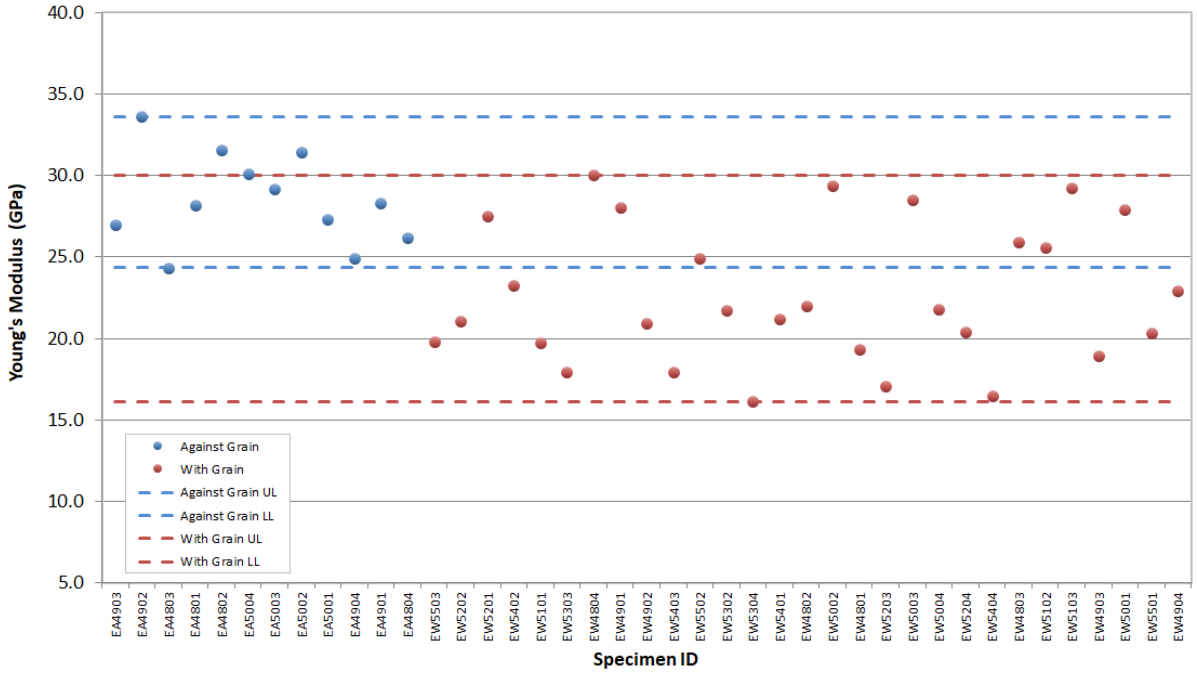

Figure A-60. IG-110 creep modulus by sonic velocity.

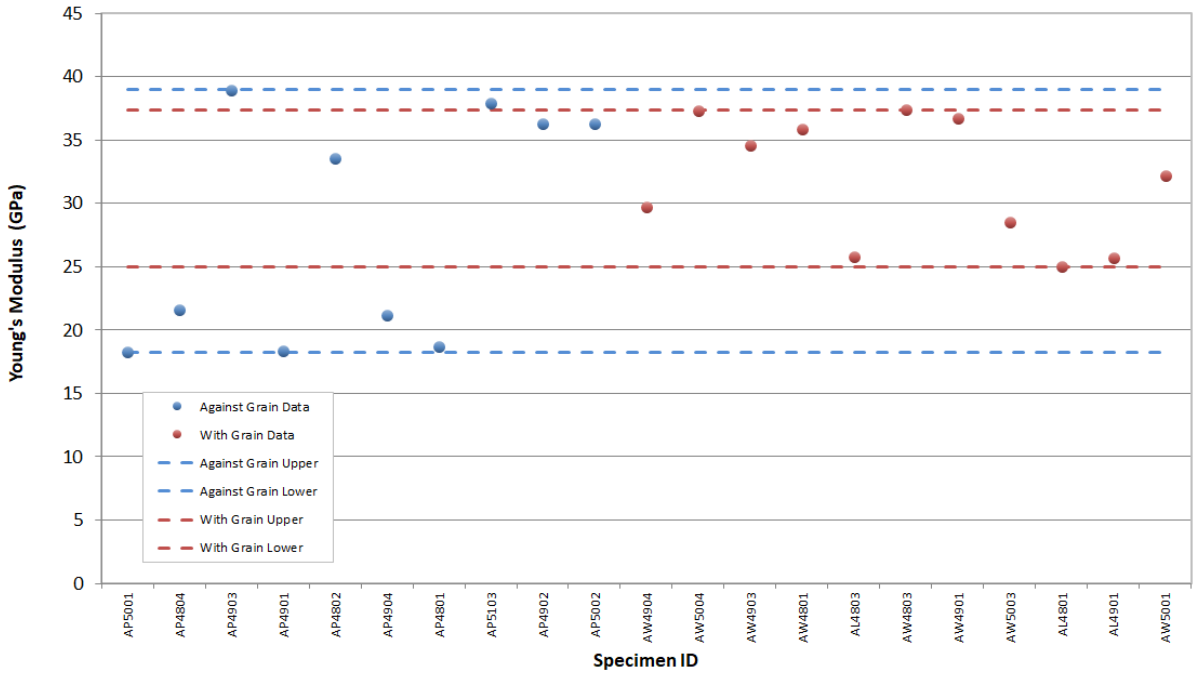

Figure A-61. NBG-17 creep modulus by sonic velocity.

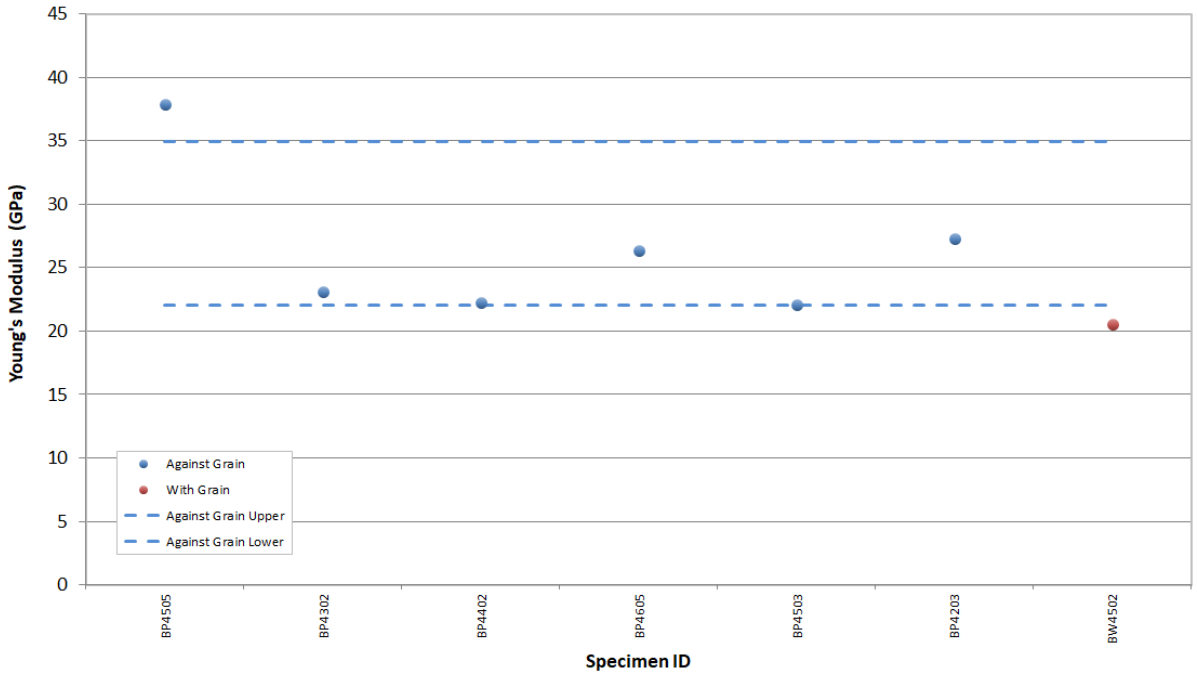

Figure A-62. NBG-18 creep modulus by sonic velocity.

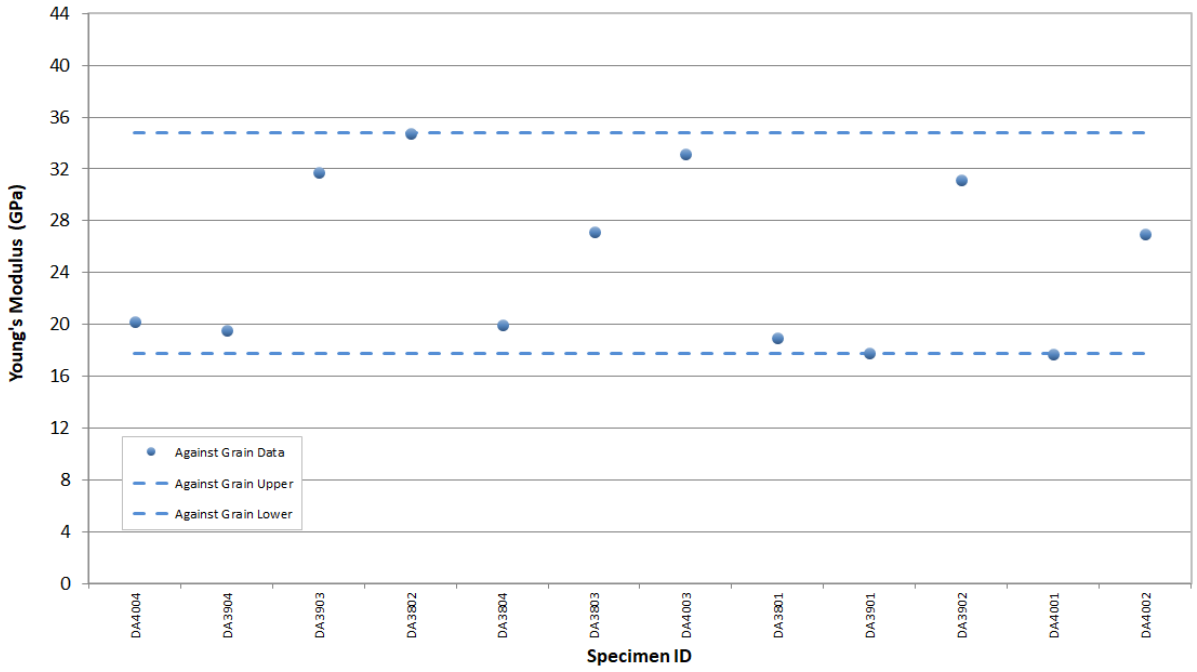

Figure A-63. PCEA creep modulus by sonic velocity.

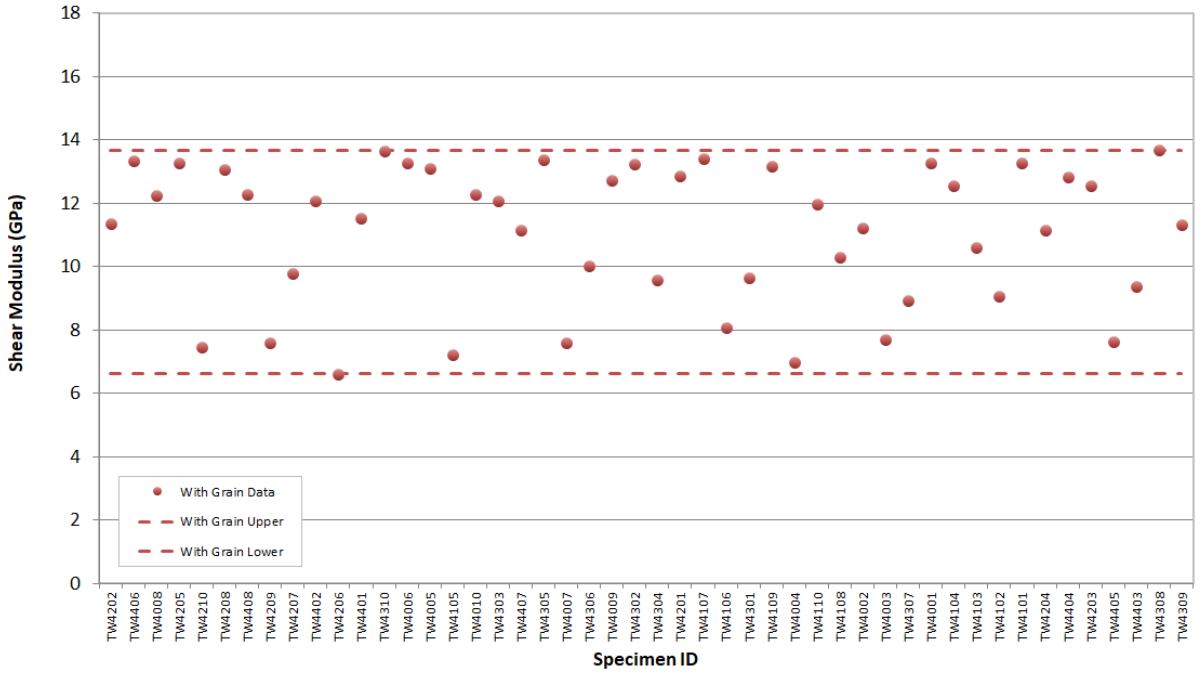

Figure A-64. 2114 creep shear modulus by sonic velocity.

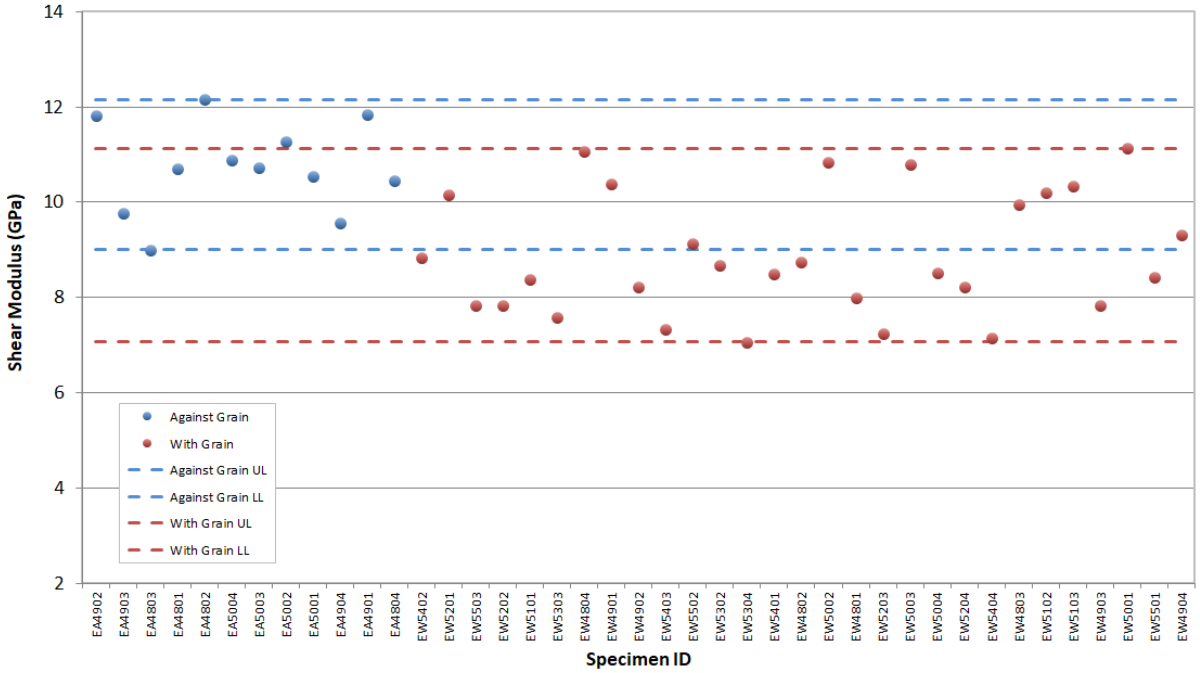

Figure A-65. IG-110 creep shear modulus by sonic velocity.

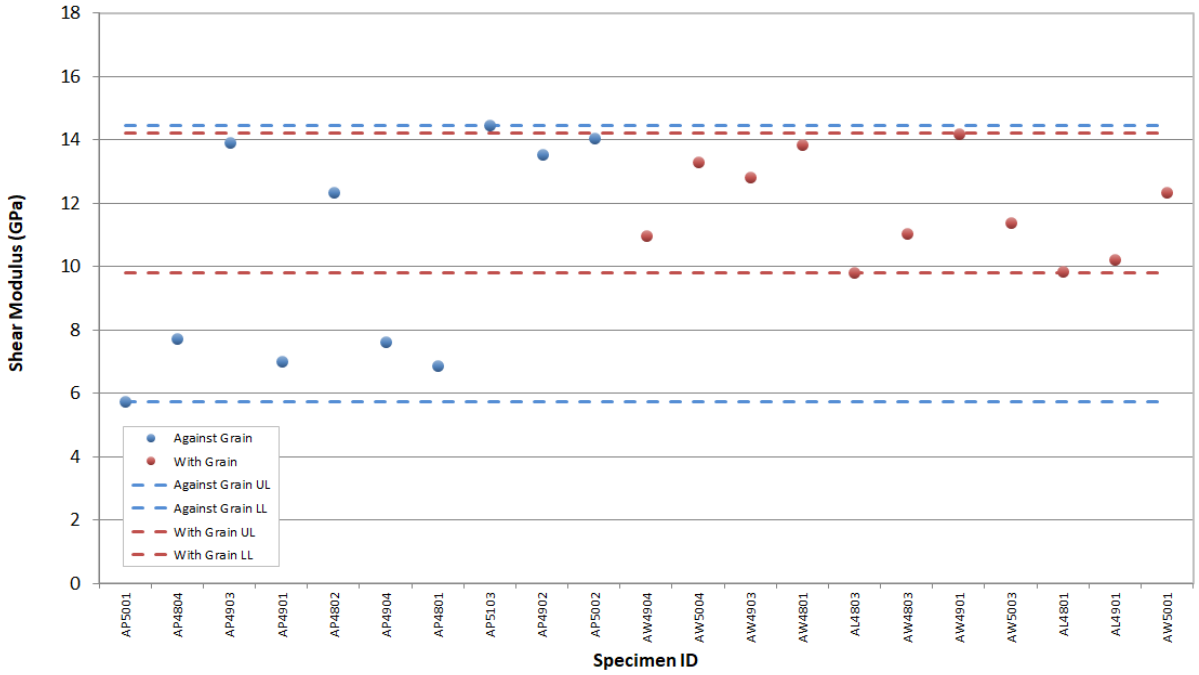

Figure A-66. NBG-17 creep shear modulus by sonic velocity.

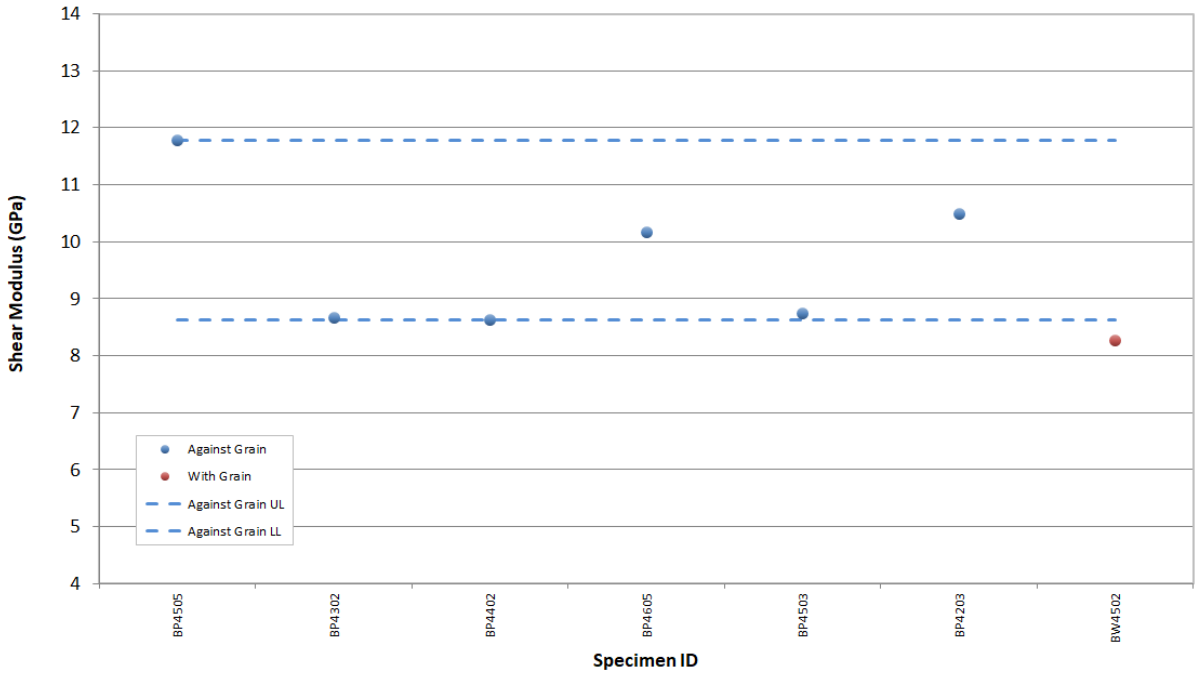

Figure A-67. NBG-18 creep shear modulus by sonic velocity.

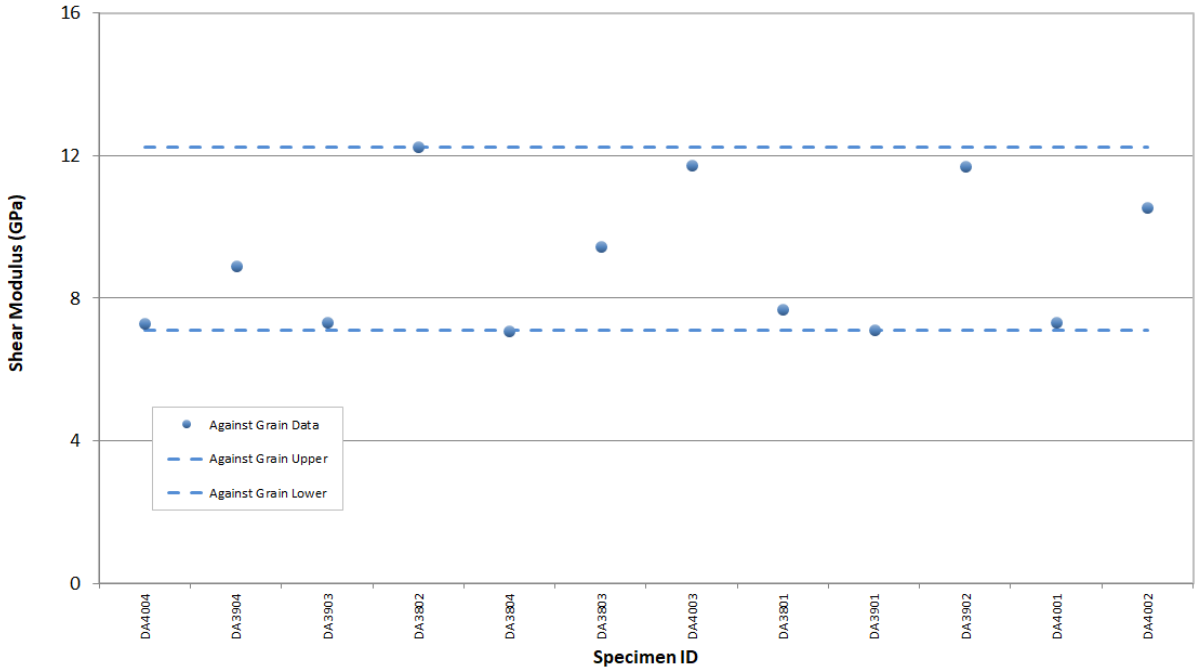

Figure A-68. PCEA creep shear modulus by sonic velocity.

Page intentionally left blank

Appendix B

Statistical Tables

Table B-1. Creep-specimen length (mm) summary statistics.

Combined Specimens	Mean	Std Dev	CoV (%)	Median	Upper Limit	Lower Limit
NBG-17	24.732	0.276	1.12	24.653	25.274	24.364
NBG-18	24.564	0.093	0.38	24.580	24.696	24.438
PCEA	24.677	0.331	1.34	24.471	25.117	24.218
2114	25.065	0.261	1.04	25.238	25.339	24.610
IG-110	24.790	0.358	1.44	24.833	25.293	24.096
Against Grain Specimens	Mean	Std Dev	CoV (%)	Median	Upper Limit	Lower Limit
NBG-17	24.880	0.269	1.08	24.824	25.274	24.563
NBG-18	24.559	0.101	0.41	24.559	24.703	24.433
PCEA	24.677	0.331	1.34	24.471	25.117	24.218
2114	-	-	-	-	-	-
IG-110	24.553	0.345	1.41	24.600	24.954	24.096
With Grain Specimens	Mean	Std Dev	CoV (%)	Median	Upper Limit	Lower Limit
NBG-17	24.597	0.213	0.86	24.523	24.949	24.364
NBG-18	24.592	-	-	24.592	24.592	24.592
PCEA	-	-	-	-	-	-
2114	25.065	0.261	1.04	25.238	25.339	24.610
IG-110	24.888	0.320	1.29	24.922	25.293	24.390

Table B-2. Creep-specimen diameter (mm) summary statistics.

Combined Specimens	Mean	Std Dev	CoV (%)	Median	Upper Limit	Lower Limit
NBG-17	12.386	0.053	0.43	12.392	12.463	12.282
NBG-18	12.413	0.027	0.22	12.409	12.447	12.378
PCEA	12.312	0.069	0.56	12.312	12.409	12.200
2114	12.492	0.050	0.40	12.478	12.623	12.423
IG-110	12.345	0.064	0.52	12.341	12.462	12.227
Against Grain Specimens	Mean	Std Dev	CoV (%)	Median	Upper Limit	Lower Limit
NBG-17	12.384	0.055	0.44	12.382	12.463	12.282
NBG-18	12.408	0.027	0.22	12.408	12.447	12.378
PCEA	12.312	0.069	0.56	12.312	12.409	12.200
2114	-	-	-	-	-	-
IG-110	12.373	0.057	0.46	12.379	12.462	12.283
With Grain Specimens	Mean	Std Dev	CoV (%)	Median	Upper Limit	Lower Limit
NBG-17	12.388	0.054	0.43	12.397	12.443	12.314
NBG-18	12.439	-	-	12.439	12.439	12.439
PCEA	-	-	-	-	-	-
2114	12.492	0.050	0.40	12.478	12.623	12.423
IG-110	12.333	0.064	0.52	12.341	12.441	12.227

Table B-3. Creep-specimen mass (g) summary statistics.

Combined Specimens	Mean	Std Dev	CoV (%)	Median	Upper Limit	Lower Limit
NBG-17	5.555	0.028	0.511	5.555	5.601	5.485
NBG-18	5.612	0.026	0.461	5.611	5.655	5.587
PCEA	5.432	0.031	0.564	5.428	5.478	5.395
2114	5.513	0.023	0.423	5.516	5.546	5.454
IG-110	5.361	0.016	0.294	5.361	5.405	5.332
Against Grain Specimens	**Mean**	**Std Dev**	**CoV (%)**	**Median**	**Upper Limit**	**Lower Limit**
NBG-17	5.562	0.015	0.271	5.564	5.584	5.541
NBG-18	5.616	0.026	0.455	5.619	5.655	5.587
PCEA	5.432	0.031	0.564	5.428	5.478	5.395
2114	-	-	-	-	-	-
IG-110	5.359	0.013	0.250	5.358	5.378	5.336
With Grain Specimens	**Mean**	**Std Dev**	**CoV (%)**	**Median**	**Upper Limit**	**Lower Limit**
NBG-17	5.549	0.036	0.653	5.538	5.601	5.485
NBG-18	5.587	-	-	5.587	5.587	5.587
PCEA	-	-	-	-	-	-
2114	5.513	0.023	0.423	5.516	5.546	5.454
IG-110	5.361	0.017	0.314	5.361	5.406	5.332

Table B-4. Creep-specimen density (g/cm^3) summary statistics.

Combined Specimens	Mean	Std Dev	CoV (%)	Median	Upper Limit	Lower Limit
NBG-17	1.8979	0.0199	1.05	1.9065	1.9235	1.8643
NBG-18	1.9207	0.0210	1.09	1.9092	1.9521	1.9002
PCEA	1.8831	0.0246	1.31	1.8895	1.9083	1.8427
2114	1.8279	0.0129	0.71	1.8320	1.8492	1.7969
IG-110	1.8406	0.0200	1.09	1.8453	1.8681	1.7951
Against Grain Specimens	Mean	Std Dev	CoV (%)	Median	Upper Limit	Lower Limit
NBG-17	1.8895	0.0246	1.30	1.8866	1.9235	1.8643
NBG-18	1.9234	0.0217	1.13	1.9209	1.9521	1.9002
PCEA	1.8831	0.0246	1.31	1.8895	1.9083	1.8427
2114	-	-	-	-	-	-
IG-110	1.8482	0.0142	0.7692	1.8520	1.8681	1.8256
With Grain Specimens	Mean	Std Dev	CoV (%)	Median	Upper Limit	Lower Limit
NBG-17	1.9056	0.0106	0.55	1.9081	1.9211	1.8870
NBG-18	1.9049	-	-	1.9049	1.9049	1.9049
PCEA	-	-	-	-	-	-
2114	1.8279	0.0129	0.71	1.8320	1.8492	1.7969
IG-110	1.8375	0.0214	1.17	1.8377	1.8663	1.7951

Table B-5. Creep-specimen Young's modulus (GPa) by sonic resonance summary statistics.

Combined Specimens	Mean	Std Dev	CoV (%)	Median	Upper Limit	Lower Limit
NBG-17	25.57	6.29	24.58	27.63	33.07	15.27
NBG-18	22.06	5.05	22.90	19.35	29.70	17.95
PCEA	20.73	5.18	25.01	19.48	28.01	14.88
2114	26.49	5.37	20.26	28.73	33.09	16.04
IG-110	21.71	3.95	18.17	22.14	28.66	14.73
Against Grain Specimens	Mean	Std Dev	CoV (%)	Median	Upper Limit	Lower Limit
NBG-17	23.79	7.96	33.46	23.12	33.07	15.27
NBG-18	22.75	5.17	22.71	21.06	29.95	19.06
PCEA	20.73	5.18	25.01	19.48	28.01	14.88
2114	-	-	-	-	-	-
IG-110	25.26	2.25	8.92	25.26	28.66	21.61
With Grain Specimens	Mean	Std Dev	CoV (%)	Median	Upper Limit	Lower Limit
NBG-17	27.19	3.99	14.68	27.63	31.99	21.85
NBG-18	17.95	-	-	17.95	17.95	17.95
PCEA	-	-	-	-	-	-
2114	26.49	5.37	20.26	28.73	33.09	16.04
IG-110	20.25	3.55	17.56	19.03	26.58	14.73

Table B-6. Creep-specimen resistivity (μΩ-m) summary statistics.

Combined Specimens	Mean	Std Dev	CoV (%)	Median	Upper Limit	Lower Limit
NBG-17	24.81	1.34	5.41	24.51	27.78	23.24
NBG-18	23.64	1.12	4.76	23.31	25.35	22.47
PCEA	23.21	1.15	4.97	22.90	24.96	21.79
2114	25.40	0.85	3.34	25.44	27.27	23.73
IG-110	26.54	1.26	4.73	26.38	29.89	24.01
Against Grain Specimens	Mean	Std Dev	CoV (%)	Median	Upper Limit	Lower Limit
NBG-17	25.24	1.59	6.30	25.14	28.37	23.51
NBG-18	23.35	0.91	3.91	23.13	25.00	22.47
PCEA	23.21	1.15	4.97	22.90	24.96	21.79
2114	-	-	-	-	-	-
IG-110	26.20	1.05	4.01	25.86	28.21	24.94
With Grain Specimens	Mean	Std Dev	CoV (%)	Median	Upper Limit	Lower Limit
NBG-17	24.43	0.99	4.05	24.19	26.25	23.24
NBG-18	25.35	-	-	25.35	25.35	25.35
PCEA	-	-	-	-	-	-
2114	25.40	0.85	3.34	25.44	27.27	23.73
IG-110	26.69	1.32	4.95	26.53	30.06	24.01

Table B-7. Creep-specimen Young's modulus (GPa) by sonic-velocity summary statistics.

Combined Specimens	Mean	Std Dev	CoV (%)	Median	Upper Limit	Lower Limit
NBG-17	30.02	7.29	24.27	32.24	38.98	18.26
NBG-18	25.66	5.90	22.99	23.13	34.54	20.59
PCEA	24.93	6.56	26.31	23.57	34.75	17.74
2114	30.76	6.48	21.08	32.86	41.82	18.72
IG-110	24.34	4.69	19.25	24.90	33.61	16.13
Against Grain Specimens	Mean	Std Dev	CoV (%)	Median	Upper Limit	Lower Limit
NBG-17	28.14	9.13	32.45	27.63	38.98	18.26
NBG-18	26.50	5.98	22.57	24.75	34.94	22.07
PCEA	24.93	6.56	26.31	23.57	34.75	17.74
2114	-	-	-	-	-	-
IG-110	28.50	2.80	9.83	28.22	33.61	24.33
With Grain Specimens	Mean	Std Dev	CoV (%)	Median	Upper Limit	Lower Limit
NBG-17	31.73	4.94	15.58	32.24	37.42	25.03
NBG-18	20.59	-	-	20.59	20.59	20.59
PCEA	-	-	-	-	-	-
2114	30.76	6.48	21.08	32.86	41.82	18.72
IG-110	22.62	4.22	18.66	21.75	30.02	16.13

Table B-8. Creep-specimen shear modulus (GPa) by sonic-velocity summary statistics.

Combined Specimens	Mean	Std Dev	CoV (%)	Median	Upper Limit	Lower Limit
NBG-17	11.10	2.76	24.88	11.38	14.46	5.74
NBG-18	9.54	1.30	13.62	8.76	11.78	8.27
PCEA	9.04	2.03	22.41	8.31	12.24	7.10
2114	11.07	2.20	19.84	11.74	13.67	6.62
IG-110	9.42	1.45	15.41	9.31	12.16	7.07
Against Grain Specimens	Mean	Std Dev	CoV (%)	Median	Upper Limit	Lower Limit
NBG-17	10.33	3.59	34.78	10.03	14.46	5.74
NBG-18	9.76	1.29	13.17	9.47	11.78	8.63
PCEA	9.04	2.03	22.41	8.31	12.24	7.10
2114	-	-	-	-	-	-
IG-110	10.73	0.96	8.97	10.70	12.16	9.00
With Grain Specimens	Mean	Std Dev	CoV (%)	Median	Upper Limit	Lower Limit
NBG-17	11.80	1.58	13.43	11.38	14.20	9.81
NBG-18	8.27	-	-	8.27	8.27	8.27
PCEA	-	-	-	-	-	-
2114	11.07	2.20	19.84	11.74	13.67	6.62
IG-110	8.88	1.27	14.32	8.51	11.13	7.07

Table B-9. Piggyback-specimen-length (mm) summary statistics.

Combined Specimens	Mean	Std Dev	CoV (%)	Median	Upper Limit	Lower Limit
NBG-17	6.2924	0.0286	0.45	6.2873	6.3515	6.2490
NBG-18	6.2805	0.0273	0.44	6.2809	6.3248	6.2260
PCEA	6.2833	-	-	6.2833	6.2833	6.2833
2114	6.3267	0.0109	0.17	6.3243	6.3520	6.3123
IG-110	6.2846	0.0341	0.54	6.2880	6.3380	6.2128
IG-430	6.3799	0.0177	0.28	6.3760	6.4108	6.3530
NBG-25	6.3130	0.0477	0.75	6.3350	6.3738	6.2278
A3-Matrix	-	-	-	-	-	-
Against Grain Specimens	Mean	Std Dev	CoV (%)	Median	Upper Limit	Lower Limit
NBG-17	6.3213	0.0280	0.44	6.3298	6.3515	6.2800
NBG-18	6.2532	0.0197	0.31	6.2543	6.2795	6.2260
PCEA	-	-	-	-	-	-
2114	-	-	-	-	-	-
IG-110	6.2566	0.0290	0.46	6.2553	6.3073	6.2128
IG-430	-	-	-	-	-	-
NBG-25	-	-	-	-	-	-
A3-Matrix	-	-	-	-	-	-
With Grain Specimens	Mean	Std Dev	CoV (%)	Median	Upper Limit	Lower Limit
NBG-17	6.2844	0.0237	0.38	6.2856	6.3338	6.2490
NBG-18	6.2941	0.0192	0.30	6.2926	6.3248	6.2655
PCEA	6.2833	-	-	6.2833	6.2833	6.2833
2114	6.3267	0.0109	0.17	6.3243	6.3520	6.3123
IG-110	6.3014	0.0250	0.40	6.3003	6.3380	6.2533
IG-430	6.3799	0.0177	0.28	6.3760	6.4108	6.3530
NBG-25	6.3130	0.0477	0.75	6.3350	6.3738	6.2278
A3-Matrix	-	-	-	-	-	-

Table B-10. Piggyback-specimen-diameter (mm) summary statistics.

Combined Specimens	Mean	Std Dev	CoV (%)	Median	Upper Limit	Lower Limit
NBG-17	12.3447	0.0447	0.36	12.3300	12.4290	12.2895
NBG-18	12.3085	0.0468	0.38	12.2908	12.3940	12.2495
PCEA	12.3450	-	-	12.3450	12.3450	12.3450
2114	12.4745	0.0423	0.34	12.4838	12.5595	12.4240
IG-110	12.3256	0.0599	0.49	12.3193	12.4185	12.2080
IG-430	12.3207	0.0805	0.65	12.2745	12.4350	12.2425
NBG-25	12.3873	0.0673	0.54	12.3940	12.5015	12.2960
A3-Matrix	-	-	-	-	-	-
Against Grain Specimens	Mean	Std Dev	CoV (%)	Median	Upper Limit	Lower Limit
NBG-17	12.3223	0.0389	0.32	12.3000	12.3790	12.2895
NBG-18	12.3018	0.0321	0.26	12.2980	12.3500	12.2675
PCEA	-	-	-	-	-	-
2114	-	-	-	-	-	-
IG-110	12.3514	0.0385	0.31	12.3555	12.4105	12.2880
IG-430	-	-	-	-	-	-
NBG-25	-	-	-	-	-	-
A3-Matrix	-	-	-	-	-	-
With Grain Specimens	Mean	Std Dev	CoV (%)	Median	Upper Limit	Lower Limit
NBG-17	12.3509	0.0452	0.37	12.3323	12.4290	12.2950
NBG-18	12.3119	0.0536	0.44	12.2908	12.3940	12.2495
PCEA	12.3450	-	-	12.3450	12.3450	12.3450
2114	12.4745	0.0423	0.34	12.4838	12.5595	12.4240
IG-110	12.3100	0.0661	0.54	12.3080	12.4185	12.2080
IG-430	12.3207	0.0805	0.65	12.2745	12.4350	12.2425
NBG-25	12.3873	0.0673	0.54	12.3940	12.5015	12.2960
A3-Matrix	-	-	-	-	-	-

Table B-11. Piggyback-specimen-mass (g) summary statistics.

Combined Specimens	Mean	Std Dev	CoV (%)	Median	Upper Limit	Lower Limit
NBG-17	1.4162	0.0073	0.52	1.4176	1.4248	1.4026
NBG-18	1.4214	0.0071	0.50	1.4230	1.4295	1.4055
PCEA	1.4243	-	-	1.4243	1.4243	1.4243
2114	1.4039	0.0050	0.36	1.4054	1.4083	1.3994
IG-110	1.3691	0.0080	0.59	1.3693	1.3832	1.3510
IG-430	1.4128	0.0035	0.25	1.4119	1.4200	1.4082
NBG-25	1.4346	0.0073	0.51	1.4366	1.4394	1.4279
A3-Matrix	-	-	-	-	-	-
Against Grain Specimens	Mean	Std Dev	CoV (%)	Median	Upper Limit	Lower Limit
NBG-17	1.4148	0.0052	0.37	1.4162	1.4203	1.4069
NBG-18	1.4185	0.0081	0.57	1.4201	1.4256	1.4096
PCEA	-	-	-	-	-	-
2114	-	-	-	-	-	-
IG-110	1.3640	0.0084	0.61	1.3653	1.3710	1.3538
IG-430	-	-	-	-	-	-
NBG-25	-	-	-	-	-	-
A3-Matrix	-	-	-	-	-	-
With Grain Specimens	Mean	Std Dev	CoV (%)	Median	Upper Limit	Lower Limit
NBG-17	1.4166	0.0079	0.56	1.4182	1.4248	1.4052
NBG-18	1.4229	0.0065	0.46	1.4258	1.4295	1.4087
PCEA	1.4243	-	-	1.4243	1.4243	1.4243
2114	1.4039	0.0050	0.36	1.4054	1.4083	1.3994
IG-110	1.3722	0.0063	0.46	1.3737	1.3832	1.3606
IG-430	1.4128	0.0035	0.25	1.4119	1.4200	1.4082
NBG-25	1.4346	0.0073	0.51	1.4366	1.4394	1.4279
A3-Matrix	-	-	-	-	-	-

Table B-12. Piggyback-specimen-density (g/cm^3) summary statistics.

Combined Specimens	Mean	Std Dev	CoV (%)	Median	Upper Limit	Lower Limit
NBG-17	1.8805	0.0181	0.96	1.8792	1.9087	1.8455
NBG-18	1.9022	0.0204	1.07	1.9056	1.9279	1.8612
PCEA	1.8939	-	-	1.8939	1.8939	1.8939
2114	1.8156	0.0157	0.86	1.8144	1.8369	1.7884
IG-110	1.8260	0.0189	1.04	1.8230	1.8686	1.7968
IG-430	1.8576	0.0233	1.25	1.8651	1.8906	1.8244
NBG-25	1.8858	0.0148	0.79	1.8853	1.9103	1.8550
A3-Matrix	-	-	-	-	-	-
Against Grain Specimens	Mean	Std Dev	CoV (%)	Median	Upper Limit	Lower Limit
NBG-17	1.8768	0.0085	0.45	1.8786	1.8886	1.8665
NBG-18	1.9086	0.0165	0.86	1.9069	1.9279	1.8854
PCEA	-	-	-	-	-	-
2114	-	-	-	-	-	-
IG-110	1.8196	0.0132	0.73	1.8199	1.8375	1.8008
IG-430	-	-	-	-	-	-
NBG-25	-	-	-	-	-	-
A3-Matrix	-	-	-	-	-	-
With Grain Specimens	Mean	Std Dev	CoV (%)	Median	Upper Limit	Lower Limit
NBG-17	1.8816	0.0200	1.06	1.8858	1.9087	1.8455
NBG-18	1.8990	0.0221	1.16	1.9038	1.9256	1.8546
PCEA	1.8939	-	-	1.8939	1.8939	1.8939
2114	1.8156	0.0157	0.86	1.8144	1.8369	1.7884
IG-110	1.8298	0.0211	1.15	1.8321	1.8686	1.7968
IG-430	1.8576	0.0233	1.25	1.8651	1.8906	1.8244
NBG-25	1.8858	0.0148	0.79	1.8853	1.9103	1.8550
A3-Matrix	-	-	-	-	-	-